

5-31-1987

Theoretical studies of a norbornane mimic of acyl-alpha-chymotrypsin

Pin-Nan Chen
New Jersey Institute of Technology

Follow this and additional works at: <https://digitalcommons.njit.edu/theses>

 Part of the [Chemical Engineering Commons](#)

Recommended Citation

Chen, Pin-Nan, "Theoretical studies of a norbornane mimic of acyl-alpha-chymotrypsin" (1987). *Theses*. 1970.

<https://digitalcommons.njit.edu/theses/1970>

This Thesis is brought to you for free and open access by the Electronic Theses and Dissertations at Digital Commons @ NJIT. It has been accepted for inclusion in Theses by an authorized administrator of Digital Commons @ NJIT. For more information, please contact digitalcommons@njit.edu.

Copyright Warning & Restrictions

The copyright law of the United States (Title 17, United States Code) governs the making of photocopies or other reproductions of copyrighted material.

Under certain conditions specified in the law, libraries and archives are authorized to furnish a photocopy or other reproduction. One of these specified conditions is that the photocopy or reproduction is not to be “used for any purpose other than private study, scholarship, or research.” If a user makes a request for, or later uses, a photocopy or reproduction for purposes in excess of “fair use” that user may be liable for copyright infringement,

This institution reserves the right to refuse to accept a copying order if, in its judgment, fulfillment of the order would involve violation of copyright law.

Please Note: The author retains the copyright while the New Jersey Institute of Technology reserves the right to distribute this thesis or dissertation

Printing note: If you do not wish to print this page, then select “Pages from: first page # to: last page #” on the print dialog screen

The Van Houten library has removed some of the personal information and all signatures from the approval page and biographical sketches of theses and dissertations in order to protect the identity of NJIT graduates and faculty.

ABSTRACT

**Title of Thesis: Theoretical Studies of A Norbornane Mimic
of Acyl-Alpha-Chymotrypsin**

Pin-Nan Chen, Master of Science, 1987

Thesis directed by: Dr. Carol A. Venanzi

Molecular mechanics calculations were used to investigate the structural flexibility of the norbornane mimic which is a model of an acyl-alpha-chymotrypsin intermediate. The Amber molecular mechanics force field was used to perform the conformational analysis.

Comparison of the optimized conformations of different energy has shown the relative structural rigidity of this molecule. Structural superposition of the minimized mimic to the native conformation of chymotrypsin shows that the mimic has a very similar spatial arrangement of its functional groups compared to the catalytic triad of the real enzyme.

Molecular electrostatic potential maps calculated in planes parallel to the average plane containing the catalytic triad indicate that the mimic presents an electrostatic pattern similar to that of chymotrypsin in the region of the carboxylate fragment.

THEORETICAL STUDIES OF A NORBORNANE MIMIC OF
ACYL-ALPHA-CHYMOTRYPSIN

by

PIN-NAN CHEN

Thesis submitted to the Faculty of the Graduate School of
the New Jersey Institute of Technology in partial
fulfillment of the requirement for the degree of
Master of Science in Chemical Engineering

1987

APPROVAL

Title of Thesis: THEORETICAL STUDIES OF A NORBORNANE MIMIC
OF ACYL-ALPHA-CHYMOTRYPSIN INTERMEDIATE

Name of Candidate: Pin-Nan Chen

Thesis and Abstract Approved: _____

Dr. CAROL A. VENANZI

Date

Department of Chemistry

5/1/87

Signatures of other members

of the thesis committee:

5/1/87

Date

5/1/87

Date

VITA

Name: Pin-Nan Chen

Present address:

Permanent address:

Degree and date to be conferred: Master of Science, 1987

Date of birth:

Place of birth:

Secondary education: Tu-Ku High School, 1977

Collegiate institutions attended	Dates	Degree	Date of Degree
-------------------------------------	-------	--------	----------------

Ming-Chi Institute of Technology	1977-1982	B.S.	Jun., 1982
-------------------------------------	-----------	------	------------

New Jersey Institute of Technology	1985-1987	M.S.	May, 1987
---------------------------------------	-----------	------	-----------

Major: Chemical Engineering

Position Held: Teaching Assistant, Sept., 1985 - Dec., 1986

Research Assistant, Jan., 1987 - May, 1987

Department of Chemistry/Chemical Engineering

New Jersey Institute of Technology

Newark, New Jersey 07104

TABLE OF CONTENTS

Chapter	Page
ACKNOWLEDGEMENT.....	ii
LIST OF TABLES.....	iii
LIST OF FIGURES.....	v
I. INTRODUCTION.....	1
A. Enzymes and Artificial Enzymes: General Aspects.....	1
B. Alpha-Chymotrypsin.....	2
C. Computer Modeling Applications for Chemists.....	5
D. Functionalized Norbornane as a Model of an Acyl-Enzyme Intermediate.....	6
E. Goals of the Present Research.....	8
II. METHODOLOGY.....	9
A. Conformational Analysis.....	9
B. Distance Analysis.....	14
C. Model Building.....	14
D. Force Field Parameters.....	16
1. Bond Stretching Parameters.....	17
2. Angle Bending Parameters.....	19
3. Torsional Parameters.....	23
E. Atomic Point Charges.....	26
F. Structural Superposition.....	27
G. Molecular Electrostatic Potential.....	29
III. RESULTS.....	33
A. Conformational Analysis.....	33
B. Energy Minimization.....	38
C. Distance Analysis.....	42
D. Structural Superposition.....	44
E. Electrostatic Potential Contours.....	50

IV. DISCUSSION AND CONCLUSION.....	53
V. TABLES.....	55-83
VI. FIGURES.....	84-112
VII. APPENDIX.....	113-117
VIII. REFERENCES.....	118

ACKNOWLEDGEMENT

I particularly wish to present my appreciation and gratitude to Dr. Carol A. Venanzi, whose kind assistance and guidance has been instrumental to the success of this study. I also wish to acknowledge Dr. Dana Knox and Dr. Tamara Gund for careful reading of the thesis, and Dr. Mark Hermsmeier and Mr. Wen-Chung Shang for help in preparing some of the figures.

LIST OF TABLES

Table		Page
1.	List of Amber atom types.....	55
	With diagram of Amber atom types (Chart 1).....	59
2.	Additional force field parameters used for the norbornane mimic.....	62
3A.	Optimization of alpha angle: O10-C9-O11-C12.....	64
3B.	Optimization of beta angle: C17-C18-C19-N23.....	65
3C.	Optimization of gamma angle: C25-C30-C31-O32.....	66
3D.	Optimization of alpha angle: O10-C9-O11-C12.....	67
3E.	Optimization of delta angle: N21-C24-C25-C30.....	68
4A.	Optimized energies for rotation around alpha angle.....	69
4B.	Optimized energies for rotation around beta angle.....	70
4C.	Optimized energies for rotation around gamma angle.....	71
4D.	Optimized energies for rotation around alpha angle.....	72
4E.	Optimized energies for rotation around delta angle.....	73
4F.	Scaling Factor Study at Constant EEL.....	74
4G.	Scaling Factor Study at Constant NB.....	75
5A.	Distance comparison between atoms for optimization of alpha angle.....	76
5B.	Distance comparison between atoms for optimization of beta angle.....	77
5C.	Distance comparison between atoms for optimization of gamma angle.....	78
5D.	Distance comparison between atoms for optimization of alpha angle.....	79
5E.	Distance comparison between atoms for optimization of delta angle.....	80

6.	RMS comparisons for selected minimized structures.....	81
7.	Comparison of distances between functional groups in mimic and enzyme.....	82
8.	Fit of Mimic to the Active Site of the Chymotrypsin.....	83

List of The Figures

Figure	Page
1. The activation process of chymotrypsinogen.....	84
2. Conformation of the charge relay system in chymotrypsin.....	85
3. Charge relay network in chymotrypsin.....	86
4. The tetrahedral transition-state intermediate in the acylation and deacylation reactions of chymotrypsin.....	87
5. The acylation stage in the hydrolysis of a peptide bond by chymotrypsin.....	88
6. The deacylation stage in the hydrolysis of a peptide bond by chymotrypsin.....	89
7. Structure of endo - 5 - [4'(5') - imidazolyl] bicyclo [2.2.1]- hept- endo- 2- yltrans- cinnamate.....	90
8. Structure of exo - 5 - [4'(5') - imidazolyl] bicyclo [2.2.1] - hept - endo - 3 - yl trans- cinnamate.....	91
9. Structure of endo, endo-5-[2-(2-carboxylphenyl)- 4-(5)- imidazolyl] bicyclo [2.2.1]-hept-2-yl trans-cinnamate.....	92
10. Synthesis of structure 3.....	93
11A. Starting structure of norbornane mimic.....	94
11B. Norbornane mimic with atom type.....	95
12. Superposition of two minimized structures of the norbornane mimic: run B16M onto run B510M....	96
13. Superposition of two minimized structures of the norbornane mimic: run B111 onto run B510M....	97
14. Superposition of two minimized structures of the norbornane mimic: run B24M onto run B510M....	98
15. Superposition of two minimized structures of the norbornane mimic: run B38M onto run B510M....	99
16. Superposition of two minimized structures of the norbornane mimic: run B31M onto run B510M...100	

17. Superposition of two minimized structures of the norbornane mimic: run B311 onto run B510M...	101
18. Superposition of two minimized structures of the norbornane mimic: run A (NB=EEL=0.5) onto run F (NB=EEL=1.0).....	102
19. Superposition of two minimized structures of the norbornane mimic: run N (NB=0.5,EEL=2.0) onto run F (NB=EEL=1.0).....	103
20. Superposition of two minimized structures of the norbornane mimic: run Q (NB=2.0,EEL=2.0) onto run F (NB=EEL=1.0).....	104
21. Superposition of the optimized norbornane mimic structure onto the active site of alpha-chymotrypsin.....	105
22. Molecular electrostatic potential contour map of norbornane mimic calculated in the x-y plane at z = 0.0 A.....	106
23. Molecular electrostatic potential contour map of norbornane mimic calculated in the x-y plane at z = 2.0 A.....	107
24. Molecular electrostatic potential contour map of norbornane mimic calculated in the x-y plane at z = 4.0 A.....	108
25. Molecular electrostatic potential contour map of norbornane mimic calculated in the x-y plane at z = 6.0 A.....	109
26. Molecular electrostatic potential contour map of norbornane mimic calculated in the x-y plane at z = -2.0 A.....	110
27. Molecular electrostatic potential contour map of norbornane mimic calculated in the x-y plane at z = -4.0 A.....	111
28. Molecular electrostatic potential contour map of norbornane mimic calculated in the x-y plane at z = -6.0 A.....	112

I. Introduction

A. Enzymes and Artificial Enzymes: General Aspects

An enzyme is a protein polymer which is formed from hundreds of amino acid monomers and is capable of catalytic activity. The complexation of an enzyme with its substrate is the first step in the enzymatic catalysis, which occurs in a specific region called the active site [1,2,3]. The active site consists of all the amino acid residues implicated in the binding of the substrate. The enzyme is selective for the substrate structures which fit within the active site, forming an enzyme-substrate complex [2,4]. As a result of specific complexation and consequent intramolecular catalysis [4], enzymes can increase the reaction velocity by a factor of up to 10^{12} over the uncatalyzed reaction by significantly decreasing the activation energy of the reaction [2,3]. Studies involving the active site of enzymes have become one of the key research focuses in enzyme chemistry.

In an effort to elucidate the mechanism of enzyme-substrate interactions, several groups have begun the design and synthesis of artificial enzymes: molecules with less than 200 atoms which can reproduce the substrate selectivity and high reaction velocity approaching that of enzymatic reactions. These artificial enzymes, or enzyme mimics, contain fragments similar to the catalytic residues of the enzyme which they model. Cyclic urea, cyclodextrin, crown ether, and norbornane have been used to mimic the hydrolysis

mechanism of alpha-chymotrypsin. Recent work by Cram [6,7], Breslow [8], and Bender [5,9] has focused on the design of compounds containing reactive hydroxyl groups intended to mimic the action of Ser-195 of chymotrypsin in acyl transfer to the substrate. These research groups have been able to demonstrate comparable enzymatic velocities with their artificial enzymes.

B. Alpha-chymotrypsin

Alpha-chymotrypsin is one of the most extensively studied enzymes. It is a digestive enzyme belonging to the enzyme family of serine proteases. The inactive precursor of the enzyme, called chymotrypsinogen, is synthesized in mammalian pancreas. Chymotrypsinogen is virtually devoid of enzymatic activity. It is converted into a fully active enzyme when the peptide bond joining Arginine-15 and Isoleucine-16 is cleaved by trypsin (Figure 1). The resulting active enzyme, called pi-chymotrypsin, then acts on other pi-chymotrypsin molecules. Two peptides are removed to yield alpha-chymotrypsin, the stable form of the enzyme. A schematic representation of the chymotrypsinogen activation process is shown in Figure 1 [2].

In the metabolic system, alpha-chymotrypsin serves in the role of catalyzing the hydrolysis of ester and peptide bonds of protein substrates in the intestines of mammals. The enzyme is very large, having a molecular weight of 24,800 Daltons with 245 amino acids residues [2,3,5]. It is

selective for peptide bonds on the carboxyl side of the aromatic side chains of tyrosine, tryptophan, phenylalanine, and of large hydrophobic residues such as methionine [2]. The structure of alpha-chymotrypsin has been resolved by X-ray crystallography [10,11]. The "catalytic triad" of alpha-chymotrypsin is composed of three amino acid residues: Histidine-57 (His-57), Aspartate-102 (Asp-102), and Serine-195 (Ser-195) [1,3]. The catalytic activity of chymotrypsin depends on the unusual reactivity of Ser-195. Generally, the $-CH_2OH$ group is quite unreactive under physiological conditions of pH 6.4 to pH 7.4. The explanation of why the active site of alpha-chymotrypsin becomes so reactive has been deduced from X-ray studies of the three dimensional structure of the enzyme. In the active site, His-57 is adjacent to Ser-195 and to the carboxyl side chain of Asp-102 (Figure 2). The juxtaposition of these three residues enhances the catalytic activity, which is also a result of intramolecular catalysis [2,4]. As a result, a charge relay network is formed by these three residues (Figure 3) [2,3].

Acylation is the first step during the protein peptide bond hydrolysis catalyzed by alpha-chymotrypsin. In this mechanism, His-57 and Ser-195 participate directly in the cleavage of the susceptible peptide bond of the substrate. The oxygen atom of the hydroxyl group of Ser-195 attacks the carbonyl carbon atom of the susceptible peptide bond, and this step marks the beginning of the peptide bond hydrolysis [2]. The carbon-oxygen bond of this carbonyl group becomes a single bond and the oxygen atom assumes a net charge

[2,3]. The four atoms bonded to the carbonyl carbon form a transient tetrahedral intermediate transition state (Figure 4). The formation of this tetrahedral intermediate transition state from a planar amide group is made possible by hydrogen bonds between the negatively charged carboxyl oxygen atom and two main-chain NH groups [2]. Simultaneously, a proton is transferred from Ser-195 to His-57 (Figure 5). This proton transfer is facilitated considerably by the existence of the charge relay network in which Asp-102 orients the imidazolyl ring of His-57 and partially neutralizes the charge on this ring that develops during the transition state. The nitrogen atom of the substrate then attracts the proton stored by the histidine-aspartate couple of this network and, as a result, the susceptible peptide bond is cleaved. At this stage, the acid component of the substrate is esterified to Ser-195, and the amine component is hydrogen bonded to His-57. This ends the acylation stage of the hydrolytic reaction [2].

The following step is deacylation (Figure 6), which is essentially the reverse of acylation. In the active site, a water molecule replaces the amine component of the substrate, which diffuses away. A proton from the water molecule is attracted by the charge relay network and the resulting OH^- ion simultaneously attacks the carbonyl carbon atom of the acyl group attached to Ser-195. His-57 then donates a proton to the oxygen atom of Ser-195, which leads to the release of the acid component of the substrate. The

acid component diffuses away and this terminates the deacylation stage, and makes the enzyme ready for another round of catalysis [2,3].

C. Computer Modeling Applications for Chemists

Computer modeling of compounds combines calculation of geometries, conformational energies, charge densities, and electrostatic potential contour maps with graphical display of the results. It gives chemists a sense of the physical properties of a compound without having to hold a molecular model of the molecule in hand. With the facility of high resolution graphics terminals interfaced to a high speed computer, color and shading in a visual presentation of the structure can highlight surface area, particular atoms or bonds, or some other feature of interest to the chemist. Software packages for molecular modeling, which are commercially available, can be used to search for correlations among molecules with common biological activity. Thus a number of artificial enzymes have been modeled on computers using such techniques as molecular mechanics to study the conformational and electrostatic properties of the biomimetic catalyst. For example, Venanzi and coworkers have used computer modeling to study the biological activity of drugs and artificial enzymes: (1) Molecular mechanics calculations were used to investigate the degree of structural preorganization and electrostatic complementarity for substrate binding exhibited by cyclic urea mimics of alpha-chymotrypsin [12]. (2) Molecular

mechanics calculations were used to calculate the conformational properties of a cyclic urea mimic of alpha-chymotrypsin proposed, but not yet synthesized, by Cram and co-workers [13,14]. (3) Quantum mechanical calculations as well as molecular mechanics calculations were used to elucidate the structures and define the conformations, the rigidity of the phenyl ring arrangement, and the structural determinants for the recognition of phencyclidine derivatives at muscarinic cholinergic receptors [15].

D. Functionalized Norbornane as a Model of an Acyl-Enzyme Intermediate

Three analogues of norbornane were designed and synthesized by Bender and coworkers [5,9] as model systems with which to explore intramolecular general base catalysis by the imidazolyl group [5]. The goal of the work was to produce a model of the acyl-enzyme intermediate which would rival chymotrypsin in the rate of the deacylation step (Figure 6). Structure 1, endo - 5 - [4'(5') -imidazolyl] bicyclo [2.2.1] - hept - endo - 2 - yl trans - cinnamate, is shown in Figure 7. The molecule has a rigid structure with the imidazolyl and esterified hydroxyl groups disposed in an orientation similar to the His-57 and Ser-195 in the serine protease, alpha-chymotrypsin. Thus structure 1 is a model of the acyl-enzyme, since catalysis by serine proteases also involves general base catalysis by the imidazolyl group of a

histidine residue [4,5]. Structure 2, exo - 5 - [4'(5') - imidazolyl] bicyclo [2.2.1] - hept - endo - 3 - yl trans-cinnamate, is shown in Figure 8. Bender found that only the imidazolyl group in the endo, endo compound, structure 1 (Figure 7), but not in the exo, endo compound, structure 2 (Figure 8), participated in the hydrolysis of the ester linkage across the bicyclic ring system. This is because the imidazolyl group in structure 2 is far from the trans-cinnamoyl ester group [5]. The rate constant for the intramolecular general base-catalyzed hydrolysis by the imidazolyl group of structure 1 is much smaller than for the deacylation (hydrolysis) of the acyl-enzyme, trans-cinnamoyl-chymotrypsin.

In addition, Figure 9 shows the structure of endo, endo - 5 - [2 - (2 - carboxylphenyl) - 4 - (5) - imidazolyl] bicyclo [2.2.1] -hept - endo - 2 - yl trans-cinnamate, structure 3. This molecule is similar to structure 1, with the addition of carboxylate ion which models the Asp-102 residue of chymotrypsin. Bender has shown [5] that the rate of catalysis by structure 3 is only 4-fold smaller than the enzymatic deacylation rate, indicating that structure 3 is a good model of the acyl-enzyme intermediate in the reaction mechanism of chymotrypsin.

Experimentally, structure 3 is synthesized by: (1) converting the endo, endo-5-acetyl-2-hydroxybicyclo-[2.2.1]heptane to endo, endo-5-(bromo-acetyl)-2-hydroxybicyclo[2.2.1]heptane; (2) condensing the product from (1) with 2-bromobenzamidine to the corresponding

imidazolyl derivative; (3) carboxylating the 2-bromophenylimidazole to give the corresponding carboxylate ion; and (4) cinnamoylating the hydroxyl group on the norbornane ring. The synthesis of this molecule is shown in Figure 10 [5].

E. Goals of the Present Research

We have studied the conformational properties of the functionalized norbornane mimic, structure 3, using the computational procedures described below. The study was undertaken in order to determine: (1) the structural flexibility and relative positions of the esterified hydroxyl oxygen, imidazolyl group, and carboxyl oxygens of the norbornane mimic; (2) the spatial orientation of the esterified hydroxyl oxygen, imidazolyl group, and carboxylate oxygens on the norbornane mimic compared to that of the similar functional groups in chymotrypsin; and (3) the molecular recognition pattern of the norbornane mimic as defined by the molecular electrostatic potential contour maps.

The goal of the research, then, is to attempt to understand the catalytic activity of the acyl-enzyme model through comparison of the steric and electrostatic features of molecular recognition exhibited by the enzyme and the mimic.

II. METHODOLOGY

A. Conformational Analysis

The AMBER [Assisted Model Building with Energy Refinement] [16] program was used to perform the conformational analysis of the functionalized norbornane mimic. The Amber force field has been developed by Kollman and coworkers [17] to treat small molecules, as well as proteins and nucleic acids. It is related to the Karplus-Gelin [18] force field for macromolecules and the Allinger [19] force field for small molecules. Amber approximates the conformational energy of a molecule as the sum of bond stretching, angle bending, torsional, nonbonded, and hydrogen bond interactions. The potential energy function is given as a sum of strain energies and non-bonded interaction terms represented by:

$$\begin{aligned} E = & \sum_{\text{bonds}} K_r (r - r_{eq})^2 \\ & + \sum_{\text{angles}} K_\theta (\theta - \theta_{eq})^2 \\ & + \sum_{\text{dihedrals}} V_n [1 + \cos(n\phi - \gamma_n)] / 2 \\ & + \sum_{i < j} [A_{ij} / R_{ij}^{12} - B_{ij} / R_{ij}^6 \\ & + q_i q_j / (\epsilon R_{ij})] \end{aligned}$$

$$+ \sum_{\text{H-bonds}} [C_{ij} / R_{ij}^{12} - D_{ij} / R_{ij}^{10}]. \quad (1)$$

The first three terms represent the difference in energy between a geometry in which the bond lengths, bond angles, and dihedral angles have ideal values and the actual geometry [17]. The remaining terms represent non-bonded van der Waals, electrostatic, and hydrogen bonded interactions, respectively. In Equation (1), r represents the bond length, θ the bond angle, ϕ the dihedral angle, R_{ij} the distance between any two atoms i and j , q_i the charge on atom i , and ϵ , the dielectric constant. ϵ is generally chosen as 1.0, but can be made distance dependent ($\epsilon = R_{ij}$) in order to simulate the effect of solvent medium. The distance dependent dielectric damps the effect of the long range interactions, thus increasing the effect of short range interactions and simulating the effect of solvent polarization.

The force field parameters are r_{eq} (the equilibrium bond length), K_r (the bond stretching constant), θ_{eq} (the equilibrium bond angle), K_θ (bond angle bending constant), γ_n (the torsional angle phase factor), V_n (the torsional angle constant), A_{ij} and B_{ij} (the nonbonded parameters), and C_{ij} and D_{ij} (the hydrogen bond parameters).

In order to extensively probe the conformational potential energy surface of the molecule (built as described in Section C), it was necessary to generate a number of different starting conformations to use as input to the

molecular mechanics energy minimization routine. This work was accomplished using the Chemgraf/Chem-X [20] "Set Torsion" command (see Appendix 1) to successively increment the torsional angles. Thus the starting structures differed in the values of the four dihedral angles: alpha (O10-C9-C11-O12), beta (C17-C18-C19-N23), gamma (C25-C30-C31-O32), and delta (N21-C24-C25-C30), as shown in Figure 11A.

For example, in the first set of starting conformations designed to probe the dependence of the conformational energy on alpha angle variation, the four dihedral angles and their values measured in degrees were : alpha (O10-C9-C11-O12): 62.22; beta (C17-C18-C19-N23): 30.23; gamma (C25-C30-C31-O32): 269.0; and delta (N21-C24-C25-C30): 0.0. For each of the successive starting conformations, the dihedral angle alpha was incremented by 30 degrees, keeping the other angles fixed at the above values. Every increment produced a new input conformation for energy minimization. These eleven starting conformations corresponded to variations in alpha from 2.21 to 300.3 degrees. The region from 330 to 20 was investigated in detail in a separate set of minimizations described below. The four dihedral angles of every starting and minimized conformation were measured using the "Calculate Geometry" command of Chemgraf/Chem-X (see Appendix 2).

The optimized value of alpha was identified as the value which corresponded to the energy minimum for rotation around the torsional angle alpha. The values of alpha (356.63), beta (76.45), gamma (218.59), and delta (321.2) that

corresponded to this minimum were used as the starting point for probing the dependence of the conformational energy on beta variation. The values of alpha, delta, and gamma were fixed while beta was incremented by 30 degrees. This procedure constructed eleven new starting conformations which probed the entire 360 degree region around the starting value of beta. Again, the optimized value of beta was identified as the value which corresponded to the energy minimum for rotation around the torsional angle beta. However, it was discovered that all the eleven new starting conformations minimized to give values of the energy higher than the optimized alpha conformation. So this conformation (alpha = 356.63, beta = 76.45, gamma = 218.59, and delta = 321.2) was used to probe the gamma dependence of the conformational energy. Alpha, beta, and delta were fixed at the above values, while gamma was incremented by 30 degrees to probe the entire 360 degree range. The dihedral angles which corresponded to the optimized value of gamma were alpha = 357.98, beta = 67.01, gamma = 216.32 and delta = 324.4.

However, when we finished the minimizations around the three angles alpha, beta, and gamma, we found that the conformational energy was not significantly affected by changes in beta and gamma. Rather the optimized conformational energy varied sharply with alpha angle rotation from -22 to 68 degrees. Thus we decided to use the optimized values of beta = 67.01 and gamma = 216.32 degrees obtained from the gamma angle optimization as input to "fine

tune" minimizations around the alpha angle. In this set of minimizations, alpha was incremented by 10 degrees, starting from -22 to 68 degrees. The optimized structure from this procedure (with alpha = 356.61, beta = 61.29, gamma = 215.70, and delta = 320.7) was chosen as the starting conformation for the delta optimization. Delta was incremented by 30 degrees to probe the entire 360 range.

In total, 54 different points on the conformational potential energy surface were evaluated by this procedure. The tables of initial and optimized angles, as well as conformational energy will be discussed in the Results Section (see Sections III A and B).

In the above cases of the energy minimization, the calculations were performed for the different starting structures at constant values of the NB and EEL (i.e. 1-4 Non-bonded and 1-4 electrostatic) scaling factors, that is, NB=EEL=1.0. In order to study how the NB and EEL scaling factors affected the structural geometry as well as the conformational energy of the enzyme mimic, the energy minimization was performed for the same starting structure using different values of the NB and EEL scaling factors. The starting structure used for the scaling factor study was the structure corresponding the global energy minimum (obtained in the above cases at constant NB=EEL=1.0). The range of values for NB and EEL were 0.5, 1.0, 1.5, and 2.0. For example, for EEL = 0.5, NB ranged from 0.5 to 2.0, and so on. The results of the scaling factor study will be discussed in the Results Section (see Sections III A and B).

B. Distance Analysis

The functionalized norbornane mimic is intended to be a model of the acyl-enzyme intermediate in the chymotrypsin hydrolysis mechanism. We, therefore, wished to compare the relative distances between the Ser-like, His-like, and Asp-like functional groups in the mimic to the same distances in the X-ray structure of the enzyme [10]. Using the "Calculate Geometry" command (see Appendix 2), we measured the distances from the imidazolyl nitrogen N23 to the ester oxygens O10 and O11, and the distances from the imidazolyl hydrogen H22 to the carboxylate oxygens O32 and O33 (see Figure 11A), for each of the optimized conformations of the mimic.

The distances will be compared to those between the catalytic functional groups in the active site of chymotrypsin in the Results Section (Section III E). In addition, the variation of the distances with conformational energy will be discussed. For a description of these comparisons, see Section F, Structural Superposition.

C. Model Building

Computer graphics modeling was used to construct the basic structural template of the mimic. Since there was no X-ray crystal structure of the complete norbornane acyl-enzyme mimic, the initial structure was built by connecting the trans-cinnamate, endo-bicyclo-2-heptane, and imidbenzoate fragments, using the bond-making facility of

Chemgraf [20]. The structures of the trans-cinnamate and imidbenzoate were obtained from the MNDO (Modified Neglected of Diatomic Overlap) [21a] geometry optimization of trans-cinnamate and imidbenzoate, respectively, using the MOPAC program [21b]. The bicyclo heptane portion was obtained from the X-ray crystal structure of [endo-bicyclo, 2-(hydroxymethyl)-6-(methylsulfinyl)-bicyclo(2,2,1) heptane] in the Cambridge Crystallographic Database [22a].

The fragments were attached, as shown in Figure 11, by: (1) deleting the hydrogen of the hydroxyl group on the trans-cinnamate and the hydroxymethyl and methylsulfinyl groups on endo-bicyclo, 2-(hydroxymethyl)-6-(methylsulfinyl)-bicyclo(2,2,1) heptane; (2) connecting the hydroxyl oxygen O11 on the trans-cinnamate to the carbon C12 on the endo-bicyclo-heptane; and (3) forming the bond between the carbon C18 of the norbornane portion and the carbon C19 the imidbenzoate group, using the bond breaking/making facility of Chemgraf/modify.

The "Fly/Modify" facility of Chemgraf/Chem-X was used to delete all the hydrogens, except the H22 on nitrogen N21 which could participate in hydrogen bonding interactions. This was necessary because the Amber "united atom" force field was to be used for the conformational analysis. In the united atom approximation, the hydrogen atoms on the aliphatic and aromatic carbons are not treated explicitly. The force field parameters and atomic point charges are derived for the group (such as -CH₃) as a unit.

The molecular modeling was accomplished on an Advanced

Electronics Design 767 (AED 767) color raster graphics terminal interfaced to a DEC VAX 11/750 - 11/785 cluster.

D. Force Field Parameters

The Amber force field has been parameterized by Kollman and coworkers [17] to treat small molecules, as well as proteins and nucleic acids. It has been used by Kollman and coworkers for conformational analysis of crown ether compounds [23] and anisole spherands [24], and by Venanzi and Bunce [12,13,14] for conformational analysis of the cyclic urea mimics of chymotrypsin. Therefore, the database contained most of the bond stretching, angle bending, and torsional parameters needed to describe the norbornane mimic. However, additional parameters were needed chiefly to describe the bonds and angles found at points of connection between the major structural fragments of the norbornane mimic: C9-O11 (trans-cinnamaldehyde portion), C18 (norbornane) - C19 (imidazole), C24 (imidazole) - C25 (benzoate), and C30 (benzoate) - C31 (benzoate), as shown in the Figure 11A. Figure 11B shows the structure of the norbornane mimic with each of the atoms labeled according to the Amber atom types [17] described in Table 1. The chemical environment of each of the atom types is illustrated in Chart 1, which accompanies Table 1. The atom type assignment was made by choosing from the list in Table 1 the atom type which most closely described the chemical environment of each atom in the mimic. Since the

list was derived to describe atoms in proteins and nucleic acids, assignment of similar atom types to the mimic resulted in a situation in which unusual combinations of atoms (that is, combinations not found in the protein or nucleic acid) occurred. For this reason, additional force field parameters were required to describe the new combinations.

The additional parameters were obtained by the Kollman protocol [17] and are summarized in Table 2. The approximations involved in the definition of these parameters is described below.

1. Bond Stretching Parameters

It was necessary to determine the stretching force constants for the following bonds which were unavailable in the parameter file, namely: C-OS, CH-CC, and CC-CA (see Table 2A). These were computed from the existing database by judicious comparison of atoms in similar chemical environments. For the bond type C-OS, four similar sets of parameters were found in the database:

Type	K_r (Kcal/mol A ²)	r_{eq} (A)
C-OH	450.0	1.364
C2-OH	386.0	1.425
C2-OS	320.0	1.425
C3-OS	320.0	1.425

As seen in Table 1, the C atom type is an sp² carbonyl

or aromatic carbon with a hydroxyl substituent. C2 and C3 are sp^3 carbons with two and three hydrogens, respectively. OH is a hydroxyl oxygen, while OS is an ether or ester oxygen. Since r_{eq} for C2-OH is the same as for C2-OS (1.425 A), the r_{eq} for C-OS was chosen to be the same as that for C-OH (1.364 A). We used the data for K_r for C2-OH and C2-OS, as well as C-OH, to interpolate a value for C-OS, as shown below:

$$\begin{aligned}\Delta K_r(C2) &= K_r(C2-OH) - K_r(C2-OS) \\ &= 386 - 320 = 66\end{aligned}$$

$$\text{Inc (C2)} = \frac{\Delta K_r(C2)}{K_r(C2-OH)} = \frac{66}{386} = 0.17$$

Assume $\text{Inc (C2)} = \text{Inc (C)}$, where $\text{Inc} = \text{Increment}$.

$$\text{So, } \Delta K_r(C) = \text{Inc (C)} \times K_r(C-OH) = 0.17 \times 450 = 76.$$

$$\text{So, } K_r(C-OS) = K_r(C-OH) - \Delta K_r(C) = 450 - 76 = 374.$$

Since C2 and CH are both sp^3 carbons with similar chemical environments (one or two hydrogen substituents), the parameters for CH-CC were assumed to be the same as for C2-CC ($K_r = 317.0 \text{ Kcal/mol A}^2$, $r_{eq} = 1.504 \text{ A}$).

The K_r and r_{eq} for the bond type CC-CA was obtained from the recent Kollman study on anisole spherands since the CC-CA bond is similar in type to the $C_{(sp^2)}-C_{(sp^2)}$ bond used in that work [24].

2. Angle Bending Parameters

The values of the additional angle parameters required for the calculation are given in Table 2B. The assignment of the parameters for these angle types is mainly based on the comparison of the hybridized state of different atom types involved in these angles and those found in the parameter database. Thus, the set of CA-CA-CD, CC-CA-CA, CC-CA-CD, CD-CA-C, and CD-CA-CJ are all angle bending terms associated with the phenyl group (see Figure 11B). The CA-CA-CD angle is found within the benzene ring; the CC-CA-CA and CC-CA-CD parameters refer to the angle formed by the CC atom of the imidazole and either the CA-CA or the CA-CD bonds of on the benzene ring. The CD-CA-C angle is formed by the CD and CA atoms on the benzene ring and the C atom of the carboxylate substituent. The CA atom type refers to an sp^2 aromatic carbon with one substituent in a six-membered ring. The CD atom type is similar. It refers to an sp^2 aromatic carbon with one hydrogen substituent in a six-membered ring. Therefore, the CA-CA-CD parameters were set equal to those of CD-CA-CD and CA-CA-CA in the database: $K_{\theta} = 85.0 \text{ Kcal/mol deg}^{-2}$ and $\theta_{eq} = 120.0 \text{ degrees}$.

The CC-CA-CA and CC-CA-CD angle bending parameters were approximated by the CD-CA-CD and CA-CA-CA parameters, $K_{\theta} = 85.0 \text{ Kcal/mol deg}^{-2}$ and $\theta_{eq} = 120.0 \text{ degrees}$. Although the CC atom type (sp^2 aromatic carbon in five-membered ring with one substituent and found next to a nitrogen) is different from that of CA and CD, which are found in six-membered

rings, this difference was deemed not to be significant to the choice of the CC-CA-CA and CC-CA-CD angle bending parameters. This is because the CC is in the end position, rather than the central position. In all four cases (CC-CA-CA, CC-CA-CD, CD-CA-CD, and CA-CA-CA), the central carbon atom is a CA type. The hybridization state and chemical environment of the central atom are the chief factors which determined the values of the angle bending parameters.

By the same reasoning, the CD-CA-C and CD-CA-CJ angle bending parameters were set equal to $K_{\theta} = 85.0$ Kcal/mol deg^{-2} and $\theta_{\text{eq}} = 120.0$ degrees.

The angle CJ-C-OS refers to the trans-cinnamic acid portion of the molecule. The CJ atom type is similar to the CM atom type. Both are sp^2 carbons in pyrimidines exhibiting more double bond than aromatic character. CJ has one hydrogen substituent, while CM has one non-hydrogen substituent. The OS atom type indicates an ether or ester oxygen. The Amber database contained the CM-C-O and CJ-C-O angle bending parameters ($K_{\theta} = 80.0$ Kcal/mol deg^{-2} , $\theta_{\text{eq}} = 125.3$ degrees), where O is a carbonyl oxygen, and the CD-C-OH parameters ($K_{\theta} = 70.0$ Kcal/mol deg^{-2} , $\theta_{\text{eq}} = 120.0$ degrees), where OH is a hydroxyl oxygen. The X-ray crystal structure [22b] shows the bond of interest in trans-cinnamic acid to be 118.6 degrees. The CJ-C-OS parameters were approximated by $K_{\theta} = 80.0$ Kcal/mol deg^{-2} and $\theta_{\text{eq}} = 120.0$ degrees.

The angle bending parameters for $\text{C}_{(\text{sp}^2)}-\text{OS}_{(\text{sp}^3)}-\text{CH}_{(\text{sp}^3)}$ were assumed to be identical to the parameters for $\text{C}_{(\text{sp}^2)}-$

O(sp³) -C(sp³) and were obtained from Kollman's study of anisole spherands [24].

The angle bending parameters for O(sp²)-C(sp²)-O(sp³) were assumed to be equivalent to the O(sp²)-C(sp²)-O(sp³) parameters available in the database.

The bond angle bending terms for C2-CH-C2, C2-CH-CC, and CH-CH-CC were all assumed to be similar because the central carbon atoms all have the same hybridization state, sp³, and a similar chemical environment. Parameter values for similar bond angle bending has been reported by Kollman [24]. They are CH-CH-C2, CH-CH-C3, and CH-CH-CH (K_θ = 63.0 Kcal/mol deg⁻², θ_{eq} = 111.5 degrees), CH-C2-CA (K_θ = 63.0 Kcal/mol deg⁻², θ_{eq} = 114.0 degrees, and CH-C2-CH (K_θ = 63.0 Kcal/mol deg⁻², θ_{eq} = 112.4 degrees). We assumed that the chemical environment of the CC atom type is close to that of CA, and that C2 is similar to CH. So for the CH-CH-CC and C2-CH-CC parameters, we used those of CH-C2-CA (K_θ = 63.0 Kcal/mol deg⁻², θ_{eq} = 114.0 degrees). For C2-CH-C2, we used the parameters of CH-CH-C2, since the C2 environment (sp³ carbon with 2 attached hydrogens) is similar to that of CH (sp³ carbon with one attached hydrogen).

Using the same reasoning, we approximated the angle bending parameters for CH-CC-CG and CH-CC-NB by the parameters for C2-CC-CG (K_θ = 70.0 Kcal/mol deg⁻², θ_{eq} = 129.05 degrees) and C2-CC-NB (K_θ = 70.0 Kcal/mol deg⁻², θ_{eq} = 121.05 degrees), respectively.

The CC-NB-CC, CG-NA-CC, and NA-CC-NB parameters

describe angle bending within the imidazole ring. The bond angle bending parameters for CC-NB-CC were determined by comparison with parameters for similar chemical environments found in the Amber database: CC-NB-CP ($K_{\theta} = 70.0$ Kcal/mol deg⁻², $\theta_{eq} = 105.3$ degrees), CB-NB-CE ($K_{\theta} = 70.0$ Kcal/mol deg⁻², $\theta_{eq} = 103.8$ degrees), and CF-NB-CP ($K_{\theta} = 70.0$ Kcal/mol deg⁻², $\theta_{eq} = 105.3$ degrees). In the above cases, the central atom is of type NB (sp² nitrogen with lone pairs in a five-membered ring). Atom types CC, CP, CB, CE, and CF all refer to sp² aromatic carbons. Since CC and CF are found in similar chemical environments (five-membered rings, next to a nitrogen), the Amber database uses the same parameters for CC-NB-CP and CF-NB-CP. Similarly, the CC and CP atom types are in a similar chemical environment (five-membered rings, next to a nitrogen). Since the value of angle bending parameters should chiefly be determined by the hybridization of the central atom, we felt justified by approximating the CC-NB-CC parameters with those of CC-NB-CP.

For a similar reason, we approximated the CG-NA-CC parameters with those of CG-NA-CP and CC-NA-CP ($K_{\theta} = 70.0$ Kcal/mol deg⁻², $\theta_{eq} = 107.5$ degrees).

Since the chemical environment and hybridization of CC is similar to that of CP and CR, we set the angle bending parameters of NA-CC-NB equal to those of NA-CP-NB and NA-CR-NB ($K_{\theta} = 70.0$ Kcal/mol deg⁻², $\theta_{eq} = 111.6$ degrees). The parameters for NA-CC-CA, where NA and CC are on the imidazole and CA is on the benzoate fragment, were obtained

by comparison with of NB-CC-C2 ($K_{\theta} = 70.0$ Kcal/mol deg⁻², $\theta_{eq} = 121.05$ degrees) and NA-CC-C2 ($K_{\theta} = 70.0$ Kcal/mol deg⁻², $\theta_{eq} = 122.2$ degrees). We assigned the value of $K_{\theta} = 70.0$ Kcal/mol deg⁻² from the above comparison. However, we took the value of $\theta_{eq} = 126.0$ degrees from our calculation of the optimized structure of imidbenzoate (see Section C of Methodology).

Similarly for NB-CC-CA (where NB and CC are on the imidazole and CA is on the benzoate fragment) were assigned the values of $K_{\theta} = 70.0$ Kcal/mol deg⁻² and $\theta_{eq} = 124.0$ degrees. The value of θ_{eq} was taken from the optimized structure of imidbenzoate.

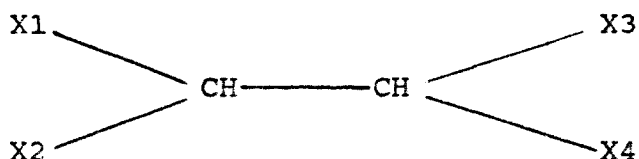
The parameters for CA-C-O2 (the carboxylate group) were approximated by those of CT-C-O2 ($K_{\theta} = 70.0$ Kcal/mol deg⁻², $\theta_{eq} = 117.0$ degrees) in the carboxylate group in Aspartate.

3. Torsional Parameters

The additional torsional parameters are summarized in Table 2C. A general torsional parameter is of the form X-Y_a-Y_b-X, where X can be any atom and Y_a and Y_b refer to specific carbon, nitrogen, or oxygen atom types. If the hybridization of the central atoms is X-Y_a(sp³)-Y_b(sp³)-X, the torsional function is often fit to a 3-fold potential barrier. If the hybridization is X-Y_a(sp²)-Y_b(sp²)-X, the function is often fit to a 2-fold torsional barrier. For hybridization X-Y_a(sp³)-Y_b(sp²)-X, the function is often fit to either a 2- or 3-fold barrier. For an n-fold torsional

barrier, the torsional parameter is $V_n/2$ with phase factor, γ_n , as shown Equation (1).

For example, the torsional angle X-CH-CH-X is of the type X-C(sp³)-C(sp³)-X, since the CH atom type is an sp³ carbon with one hydrogen. In the united atom force field, the CH group is taken as a unit. Therefore, the carbon atom has 2 "X"-type substituents and one "CH" substituent, as shown below:



Each torsional angle is made up of equal contributions from 4 bonds: X1-CH-CH-X3, X1-CH-CH-X4, X2-CH-CH-X3, and X2-CH-CH-X4. The phase factor γ_3 is determined so that the mathematical expression $V_3 [1 + \cos(3\phi - \gamma_3)]/2$ reproduces the known experimental torsional barrier of 2.0 Kcal/mol and the preferred conformational arrangement of staggered over eclipsed bonds. In this case, $V_3/2 = 2.0$ Kcal/mol and $\gamma_3 = 0$ degrees.

The dihedral angle parameters for CJ-C-OS-CH and O-C-OS-CH arise due to the rotation of ester linkage in the molecule. They belong to the general type of torsional angle parameter X-C-OS-X, where X = any atom. Parameters for a similar case, where an sp² aromatic carbon is bonded to ester oxygen in methyl anisole, were given by Kollman in a study of anisole spherands [24]. We used these parameters for CJ-C-OS-CH and O-C-OS-CH: $n = 2$, $V_n/2 = 5.0$ Kcal/mol,

and $\gamma_n = 180$.

The angle CH-CH-CC-CG and CH-CH-CC-NB are of the type X-CH-CC-X. The angle refers to the bond between the CH of the norbornane fragment and the CC of the imidazole. This is similar to the X-C2-CC-X torsional angle in the Amber database ($V_2/2 = 0.0$ Kcal/mol, $\gamma_2 = 0$ degrees). Because of the additional substituent on CH compared to C2, we used a 4-fold potential of the same barrier height ($V_4/2 = 0.0$ Kcal/mol, $\gamma_4 = 0$ degrees) for CH-CH-CC-CG and CH-CH-CC-NB.

The angles NA-CC-CA-CD, NA-CC-CA-CA, NB-CC-CA-CD, and NB-CC-CA-CA are of the type X-CC-CA-X, in which the bond is between the CC atom of the imidazole and the CA atom of the benzoate fragment. A 4-term torsional potential function for phenyl-imidazole rotation was derived by Venanzi and Rance [13] in their study of cyclic urea mimics of chymotrypsin. The form of the potential function for the phenyl-imidazole dihedral angle was:

$$\sum_{i=1}^4 V_i/2 (1 + \cos(n_i\phi - \gamma_i)) \quad (2)$$

The values of $V_1 - V_4$ and $\gamma_1 - \gamma_4$ are given in Table 2C. The values in Table 2C result from a fit to 9 data points; whereas parameters for the fit to 8 data points were presented in that work [13].

Finally, although the X-CA-CJ-X angle parameters were given in the Amber database, the chemical environment of the atom types as defined Kollman was different than that of the norbornane mimic. In Kollman's definition [17], CA and CJ

form an endo-bicyclic bond within a ring, as in cytosine (Chart 1A of Table 1). Therefore, Kollman used a rather large value for the X-CA-CJ-X $V_2/2$ parameter ($V_2/2 = 3.7$ Kcal/mol). In the case of the mimic, CA is in a benzene ring and CJ is external to the ring, in the trans-cinnamate fragment. The chemical environment is similar to that of the compound styrene [25]. In order to allow greater freedom of rotation around the X-CA-CJ-X angle, we used a lower value of the $V_2/2$ term than found in the database (see Table 2C).

E. Atomic Point Charges

The atomic point charges for the norbornane mimic used in the Amber force field were chosen as the "potential derived" charges obtained from an STO-3G basis set calculation on the trans-cinnamate, endo-bicyclo-heptane, and the imidbenzoate fragments. The calculations were carried out using the GAUSSIAN 80 UCSF software package [26].

A Gaussian basis set supports four types of shells: s-shells, p-shells, d-shells, and sp-shells. A shell is a set of basis functions (φ_μ) with shared exponents. An s-shell contains a single s-type basis function, while an sp-shell contains four basis functions with common gaussian exponents: one s-type function and three p-functions p_x , p_y , and p_z . A single basis function is generally comprised of more than one primitive gaussian function. Therefore, the equation representing a basis function ($\varphi_\mu(r)$) for an s-

type function, may be of the form:

$$\rho_{\mu}(r) = \sum_{i=1}^N d_{i\mu} \exp(-\alpha_i f^2 r^2) \quad (3)$$

in which N, the degree of contraction, is the number of primitive functions comprising the basis function; $d_{i\mu}$ are the contraction coefficients; $\{\alpha_i\}$ are the exponents; and f is the scale factor for the basis function. The STO-3G basis on any first row atom (Li \rightarrow Ne) consists of only 2 shells. An s-shell consisting of a set of 3 primitive gaussian functions least-squares fitted to a Slater 1s orbital with an appropriate scale factor. The other is an sp-shell that is obtained by a least-squares fit of 3 Gaussians to Slater 2s and 2p orbitals with the constraint that the s and p functions have equal exponents [26].

Potential derived charges were calculated in the united atom approximation for each of the molecular fragments of the mimic: trans-cinnamaldehyde, endo-bicyclo-heptane, and imidbenzoate. In this procedure the heavy (non-hydrogen) atom charges were fit in order to effectively reproduce the electrostatic potential calculated on the surface of the molecule. The charges approximated in this fashion are known as "potential-derived" point charges.

F. Structural Superposition

In order to investigate the degree of structural difference between molecules of different conformational

energy, structures with high conformational energy were compared to those of low conformational energy. The comparison was made by superimposing one structure upon the other using the RMS (Root Mean Square) [27] fitting facility of Amber. In this procedure, a set of selected atoms of one molecule are superimposed on a set of selected atoms in a second molecule by a least-squares fitting algorithm. Differences in atomic positions in the superimposed structures highlight regions of significant conformational change.

For the norbornane mimic, we selected the atoms of the endo-bicyclo-heptane fragment (C12, C13, C14, C15, C16, C17; see Figure 11A) to be superimposed. The endo-bicyclo-heptane portion is rigid and is not significantly altered during the minimization. Therefore structural superposition of the rigid portion of each molecule highlights the orientation of any structural differences. In order to have a clear view of the superimposed structures on the graphics terminal, the optimized conformation corresponding to the global energy minimum was first oriented into a good orientation using the "Fly" command of Chemgraf/Chem-X. Then, each chosen structure of higher energy was separately fit to it by the RMS facility of Amber.

In order to investigate the effect of the choice of 1-4 nonbonded interaction scaling factors (NB and EEL) on conformation, structures minimized with different scaling factors were superimposed. In addition, the X-ray crystal

structure of the active site of the alpha-chymotrypsin in its native conformation [10] was retrieved from the Protein Data Bank [28] to compare to the optimized acyl-enzyme mimic. The chosen atoms of the active site of alpha-chymotrypsin and the optimized enzyme mimic were those corresponding to the catalytic triad: the imidazolyl ring, the carboxylate oxygens, and the hydroxyl oxygen.

G. Molecular Electrostatic Potential

The molecular electrostatic potential is a physical observable [29], measured by X-ray diffraction and scattering experiments. The calculation of the molecular electrostatic potential enables one to investigate the general pattern of the electrostatic interaction between the enzyme mimic and substrate via the use of two-dimensional or three-dimensional molecular electrostatic potential contour maps. The electrostatic interaction of a positive point charge with the static charge distribution of the molecule can be expressed by:

$$V(\vec{r}) = \sum_{\text{nuclei } A} (Z_A / |\vec{R}_A - \vec{r}|) - \int \rho(\vec{r}') d\vec{r}' / |\vec{r}' - \vec{r}| \quad (4)$$

where $V(\vec{r})$ is the electrostatic potential of the molecule at point \vec{r} , Z_A is the charge on nucleus A located at \vec{R}_A , and $\rho(\vec{r}')$ is the electron density distribution derived

from the quantum mechanical wave function. Since the calculation of the wave-function of such a large molecule as the norbornane mimic is outside the range of central processing memory for most present computers, it is desirable to approximate Equation (4). The electrostatic interaction of a positive point charge with the static charge distribution of the molecule modeled by point charges placed at the positions of the atomic nuclei can be approximated by the following:

$$V(\vec{r}) = \sum_{\text{nuclei } A} (Q_A / \left| \vec{R}_A - \vec{r} \right|) \quad (5)$$

where Q_A is the point charge of atom A, calculated as described in Section E.

For the 2-dimensional map, the enzyme mimic was oriented in the x-y plane with the "Set View/Plane" command (see Appendix 3) of Chemgraf/Chem-X. The "Set View" command orients the molecule with the x-y plane (at arbitrary z-value) passing through the selected atoms that define the plane. The atoms chosen to approximately define the same x-y plane were O10, O11, N21, and O32, since they have very similar z-coordinates and belong to the catalytic triad, as shown in Figure 11A. Then the "Manipulate" command was used to shift the entire molecule along the z-axis so that the x-y plane at $z = 0$ Å passed through the selected atoms.

The maps were produced in planes parallel to the plane containing the selected atoms. The "Set Dummy" command was used to produce a centroid with cartesian coordinates which

were the average of the x, y, and z positions of the selected atoms.

The "Set Map" command (see Appendix 4) calculates the 2-dimensional electrostatic potential contour map at the z-coordinate of a selected atom; in this case, the centroid. The map was calculated in different planes parallel to that containing the selected atoms, by first altering the z-coordinate of the centroid and then recalculating the map with the "Set Map" command.

The z-coordinate of the centroid was altered by the "Modify Geometry" command, which allows the user to define any new x, y, or z position. In this case, the z-coordinate of the centroid was changed at an increment of 2.0 Å along with the positive direction to 6.0 Å and at a decrement of 2.0 Å along with the negative direction to -6.0 Å. Thus seven 2-dimensional molecular electrostatic potential contour maps (i.e. z=0 Å, z=2 Å, z=4 Å, z=6 Å, z = -2 Å, z = -4 Å, and z=-6 Å x-y planes, respectively) were produced in this fashion.

Equi-energy curves of different values were used to indicate the different electrostatic potential energy levels around the molecule. The energy levels were calculated based on the unit of Kcal/mol. Through a series of "trial and error" tests, the levels of -200, -150, -100, and -50 Kcal/mol were chosen to show the electrostatic potential energy levels around the norbornane mimic. Without having to use the "Set View/Plane" and "Modify/Geometry"

commands, the 3-dimensional electrostatic potential contour maps were produced directly with the "Set Map/Contour" command of Chem-X (see Appendix 5). The potential energy levels were shown by the curvilinear planes of different values. The range used to indicate the energy levels was the same as that used in the 2-dimensional cases. Since these 3-dimensional plots do not reproduce well in black and white, none will be presented in the Results Section.

III. Results

A. Conformational Analysis

The results of the conformational analysis of the norbornane mimic are given in Tables 3A - 3E. The tables contain the values of the initial and the optimized alpha, beta, gamma, and delta dihedral angles, and the optimized energy for each run. The values of the dihedral angles in the optimized structure were obtained by using the "Calculate Geometry" command of Chemgraf/Chem-X (see Appendix 3).

In the tables, the symbol BabM indicates each of the different runs of the optimizations. The symbol B represents the norbornane mimic; symbol a, ranging from 1 to 5, indicates different sets of optimizations around the dihedral angles (i.e. 1 = alpha, 2 = beta, 3 = gamma, 4 = alpha, and 5 = delta, respectively); symbol b, ranging from 1 to 11 in each set of optimizations, indicates the different structures obtained by successive increment of the dihedral angles; and the symbol M means the minimized structure and energy. For example, for the run B34M (Table 3C), B is norbornane mimic, 3 refers to the set of gamma angle optimizations, 4 indicates that this structure was obtained from the fourth increment around the gamma dihedral angle (while other dihedral angles were kept constant), and M indicates the minimized structure and energy. Similarly, run B56M (Table 3E) means the minimized norbornane mimic obtained from the sixth increment around the delta dihedral

angle. Due to lack of space in the tables, files such as B10, B111, etc. are understood to refer to the minimized structure, even though an "M" is not explicitly given in the file name.

The general trends in the relationship between the initial and optimized dihedral angles, and the optimized energy, are as follows:

(1) Optimization of the alpha dihedral angle (Table 3A) shows that the optimized values of the alpha angle tend to be one of two values, depending on the choice of starting value. For an initial value in the range of 92.26 - 242.3 degrees, the optimized value of alpha is in the narrow range of 168 - 174 degrees, corresponding to an optimized energy of 37.00 to 42.68 Kcal/mol. For an initial value in the range of 272.3 - 62.22 degrees, alpha optimizes to 353.85 - 0.68 degrees, with energy ranging from 34.08 to 42.30 Kcal/mol. This behavior indicates the presence of two local minima with respect to alpha angle rotation. The wide range of optimized energy values suggests the possible existence of other local minima. We, therefore, studied the region from 328.0 to 68.2 degrees in smaller alpha angle increments. The results are given in Table 3D and are discussed in item (4) below.

In the alpha angle rotations (Table 3A), the optimized value of beta falls within the range of 59.18 to 85.47 degrees from a starting value of 30 degrees. Gamma optimizes to 207.58 - 222.61 degrees from an initial value

of 269 degrees, and delta gives 315.0 to 329.4 degrees from a starting value of zero degrees. The optimized conformation which corresponds to the global energy minimum for the alpha angle rotation is run B11M, with optimized values of alpha = 356.63, beta = 76.45, gamma = 218.59, and delta = 321.2 degrees, and optimized energy = 34.08 Kcal/mol.

(2) Optimization of the beta dihedral angle (Table 3B) shows that the optimized values of beta range from 28.94 to 353.9 degrees, with the optimized value of beta being close to the initial value. The final values of alpha tend to be consistently in the range of 355.66 to 358.01 degrees, indicating that the starting value of 356.6 degrees for alpha was close to the minimum value. Gamma optimized to 209.36 - 218.58 from a starting value of 218 degrees, and delta optimized to 310.6 - 321.8 degrees from a starting value of 321 degrees. There is no significant change in the optimized energy with rotation around the beta angle. The energy of the mimic is 37 - 38 Kcal/mol for optimized beta in the range of 136.6 - 353.9 degrees. The energy decreases from 37.09 Kcal/mol at 353.9 degrees to 34.07 Kcal/mol at 76.45 degrees, increasing to 35.53 Kcal/mol at 91.00 degrees.

Since the energy is approximately constant over a large range of final beta values, the energy does not appear to be sensitive to the choice of beta. Since for each run, the initial value of beta is close to the optimized value, there do not appear to be any steep potential energy minima with respect to rotation around beta. The optimized conformation

which corresponds to the global energy minimum is run B21M, with optimized values of the dihedral angles: alpha = 356.64, beta = 76.45, gamma = 218.58, and delta = 321.2 degrees, and optimized energy = 34.07 Kcal/mol. The optimized conformation obtained from B21M is basically the same as that of B11M.

(3) Optimization of the gamma dihedral angle (Table 3C) shows that the final values of alpha tend to be in a range from 354.64 to 359.49 degrees, very close to the starting value of 356 degrees. The final value of beta ranges from 64.46 to 78.02 degrees, close to the starting value of 76.4 degrees. The final value of delta ranges from 315.0 to 328.0 degrees, close to the starting value of 321 degrees.

The optimization of gamma exhibits two local minima of approximately equal energy. Table 3C shows that starting values for gamma from 308.6 - 98.6 degrees tend to minimize to a value of 24 - 31 degrees, at an optimized energy of 33 - 34 Kcal/mol. On the other hand, starting values of gamma from 128.6 to 278.6 degrees tend to optimize to a final value of 200 - 218 degrees with energy of 33 - 34 Kcal/mol. This indicates the presence of two rather steep potential energy wells of approximately equal depth related to the value of gamma.

The optimized conformation which corresponds to the global energy minimum in this set is run B311, having optimized values of the dihedral angles: alpha = 357.98,

beta = 67.01, gamma = 216.32, and delta = 324.4 degrees, and optimized energy = 33.37 Kcal/mol.

(4) The results of "fine tuning" the optimization of the alpha angle are shown in Table 3D. Starting values of alpha in the range of 328.0 to 48.0 degrees all minimize to an alpha equal to approximately 357 - 360 degrees and an energy of 32 - 36 Kcal/mol. The final values of beta, gamma, and delta are consistently close to the starting values. The "fine tuning" procedure has uncovered a new energy minimum with respect to alpha rotation. The optimized conformation which corresponds to the global energy minimum is run B410, with optimized values of the dihedral angles: alpha = 356.61, beta = 61.29, gamma = 215.70, and delta = 320.7 degrees, and optimized energy = 32.12 Kcal/mol.

(5) The optimization of the delta dihedral angle (Table 3E) shows that the final values of the alpha angle tend to be very close to the starting value of 356.7 degrees. The final values of beta and gamma tend to differ from the starting value. For example, the starting value of 61.28 degrees for beta results in the final values clustering around 60, 100, or 330 degrees. The starting value of 215.8 degrees for gamma results in final values around 214 or 150 degrees. Therefore, beta and gamma, but not alpha, are influenced by changes in delta.

Table 3E indicates the presence of two steep potential energy wells related to rotation around delta. For starting values of delta in the range 200.7 to 350.6 degrees, the

optimized values of delta cluster around 315 degrees, at energies of 32 - 35 Kcal/mol. For starting values in the range 20.7 - 170.7 degrees, the final values of delta range from 35 - 83 degrees, with energies of 35 - 42 Kcal/mol.

The optimized conformation which corresponds to the global energy minimum in this set is run B510, having the optimized values of alpha = 356.64, beta = 60.17, gamma = 214.93, and delta 319.19 degrees, and the optimized energy of 32.06 Kcal/mol.

(6) A general comparison of the optimized conformations of the norbornane mimic has shown that the conformations of lower conformational energy of around 33.00 Kcal/mol, such as B33M, B311, B41M, B49M, B410, B411, B51M, B510 and B511, have very similar values of the four dihedral angles. In other words, their structures are very similar.

(7) In addition, the conformational energy seems to be most sensitive to changes in the alpha and delta angles. This can be seen from the range of energies in Tables 3A, 3D, and 3E.

B. Energy Minimization

The results of the conformational energy minimization for the norbornane mimic are presented in Tables 4A through 4G. The total conformational energy (T.E.) is decomposed into contributions from bond stretching (BOND), angle bending (B.A.), torsional (DIH), van der Waals (VDW),

electrostatic (ELEC), hydrogen bonding (H-B), 1-4 van der Waals (1-4VDW), and 1-4 electrostatic (1-4EEL) terms. The data in Tables 4A - 4E correspond to those in Tables 3A - 3E. For example, Table 4A gives the total and component energies for the optimization of the alpha angle with the initial and optimized values given in Table 3A. As in Table 3A, the first column gives the file name, while columns 2 - 10 of Table 4A give the total and component energies. Tables 4F and 4G give the results of the energy minimization for the norbornane mimic using various values of the NB and EEL scaling factors which modify the 1-4 van der Waals and 1-4 electrostatic terms, respectively. Calculations were carried out using the same starting structure, B510, in each case. Column 1 of Tables 4F - 4G gives a letter which is related to the choice of the NB and EEL parameters in columns 11 and 12. Columns 2 - 9 contain the total and component conformational energies. The data in Table 4F is arranged to show the trends in conformational energy as a function of the NB parameter. The same data is rearranged in Table 4G to show the trends in conformational energy as a function of EEL.

The general trends observed for the final and component energies obtained from the optimization around the alpha, beta, gamma, and delta dihedral angles, at constant value of NB=EEL=1.0 (Table 4A - 4E), are as follows:

(1) Optimizations around the alpha (Tables 4A and 4D), beta (Table 4B), gamma (Table 4C), and delta (Table 4E) dihedral angles show that the total energy and the component

energies exhibit little fluctuation in value. The total energy ranges from 32.06 Kcal/mol (B510 of Table 4E) to 42.68 Kcal/mol (B16M of 4A). The component energies show similarly little variation. The bond stretching term is consistently around 2.5 - 2.7 Kcal/mol, the bond angle bending term is around 25 - 29 Kcal/mol, the dihedral term is around 13 - 16 Kcal/mol, the van der Waals term is -2 to -11 Kcal/mol, the electrostatic term is usually around -71 to -74 Kcal/mol, the hydrogen-bond term is close to 0 Kcal/mol, the 1-4 van der Waals term is 13 - 16 Kcal/mol, and the 1-4 electrostatic term is 56 - 59 Kcal/mol.

(2) The hydrogen-bond component contributes very little to the total energy. The van der Waals and the electrostatic terms have negative values, with the electrostatic term dominating the contribution to the total energy. The 1-4 electrostatic term makes the largest positive contribution to the total energy, followed by the bond angle bending term. The torsional and 1-4 van der Waals terms contribute positive values of equal weight to the total conformational energy. The bond stretching term contributes the least, next to the hydrogen-bond term, to the total energy.

(3) Generally, the conformations of lowest energy, such as B11M, B21M, B311, B410, B411, B51M, B510, and B511, have the largest negative values of either the van der Waals and/or the electrostatic component energies. This indicates that the range of the total energy is mainly determined by

the magnitude of the van der Waals and electrostatic interactions.

The final and component energies for the norbornane mimic, at constant EEL and varying NB, are given in Table 4F. The general trends are as follows: (1) There are decreasing trends in the total energy, bond stretching, bond angle bending, dihedral, and 1-4 van der Waals energies with the increasing values of the NB factor. The most significant change is in the 1-4 van der Waals term. This is not unexpected since scaling of the 1-4 van der Waals term involves multiplication of the term by the inverse of NB. (2) There is no significant variation in the values of the van der Waals, electrostatic, and hydrogen-bond component energies with changes in NB. (3) There is a significant decrease in the total energy with increase in EEL proceeding from one constant EEL group to another (i.e. EEL = 0.5 to EEL = 1.0, or EEL = 1.0 to EEL = 1.5), due to the decrease in the contribution from the 1-4 electrostatic component energy.

The same data are rearranged, at constant NB and varying EEL in Table 4G. The general trends are as follows: (1) In addition to the significant decrease in the total energy and 1-4 electrostatic energy with an increase in EEL, the bond stretching, bond angle bending, and electrostatic component energies also display a smoothly decreasing trend with increasing EEL factor. (2) However, unlike the case of increasing NB at constant EEL, the dihedral component energy shows an increasing trend with increasing EEL factor at constant NB. (3) The decreasing trends for the total energy

seems to be dominated by the decrease in the 1-4 electrostatic component energy in different groups of constant NB factors.

C. Distance Analysis

The results of the analysis of the distances between atoms of the catalytic functional groups in the norbornane mimic (see Figure 11A) are presented in Tables 5A through 5E. The tables contain the distances between the imidazolyl nitrogen N23 and the ester oxygen O11 (column 2) and O10 (column 3), and the imidazolyl hydrogen H22 to the carboxylate oxygens O33 (column 4) and O32 (column 5). The distance are all given in Angstrom units. The data in Tables 5A - 5E correspond to the results presented in Tables 3A - 3E and 4A - 4E. For example, Table 5A presents the distances between atoms of the catalytic functional groups in the structures obtained from rotation around the initial alpha angles listed in Table 3A, corresponding to the minimized energies in Table 4A.

The general trends are summarized below, with the maximum and minimum distances listed in Angstroms:

Set of Optimizations	Range of Distances			
	N23-O11	N23-O10	H22-O33	H22-O32
Alpha	3.149-4.250	4.097-5.205	3.510-3.684	1.684-1.706
Beta	3.149-5.143	4.877-6.909	3.646-3.772	1.684-1.714
Gamma	3.065-3.231	4.764-4.891	1.687-1.708 or 3.643-3.813	3.563-3.745 or 1.690-1.705
Alpha	3.059-3.450	3.218-4.895	3.642-3.771	1.690-1.711
Delta	3.017-4.252	4.754-6.119	3.729-4.692	1.687-2.702

In comparing the distances H22-O33 and H22-O32, it can be seen that there is always one hydrogen-oxygen distance which ranges around 1.69 A while the other is around 3.6 A. This indicates that there is a hydrogen bond between the imidazolyl hydrogen H22 and one of the carboxylate oxygens, O32 or O33. Geometrically, the hydrogen-bond serves in the role of fixing the orientation of the imidazolyl ring toward the two carboxylate oxygens (see Figure 11A). This is similar to the structure of the catalytic site in chymotrypsin where the nitrogen of His-57 is within 3 - 4 A of one of the carboxylate oxygens of Asp-102 [10]. The distance N23-O11 appears to fall in the range of 3 - 4 A. This corresponds to the active site of chymotrypsin in which the other nitrogen of His-57 is within 3 - 4 A of the oxygen of Ser-195.

D. Structural Superposition

The results of structural superposition are presented in Figures 12 through 17 for conformations calculated at NB=EEL=1.0, and Figures 18 through 21 for conformations calculated with various values of NB and EEL. In those figures, structure a, B510, is the optimized conformation corresponding to the global energy minimum at 32.06 Kcal/mol, and structure b is the optimized conformation of either: (1) higher energy, or (2) calculated by different values of the NB and EEL scaling factors. The maps illustrate the geometrical differences as well as the geometrical similarity between the optimized conformations of the norbornane mimic.

(1) In Figure 12, the superposition of B16M (the optimized conformation corresponding to the energy maximum for the rotation around the alpha angle; at 42.68 Kcal/mol) onto B510 shows that there is a very significant structural difference in the position of the trans-cinnamaldehyde fragment. This is because the optimization is performed only with respect to the alpha angle and, among all the optimized conformations, B16M is the one with the highest total conformational energy.

(2) In Figure 13, the superposition of B111 (the optimized conformation corresponding to the mid-range energy at 36.82 Kcal/mol for rotation around the alpha angle), onto B510 shows that the 5 Kcal difference in conformational energy corresponds mainly to a change in the trans-

cinnamaldehyde fragment.

(3) In Figure 14, the superposition of B24M (the optimized conformation corresponding to the energy maximum for the rotation around the beta angle; at 38.76 Kcal/mol) onto B510 shows that the 7 Kcal/mol energy difference is due to a reorientation of the imidbenzoate fragment.

(4) In Figure 15, the superposition of B38M (the optimized conformation corresponding to the energy maximum for the rotation around the gamma angle; at 34.43 Kcal/mol) onto B510 shows that the structural difference in the position of the trans-cinnamaldehyde fragment is not as significant as in Figure 13; the structural difference in the imidbenzoate fragment is almost the same as in Figure 13. Although B38M is the global energy maximum in the set of gamma optimizations, and it is expected that there should be some structural difference in the orientation of the carboxylate fragment, the results do not show a large structural deviation in the position of carboxylate. This can be explained because of the existence of the hydrogen-bond between the imidazolyl hydrogen H22 and one of the carboxylate oxygens, O32 or O33, as described above. The hydrogen-bond interaction "locks" one of the carboxylate oxygens into position near H22. As a result, the relative position of the imidazolyl ring and the benzoate ring is fixed. Thus, there is no large difference in the position of the carboxylate in the structural superposition of B38M onto B510.

(5) For the cases in Figure 16, the superposition of

B31M (the optimized conformation corresponding to the mid-range energy for the rotation around the gamma angle; at 34.07 Kcal/mol) onto B510, and in Figure 17, the superposition of B311 (the optimized conformation corresponding to the energy minimum for the rotation around the gamma angle; at 33.37 Kcal/mol) onto B510, the structural deviation is roughly the same. This is primarily because the two optimized conformations were obtained from the gamma angle optimization and the difference in their total conformational energies is not large (1 - 2 Kcal).

(6) By comparison of Figures 12 to 17, it can be seen that the larger the conformational energy of the optimized conformation, the larger the magnitude of the structural deviation in the trans-cinnamaldehyde fragment. In addition, the magnitude of the minimized energy also seems to affect the distance difference between the benzene ring on the trans-cinnamaldehyde and that of the benzoate.

(7) Figures 18 - 20 show the structural superposition of the optimized conformations calculated from the same starting structure with different values of the NB and EEL scaling factors. There is no significant difference in any of the figures. Figure 18 compares the optimized structure with NB = 1, EEL = 1, and energy = 32.12 Kcal/mol to that with NB = 0.5, EEL = 0.6, and energy 100.70 Kcal/mol. Although the difference in conformational energy between the two structures is approximately 70 Kcal/mol, the structures appear to be equivalent.

Figure 19 compares the structure with NB = 1, EEL = 1, and energy = 32.12 Kcal/mol to that with NB = 0.5, EEL = 2.0, and energy = 15.32 Kcal/mol. Although the energy difference between the two structures is much less than in Figure 18, the two figures appear similar.

Figure 20 compares the structure with NB = 1, EEL = 1, and energy = 32.12 Kcal/mol to that with NB = 2.0, EEL = 2.0, and energy = -5.27 Kcal/mol. The two structures exhibit little obvious difference.

Analysis of Figures 18 - 20 shows that, although the scaling factors alter the numerical value of the conformational energy, they have little effect on the optimized structure of the molecule. This indicates that the conformational potential energy minima are not particularly sensitive to the choice of scaling factors, if the same starting structure is used in each optimization. This is contrasted by Figures 12 - 17 which show the range of conformational potential energy minima for different starting structures with a single choice (NB = 1 = EEL) of scaling factors.

Quantitatively, Table 6 gives the results of the comparisons shown in Figures 12 - 17 (top table, 6A) and Figures 18 - 20 (bottom table, 6B). It contains the RMS deviation of the 6 atoms chosen to fit, the RMS deviation for all atoms, the mean deviation, the standard deviation, the maximum deviation, and the atom which displays the maximum difference in position. All the deviations shown for the 6 selected atoms in the fit are very small (about

0.01 Å), indicating that the endo-bicyclo-heptane ring is rigid and is not significantly altered during the minimization. The deviations are given in Angstroms. As shown in Figure 12, B16M has the largest value of the structural deviation, and also the largest energy difference compared to B510. Atom C3 (on the benzene ring of the trans-cinnamate fragment) shows the largest difference in atomic position (12.7 Å). B24M (Figure 14) has the second largest conformational energy difference among this set of RMS comparisons and also the second largest maximum atomic deviation (at C27). B111 (Figure 13) exhibits the third largest conformational energy difference when compared to B510 and the third largest maximum atomic deviation (3.4 Å at C4). The trend is continued by B38M (Figure 15), B31M (Figure 16), and B311 (Figure 17).

The deviation data (Table 6B) for the RMS comparison of optimized structures with different values of the NB and EEL scaling factors are not significantly different from Table 6A. The RMS deviations for the 6 atoms and for the all atoms are approximately the same order of magnitude as those in Table 6A.

In addition, the structural superposition of the optimized norbornane mimic on the active site of alpha-chymotrypsin is shown on Figure 21. The figure shows that the norbornane portion corresponding to the catalytic triad has a very similar geometrical orientation to that of the active site of alpha-chymotrypsin. The Ser-195 oxygen (OG)

is close to O11 of the mimic, the His-57 imidazolyl ring is near that of norbornane, and the Asp-102 oxygens are near to the two carboxylate oxygens of the mimic, although the carboxylate groups are pointing in different directions. The figure shows that the enzyme and the mimic have a similar spatial arrangement in their catalytic triads, indicating that the norbornane mimic may be a reasonable model of the acyl-derivative of chymotrypsin.

The results of the superposition of the catalytic functional groups in selected structures of the norbornane mimic on those of chymotrypsin are given in Table 7. In comparison with the distances in chymotrypsin (bottom row), all the data of the optimized conformations show that the range of deviation is within 1 Å of the enzyme values. In particular, the distances for B510, the global energy minimum structure, are very close to the distances in chymotrypsin: 4.4 Å for O32-N23 (mimic) compared to 4.6 Å for OD2-NE2 (enzyme); 2.6 Å for O32-N21 (mimic) versus 2.6 Å for OD2-ND1 (enzyme) for 5.8 Å for O33-N23 (mimic) versus 5.4 Å for OD1-NE2 (enzyme); 4.3 Å for O33-N21 (mimic) versus 3.3 Å for OD1-ND1 (enzyme); 3.1 Å for O11-N23 (mimic) versus 2.8 Å for OG-NE2 (enzyme); and 5.3 Å for O11-N21 (mimic) versus 4.7 Å for OG-ND1 (enzyme). In particular, the distances between the potential proton transfer partners are very similar: 2.6 Å (O32-N21) versus 2.6 Å (OD1-ND1) and 3.1 Å (O11-N23) versus 2.8 Å (OG-NE2).

The results of the structural superposition of B510 onto the active site of chymotrypsin are shown in Table 8.

As described in the Methodology Section, only the atoms of the catalytic functional groups were used in the fit. The distance between an atom of the mimic (Column 1) and the similar atom of the enzyme (Column 2) is given in Column 3. The table shows that the largest deviation in the spatial arrangement of the catalytic triads is 1.325 Å (O33 of mimic to OD1 of Asp-102) and the smallest deviation is 0.472 Å (N23 of the mimic to NE2 of His-57). Figure 21 and Table 7 indicate that neither OD1 nor O33 seem to be involved in the proton transfer mechanism. Therefore, the large deviation in their positions may not be significant.

The fact that the atoms of the mimic appear to be in the same position as those of the enzyme provides powerful evidence that the norbornane mimic has a catalytic triad similar in conformation to that of alpha-chymotrypsin.

E. Electrostatic Potential Contours

The general pattern of the two-dimensional molecular electrostatic potential contour maps of the optimized norbornane mimic are given in Figures 22 through 28. The 2-dimensional maps were calculated in the $z=0.0$ Å (Figure 22), $z=2.0$ Å (Figure 23), $z=4.0$ Å (Figure 24), $z=6.0$ Å (Figure 25), $z=-2.0$ Å (Figure 26), $z=-4.0$ Å (Figure 27), and $z=-6.0$ Å (Figure 28) x - y planes. The norbornane mimic was oriented so that the x - y ($z=0$) plane passed through the ester oxygen (O10), the histidine nitrogens (N21, N23) and the oxygen (O32) in the carboxylate group. The maps were calculated at

constant scaling factors of $NB=EEL=1.0$. The equi-energy curves were used to indicate the different molecular electrostatic potential energy levels around the enzyme mimic. The energy is represented by contours at levels of -200, -150, -100, and -50 Kcal/mol. Each map shows only negative contours, indicating that this enzyme mimic presents a negative electrostatic potential pattern. The maps also show a very negative potential energy region around the two carboxylate oxygens on the benzoate fragment, primarily due to the high negative charges on the two oxygens. The trends are as follows:

(1) In Figure 22, the electrostatic potential contour map was calculated in the x-y plane at $z = 0.0$ A. The map shows that there are -200 and -150 Kcal/mol equi-energy curves surrounding the carboxylate fragment, a -100 Kcal/mol curve around the benzoate and the imidazolyl groups, and a -50 Kcal/mol curve around the other portion of the molecule. The map shows that the carboxylate fragment presents the most negative area of the potential energy. This is similar to the pattern presented by the Asp-102 carboxylate group in the chymotrypsin [12].

(2) Figure 23, the map calculated in x-y plane at $z = 2.0$, shows that there is a -100 Kcal/mol curve surrounding the benzoate group and a -50 Kcal/mol curve surrounding the outer portion of the molecule. The general features of the map at $z=0$ A are preserved, in that the area around the carboxylate anion is the most negative region.

(3) Figure 24, the map calculated in the x-y plane at z

= 4.0 A, shows that there are -50 Kcal/mol curves surrounding the imidbenzoate and the trans-cinnamaldehyde groups. This figure is different from the previous ones in that the electrostatic potential pattern is nearly symmetrical.

(4) Figure 25, the map calculated in the x-y plane at $z = 6.0$ A, shows that there is a -50 Kcal/mol contour surrounding the benzoate group of the molecule.

(5) A similar trend in the potential energy pattern in the negative z-direction is shown in Figures 26 to 28. Comparison of Figures 22 - 25 and 26 - 28 shows how the electrostatic pattern of the molecule changes with distance. At a large distance ($z=6$ A, Figure 25, or $z=-6$ A, Figure 28), the pattern reveals few details. This is in contrast to Figure 22 ($z=0$ A) which shows the detailed pattern due to the individual atoms in the molecule.

Since the contours of the 3-dimensional electrostatic potential maps cannot be clearly indicated on a black-and-white hard copy, none of these maps will be presented. However, the maps are qualitatively consistent with the 2-dimensional ones.

IV. DISCUSSION AND CONCLUSION

The immediate goal of this research was to study the structural flexibility of the acyl-enzyme intermediate model and to determine how the orientation of the catalytic functional groups is related to the mimic's catalytic power. The results of the conformational analysis, energy minimization, and distance analysis have shown that the geometry of the norbornane mimic is directly related to the conformational energy. In particular, structures of high conformational energy have a poor arrangement of the catalytic functional groups, whereas structures of low conformational energy exhibit an orientation of the catalytic groups similar to that in chymotrypsin. We have shown that the geometry is particularly sensitive to changes in the alpha and delta angles. These two dihedral angles affect the position of the catalytic components: the esterified hydrogen O11 (alpha angle), and the imidazolyl nitrogen N21 and carboxylate oxygens O32 (delta angle). In particular, we have shown the existence of several steep potential energy wells associated with rotation around each of the dihedral angles except beta. This indicates that the molecule does not exhibit significant structural flexibility because many starting structures minimize to give the same conformation. A flexible molecule, in contrast, could have exhibited a different minimized conformation for each starting structure.

The intramolecular interaction that affects the

geometry of the optimized conformations and, therefore, the orientation of the catalytic functional groups, is the hydrogen bond between the imidazolyl hydrogen H22 and one of the carboxylate oxygens, O32 or O33. We have shown that the hydrogen bond tends to "lock" the imidazolyl ring in place next to the carboxylate fragment. That is, the relative position of the imidbenzoate group is determined by the formation of the hydrogen bond with the carboxylate.

In addition, the results of the RMS structural superposition have shown that the values of the NB and EEL scaling factors do not significantly affect the geometry, if the same starting structure is used for the calculations in which the parameters are varied. However, the magnitude of the final optimized energy was significantly affected by the values of NB or EEL.

In summary, the structural superposition of the mimic onto the active site of chymotrypsin has shown that the functional groups of the norbornane mimic have a spatial orientation similar to that of the catalytic triad in the active site of chymotrypsin. In addition, the general molecular recognition pattern of the norbornane mimic has been shown to be similar to that of chymotrypsin. Therefore, by probing the conformational energy surface and molecular properties of the mimic, we have uncovered structural and electrostatic features that could account for its excellent performance as an artificial enzyme.

TABLE 1

LIST OF AMBER ATOM TYPES^{a,b}

ATOM	TYPE
Carbons United ^c	
C2	sp ³ carbon with two hydrogens
C3	sp ³ carbon with three hydrogens
CD	sp ² aromatic carbon in six-membered ring with one hydrogen
CE	sp ² aromatic carbon in five-membered ring between two nitrogens with one hydrogen (in purines)
CF	sp ² aromatic carbon in five-membered ring next to a nitrogen without a hydrogen (e.g., C _δ -N _ε =C _ε in histidine)
CG	sp ² carbon in five-membered ring next to a N-H (e.g., C _δ -N _ε =C _ε in histidine)
CH	sp ³ carbon with one hydrogen
CI	sp ² carbon in six-membered ring of purines between two "NC" nitrogens
CJ	sp ² carbon in pyrimidines at positions 5 and 6 (more pure double bond than aromatic) with one hydrogen
CP ^e	sp ² aromatic carbon in five-membered ring between two nitrogens with one hydrogen (in His)
All Atom ^d	
C	sp ² carbonyl carbon and aromatic carbon with hydroxyl substituent in tyrosine
C*	sp ² aromatic carbon in five-membered ring with one substituent (e.g., CE _γ in Trp)

CA	sp^2	aromatic carbon in six-membered ring with one substituent
CB	sp^2	aromatic carbon at junction between five and six-membered rings (e.g., CE_6 in Trp, C4 and C5 in purines)
CC	sp^2	aromatic carbon in five-membered ring with one substituent and next to a nitrogen group (e.g., C_γ in His)
CM	sp^2	same as CJ but one substituent
CN	sp^2	aromatic junction carbon in between five and six-membered rings (e.g., C_ϵ in Trp)
CT	sp^3	carbon with four explicit substituents

Nitrogens

NC	sp^2	nitrogen in six-membered ring with lone pairs (e.g., N3 in adenine)
NA	sp^2	nitrogen in five-membered ring with hydrogen attached (e.g., protonated His)
NB	sp^2	nitrogen in five-membered ring with lone pairs (e.g., N7 in purines)
N*	sp^2	nitrogen in purines and pyrimidines with alkyl group attached (N9 in purines, N1 in pyrimidines)
N	sp^2	nitrogen in amide groups
N2	sp^2	nitrogen in base NH_2 groups and arginine NH_2
N3	sp^3	nitrogen with four substituents (e.g., Lys N_ξ)
NT	sp^3	nitrogen with three substituents (e.g., unprotonated amines)

Oxygens

O	carbonyl oxygen
O2	carboxyl and phosphate nonbonded oxygens
OS	ether and ester oxygens
OH	alcohol oxygens

Hydrogens

H3	hydrogens of lysine and arginine (positively charged)
H2	amino hydrogens from NH ₂ in purines and pyrimidines
HC	explicit hydrogen attached to carbon amide and imino hydrogens
H	amide and imino hydrogens
HO	hydrogen on hydroxyl or water oxygen
HS	hydrogen attached to sulfur

Sulfurs

S	sulfurs in disulfide linkages and mentioning
SH	sulfur in cystine

Phosphorus

P	phosphorus in phosphate groups
---	--------------------------------

Lone Pair

LP	lone pairs
----	------------

-
- a. See the following chart for amino acid and nucleic acid structures and atom types. The nomenclature (C_e , N_f , etc.) refers to standard protein crystallographic naming conventions.
 - b. Reproduced from [17].
 - c. United-atom carbons with implicit inclusion of hydrogens.
 - d. Carbons with explicit hydrogens.
 - e. Structural differences in the internal angles of the five-membered rings are the reason why these atoms, which appear in the same environment by definition, are assigned different atom types.
-

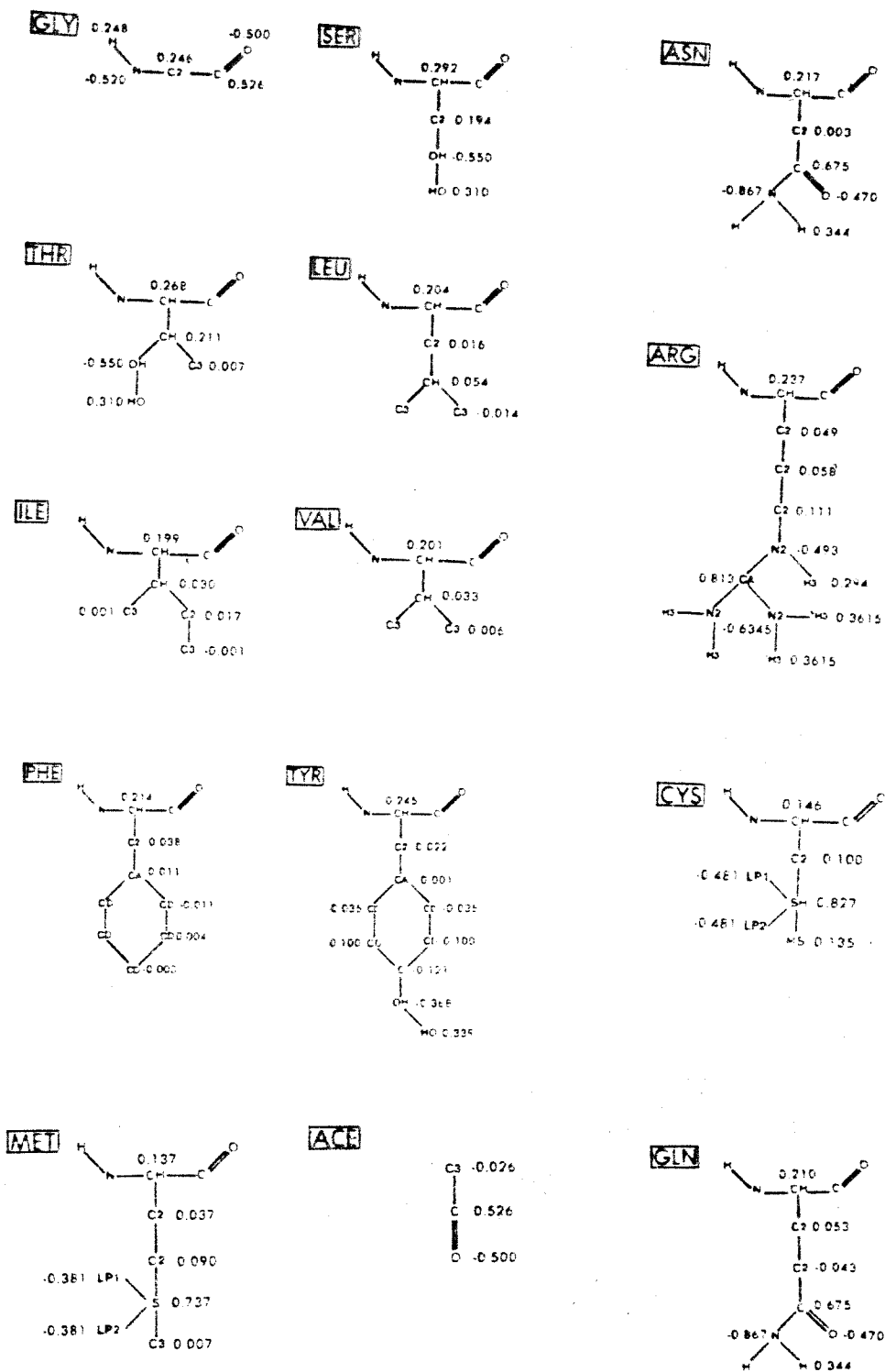


Chart 1A^a

Amino acid structures and atom types.

a. Reproduced from [17].

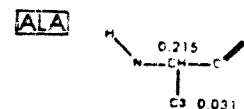
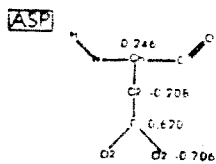
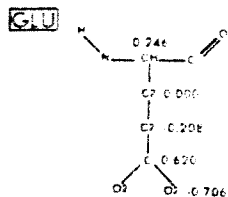
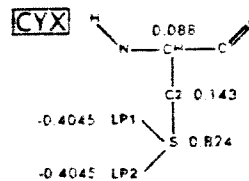
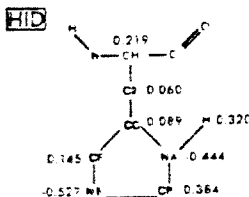
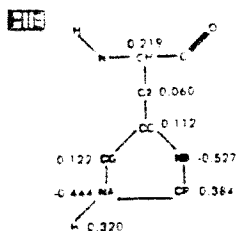
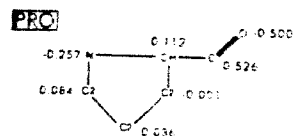
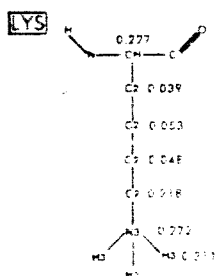
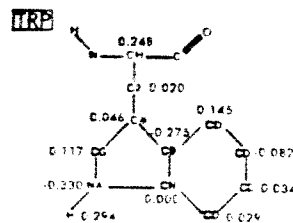
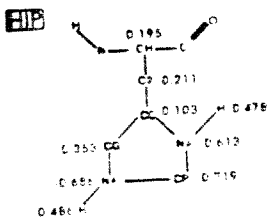


Chart 1A (Continued)

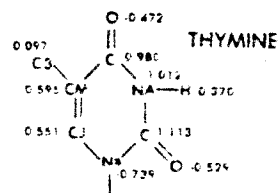
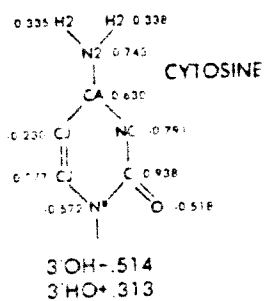
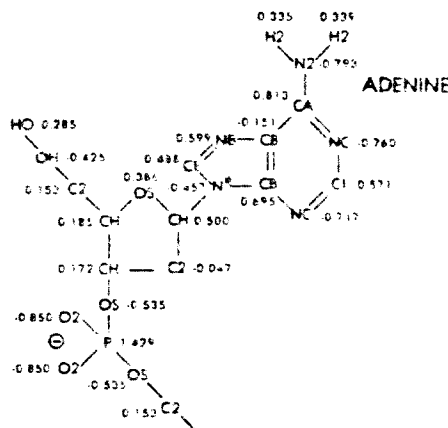
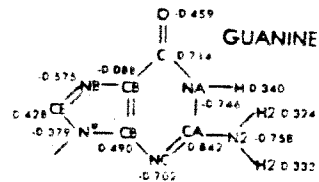
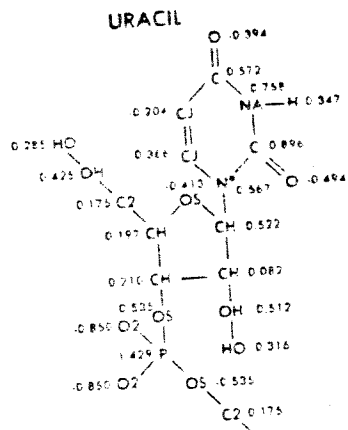


Chart 1B^a

Nucleic acid structures and atom types.

a. Reproduced from [17].

TABLE - 2

ADDITIONAL FORCE FIELD PARAMETERS

A. Bond Stretching Parameters

Bond	Equilibrium Bond Stretching Constant K_r (Kcal/mol A ²)	Equilibrium Bond Length r_{eq} (A)
C-OS	374.0	1.364
CC-CA	300.0	1.510
CH-CC	317.0	1.504

B. Angle Bending Parameters

Bond Angle	Force Constant K_θ (Kcal/mol deg ²)	Equilibrium Bond θ_{eq} (Degree)
CA-CA-CD	85.0	120.0
CC-CA-CA	85.0	120.0
CC-CA-CD	85.0	120.0
CD-CA-C	85.0	120.0
CD-CA-CJ	85.0	120.0
CJ-C-OS	80.0	120.0
C-OS-CH	46.5	113.0
O-C-OS	70.0	120.0
C2-CH-C2	63.0	111.5
C2-CH-CC	63.0	111.5
CH-CH-CC	63.0	114.0
CH-CC-CG	70.0	129.05
CH-CC-NB	70.0	121.05
CC-NB-CC	70.0	105.3

CG-NA-CC	70.0	107.5
NA-CC-NB	70.0	111.6
NA-CC-CA	70.0	126.0
NB-CC-CA	70.0	124.0
CA-C-O2	70.0	117.0

C. General Torsional Parameters

Dihedral	n	$V_n/2^a$ (Kcal/mol)	γ_n^a (degrees)
CJ-C-OS-CH	2	5.0	180
O-C-OS-CH	2	5.0	180
CH-CH-CC-CG	4	0.0	0
CH-CH-CC-NB	4	0.0	0
NA-CC-CA-CD ^b	1	0.5830	216
NA-CC-CA-CA ^b	2	-0.6213	252
NB-CC-CA-CD ^b	3	1.2006	288
NB-CC-CA-CA ^b	4	0.2980	324
X-CA-CJ-X	4	0.395	180

- a. V_n is the torsional force constant (Kcal/mol) for n-fold torsional barrier. γ_n is the torsional phase angle in degrees.
- b. Note that each of these dihedral angles is represented by a potential function which is the sum of 4 terms (see Equation (2)). The parameters $V_1 - V_4$ and $\gamma_1 - \gamma_4$ were derived by Venanzi and Bunce (unpublished data).

TABLE - 3A

OPTIMIZATION OF ALPHA ANGLE^a : O10-C9-O11-C12

A Comparison Between Initial and Optimal Values

FILE	ALPHA ^b		BETA ^c		GAMMA ^d		DELTA ^e		Tct. Op. ^f Energy
	ini ^g	opt ^h	ini	opt	ini	opt	ini	opt	
B11M	62.22	356.63	30.23	76.45	269.0	218.59	0.0	321.2	34.08
B12M	92.26	168.78	30.23	63.03	269.0	216.88	0.0	327.1	38.22
B13M	122.2	172.27	30.25	66.81	269.0	212.93	0.0	321.3	37.00
B14M	152.2	169.98	30.22	68.01	269.0	210.61	0.0	317.1	39.63
B15M	182.3	174.22	30.18	74.40	269.0	215.97	0.0	315.0	41.45
B16M	212.3	170.75	30.18	85.47	269.0	215.50	0.0	319.8	42.68
B17M	242.3	176.83	30.18	81.61	269.0	216.32	0.0	321.8	42.61
B18M	272.3	353.85	30.18	59.18	269.0	216.80	0.0	329.4	42.30
B19M	300.3	0.68	30.33	70.55	269.0	222.61	0.0	324.9	41.86
B110	2.217	3.73	30.23	66.76	269.0	214.78	0.0	322.0	38.71
B111	32.20	356.20	30.23	78.16	269.0	207.58	0.0	320.6	36.82

a. Angles given in degrees.

b. ALPHA : O10-C9-C11-O12

c. BETA : C17-C18-C19-N23

d. GAMMA : C25-C30-C31-O32

e. DELTA : O10-C9-C11-O12

f. Tot. Op. : Total Optimized Energy.

g. ini : initial dihedral angle for input.

h. opt : optimized dihedral angle.

TABLE - 3B

OPTIMIZATION OF BETA ANGLE^a: C17-C18-C19-N23

A Comparison Between Initial and Optimal Values

FILE	ALPHA ^b		BETA ^c		GAMMA ^d		DELTA ^e		Tot. Op. ^f Energy
	ini ^g	opt ^h	ini	opt	ini	opt	ini	opt	
B21M ⁱ	356.6	356.64	76.45	76.45	218.6	218.58	321.2	321.2	34.07
B22M	356.6	355.66	106.5	91.00	218.6	213.30	321.2	319.5	35.53
B23M	356.6	356.71	136.4	136.5	218.6	218.61	321.3	321.2	37.58
B24M	356.6	357.19	166.5	167.4	218.5	218.31	321.3	321.2	38.76
B25M	356.6	356.70	196.5	207.5	218.5	211.81	321.3	312.5	38.19
B26M	356.7	357.84	226.4	238.9	218.5	209.36	321.3	312.0	37.59
B27M	356.7	357.35	256.4	257.1	218.5	218.23	321.3	321.6	37.93
B28M	356.7	357.50	286.4	287.0	218.5	218.26	321.3	321.8	37.96
B29M	356.6	357.68	316.4	317.0	218.5	218.20	321.2	321.7	37.98
B210	356.7	358.01	346.4	353.9	218.5	212.76	321.3	313.3	37.09
B211	356.7	357.19	16.5	28.94	218.6	213.46	321.2	310.6	36.57
B212	356.7	355.36	46.5	61.28	218.5	213.46	321.2	309.6	35.18

a. Angles given in degrees.

b. ALPHA : O10-C9-C11-O12

c. BETA : C17-C18-C19-N23

d. GAMMA : C25-C30-C31-O32

e. DELTA : O10-C9-C11-O12

f. Tot. Op. : Total Optimized Energy.

g. ini : initial dihedral angle for input.

h. opt : optimized dihedral angle.

i. B21M is the optimized structure of Table 3A, B11M.

TABLE - 3C

OPTIMIZATION OF GAMMA ANGLE^a : C25-C30-C31-O32

A Comparison Between Initial and Optimal Values

FILE	ALPHA ^b		BETA ^c		GAMMA ^d		DELTA ^e		Tot. Op. ^f
	ini ^g	opt ^h	ini	opt	ini	opt	ini	opt	Energy
B31M ⁱ	356.6	356.64	76.45	76.52	218.6	218.57	321.2	321.2	34.07
B32M	356.6	356.65	76.45	78.00	248.6	214.30	321.2	317.7	33.78
B33M	356.6	357.16	76.45	73.14	278.6	214.21	321.2	316.3	33.38
B34M	356.6	356.98	76.45	67.55	308.6	24.69	321.1	316.5	33.38
B35M	356.7	358.00	76.45	64.46	338.6	31.24	321.1	328.0	34.11
B36M	356.7	359.49	76.42	74.08	8.6	22.73	321.1	315.8	34.00
B37M	356.7	357.85	76.42	73.67	38.6	24.34	321.1	315.0	33.98
B38M	356.7	356.66	76.42	78.02	68.6	24.08	321.1	316.9	34.43
B39M	356.7	356.66	76.42	71.68	98.6	29.24	321.1	319.5	33.91
B310	356.7	359.49	76.42	76.56	128.6	199.67	321.1	321.7	34.18
B311	356.7	357.98	76.42	67.01	158.6	216.32	321.1	324.4	33.37
B312	356.5	358.70	76.43	75.68	188.6	218.69	321.1	315.2	33.48

a. Angles given in degrees.

b. ALPHA : O10-C9-C11-O12

c. BETA : C17-C18-C19-N23

d. GAMMA : C25-C30-C31-O32

e. DELTA : O10-C9-C11-O12

f. Tot. Op. : Total Optimized Energy.

g. ini : initial dihedral angle for input.

h. opt : optimized dihedral angle.

i. B31M is the optimized structure of Table 3B, B21M.

TABLE - 3D

OPTIMIZATION OF ALPHA ANGLE^a : O10-C9-O11-C12

A Comparison Between Initial and Optimal Values

FILE	ALPHA ^b		BETA ^c		GAMMA ^d		DELTA ^e		Tot. Op. ^f Energy
	ini ^g	opt ^h	ini	opt	ini	opt	ini	opt	
B41M ⁱ	358.0	358.08	67.01	66.99	216.4	216.34	324.4	324.3	33.37
B42M	8.2	356.76	66.98	68.23	216.4	219.32	324.4	316.9	32.84
B43M	18.0	359.90	67.06	70.53	216.4	212.04	324.4	313.9	34.08
B44M	28.2	359.77	67.05	72.01	214.4	211.32	324.4	313.7	34.82
B45M	38.2	0.46	67.02	72.83	216.4	212.09	324.4	314.9	35.56
B46M	48.1	358.74	67.01	72.89	216.5	214.59	324.4	315.3	36.18
B47M	58.2	3.94	66.99	76.92	216.4	210.83	324.4	314.6	36.50
B48M	68.2	345.04	66.98	64.14	216.4	209.62	324.5	310.2	39.61
B49M	348.1	355.47	67.03	69.62	216.4	215.74	324.3	317.8	32.46
B410	338.0	356.61	67.02	61.29	216.3	215.70	324.1	320.7	32.12
B411	328.0	357.74	67.05	59.20	216.3	210.55	324.2	319.6	32.21

a. Angles given in degrees.

b. ALPHA : O10-C9-C11-O12

c. BETA : C17-C18-C19-N23

d. GAMMA : C25-C30-C31-O32

e. DELTA : O10-C9-C11-O12

f. Tot. Op. : Total Optimized Energy.

g. ini : initial dihedral angle for input.

h. opt : optimized dihedral angle.

i. B41M is the optimized structure from Table 3C, B311.

TABLE - 3E

OPTIMIZATION OF DELTA ANGLE^a : N21-C24-C25-C30

A Comparison Between Initial and Optimal Values

FILE	ALPHA ^b		BETA ^c		GAMMA ^d		DELTA ^e		Tot. Op. ^f Energy
	ini ^g	opt ^h	ini	opt	ini	opt	ini	opt	
B51M ⁱ	356.7	355.48	61.28	66.38	215.8	218.81	350.6	317.85	32.33
B52M	356.7	354.19	61.28	50.39	215.8	163.13	20.7	35.42	35.58
B53M	356.7	354.79	61.28	67.68	215.8	148.89	50.7	47.97	35.34
B54M	356.7	353.39	61.28	91.07	215.8	157.46	80.7	49.24	37.63
B55M	356.7	351.94	61.28	96.39	215.8	148.98	110.7	47.55	36.51
B56M	356.7	353.34	61.28	109.63	215.8	150.13	140.7	53.60	37.01
B57M	356.7	354.97	61.28	110.06	215.8	160.56	170.7	83.02	42.04
B58M	356.7	357.83	61.28	329.23	215.8	216.67	200.7	315.56	34.68
B59M	356.7	358.30	61.28	331.75	215.8	214.16	230.7	313.81	34.70
B510	356.7	356.64	61.28	60.17	215.8	214.93	260.7	319.19	32.06
B511	356.7	356.42	61.28	56.39	215.8	214.23	290.7	318.24	32.07

a. Angles given in degrees.

b. ALPHA : O10-C9-C11-O12

c. BETA : C17-C18-C19-N23

d. GAMMA : C25-C30-C31-O32

e. DELTA : O10-C9-C11-O12

f. Tot. Op. : Total Optimized Energy.

g. ini : initial dihedral angle for input.

h. opt : optimized dihedral angle.

i. B51M is the structure obtained from B410 by increasing delta by 30 degrees.

TABLE - 4A

OPTIMIZED ENERGIES FOR ROTATION AROUND ALPHA ANGLE: O10-C9-O11-C12

FUNCTIONALIZED NORBORNANE MIMIC

FILE	T.E. ^a	BOND ^b	B.A. ^c	DIH. ^d	VDW ^e	ELEC ^f	H-B ^g	1-4VDW ^h	1-4EEL ⁱ
B11M	34.08	2.54	25.95	14.00	-6.74	-73.86	-0.001	14.35	57.84
B12M	38.22	2.43	27.25	14.14	-4.39	-73.69	-0.043	14.05	58.46
B13M	37.00	2.67	26.64	13.38	-5.01	-73.23	0.028	14.32	58.21
B14M	39.63	2.52	26.98	13.72	-3.48	-73.32	-0.068	14.56	58.72
B15M	41.45	2.50	27.39	14.37	-3.14	-72.64	-0.136	14.31	58.79
B16M	42.68	2.67	25.68	15.82	-3.45	-71.24	-0.019	15.23	57.98
B17M	42.61	2.69	26.49	14.37	-3.48	-71.41	-0.100	16.19	57.76
B18M	42.30	2.73	29.94	13.98	-2.22	-73.88	0.105	13.56	58.08
B19M	41.86	2.56	28.85	15.10	-2.88	-73.27	0.003	13.59	57.90
B110	38.71	2.72	27.11	14.31	-3.51	-74.10	0.040	14.18	57.96
B111	36.82	2.78	26.43	13.39	-4.40	-73.25	0.005	14.99	56.88

a. T.E. - TOTAL ENERGY; UNIT: Kcal/mol

b. BOND - BOND STRETCHING

g. H-B - HYDROGEN BONDING

c. B.A. - BOND ANGLE BENDING

h. 1-4VDW - 1-4 VAN DER WAALS

d. DIH. - TORSIONAL

i. 1-4EEL - 1-4 ELECTROSTATIC

e. VDW - VAN DER WAALS

f. ELEC - ELECTROSTATIC

TABLE - 4B

OPTIMIZED ENERGIES FOR ROTATION AROUND BETA ANGLE : C17-C18-C19-N23

FUNCTIONALIZED NORBORNANE MIMIC

FILE	T.E. ^a	BOND ^b	B.A. ^c	DIH. ^d	VDW ^e	ELEC ^f	H-B ^g	1-4VDW ^h	1-4EEL ⁱ
B21M	34.07	2.53	25.93	14.01	-6.75	-73.84	-0.005	14.36	57.84
B22M	35.53	2.61	25.86	13.99	-6.02	-73.24	-0.042	14.78	57.57
B23M	37.58	2.54	25.92	14.02	-5.06	-72.06	-0.007	15.30	56.93
B24M	38.76	2.63	25.68	14.05	-3.31	-71.51	0.022	14.79	56.41
B25M	38.19	2.66	26.19	13.46	-2.94	-71.25	-0.131	14.08	56.11
B26M	37.59	2.63	26.14	13.29	-3.04	-71.58	-0.113	14.12	56.14
B27M	37.83	2.62	25.83	13.97	-3.30	-71.86	0.027	14.24	56.31
B28M	37.96	2.64	25.85	13.96	-3.53	-72.53	0.034	14.70	56.84
B29M	37.98	2.63	25.79	13.96	-3.46	-73.39	0.032	14.91	57.49
B210	37.09	2.64	25.90	13.55	-3.31	-74.27	-0.173	14.57	58.18
B211	36.06	2.51	26.17	13.69	-3.33	-74.52	-0.189	13.99	58.26
B212	35.18	2.73	25.79	13.42	-5.01	-74.09	-0.184	14.61	57.91

a. T.E. - TOTAL ENERGY; UNIT: Kcal/mol

b. BOND - BOND STRETCHING

g. H-B - HYDROGEN BONDING

c. B.A. - BOND ANGLE BENDING

h. 1-4VDW - 1-4 VAN DER WAALS

d. DIH. - TORSIONAL

i. 1-4EEL - 1-4 ELECTROSTATIC

e. VDW - VAN DER WAALS

f. ELEC - ELECTROSTATIC

TABLE - 4C

OPTIMIZED ENERGIES FOR ROTATION AROUND GAMMA ANGLE: C25-C30-C31-O32

FUNCTIONALIZED NORBORNANE MIMIC

FILE	T.E. ^a	BOND ^b	B.A. ^c	DIH. ^d	VDW ^e	ELEC ^f	H-B ^g	1-4VDW ^h	1-4EEL ⁱ
B31M	34.07	2.56	25.93	14.00	-6.75	-73.84	0.001	14.37	57.83
B32M	33.78	2.61	26.10	13.55	-6.85	-73.65	-0.014	14.52	57.52
B33M	33.38	2.52	25.91	13.61	-7.04	-73.96	-0.088	14.48	57.96
B34M	33.38	2.70	26.11	13.61	-7.70	-73.05	-0.100	14.28	57.53
B35M	34.11	2.54	26.25	14.24	-7.39	-73.17	0.022	14.06	57.86
B36M	34.00	2.68	26.07	13.36	-7.16	-72.73	-0.134	14.35	57.56
B37M	33.98	2.53	25.55	14.11	-7.21	-73.03	-0.151	14.37	57.81
B38M	34.43	2.62	26.04	13.53	-6.89	-72.63	-0.078	14.53	57.31
B39M	33.91	2.58	25.78	14.01	-7.28	-73.04	-0.078	14.24	57.70
B310	34.18	3.22	27.97	11.93	-6.97	-72.96	-0.125	14.73	56.38
B311	33.37	2.76	26.23	13.86	-7.51	-73.78	-0.026	14.18	57.66
B312	33.48	2.53	25.41	13.93	-7.25	-73.86	-0.149	14.62	58.24

a. T.E. - TOTAL ENERGY; UNIT: Kcal/mol

b. BOND - BOND STRETCHING g. H-B - HYDROGEN BONDING

c. B.A. - BOND ANGLE BENDING h. 1-4VDW - 1-4 VAN DER WAALS

d. DIH. - TORSIONAL i. 1-4EEL - 1-4 ELECTROSTATIC

e. VDW - VAN DER WAALS

f. ELEC - ELECTROSTATIC

TABLE - 4D

OPTIMIZED ENERGIES FOR ROTATION AROUND ALPHA ANGLE: O10-C9-O11-C12

FUNCTIONALIZED NORBORNANE MIMIC

FILE	T.E. ^a	BOND ^b	B.A. ^c	DIH. ^d	VDW ^e	ELEC ^f	H-B ^g	1-4VDW ^h	1-4EEL ⁱ
B41M	33.37	2.73	26.24	13.86	-7.51	-73.79	-0.022	14.19	57.66
B42M	32.84	2.52	25.76	14.21	-7.74	-74.19	-0.081	14.23	58.14
B43M	34.08	2.56	26.24	13.34	-6.35	-73.78	-0.169	14.48	57.75
B44M	34.82	2.67	26.52	13.46	-5.73	-73.83	-0.109	14.22	57.61
B45M	35.56	2.45	26.44	13.68	-5.16	-73.98	-0.066	14.30	57.88
B46M	36.18	2.55	26.75	13.88	-4.90	-73.78	-0.089	14.00	57.78
B47M	36.50	2.63	26.67	13.96	-4.93	-73.58	-0.031	14.30	57.47
B48M	39.61	2.66	26.65	14.61	-5.16	-71.62	-0.052	14.42	58.11
B49M	32.46	2.61	26.07	13.87	-8.05	-74.30	-0.068	14.48	57.84
B410	32.12	2.63	26.20	14.01	-8.46	-74.55	-0.012	14.34	57.96
B411	32.21	2.72	26.66	13.60	-8.44	-74.60	-0.017	14.46	57.81

a. T.E. - TOTAL ENERGY; UNIT: Kcal/mol

b. BOND - BOND STRETCHING

c. B.A. - BOND ANGLE BENDING

d. DIH. - TORSIONAL

e. VDW - VAN DER WAALS

f. ELEC - ELECTROSTATIC

g. H-B - HYDROGEN BONDING

h. 1-4VDW - 1-4 VAN DER WAALS

i. 1-4EEL - 1-4 ELECTROSTATIC

TABLE - 4E

OPTIMIZED ENERGIES FOR ROTATION AROUND DELTA ANGLE: N21-
C24-C25-C30

FUNCTIONALIZED NORBORNANE MIMIC

FILE	T.E. ^a	BOND ^b	B.A. ^c	DIH. ^d	VDW ^e	ELEC ^f	H-B ^g	1-4VDW ^h	1-4EEL ⁱ
B51M	32.33	2.62	26.01	14.43	-8.51	-74.31	-0.086	14.17	57.99
B52M	35.58	3.11	28.40	12.87	-6.06	-74.01	0.014	14.89	56.36
B53M	35.34	2.59	25.66	15.10	-6.02	-74.28	-0.156	14.47	57.97
B54M	37.63	2.91	25.71	15.73	-6.39	-73.51	-0.187	15.94	57.43
B55M	36.51	2.64	25.79	15.10	-6.36	-73.22	-0.175	15.46	57.27
B56M	37.01	2.70	25.46	15.82	-7.11	-72.68	-0.280	15.88	57.24
B57M	42.04	2.60	24.42	14.91	-11.45	-63.59	-0.035	16.31	59.04
B58M	34.68	2.68	25.24	14.28	-6.84	-74.29	-0.078	15.39	58.30
B59M	34.70	2.70	25.53	13.84	-6.34	-74.28	-0.126	15.10	58.27
B510	32.06	2.64	26.44	13.77	-8.39	-74.59	-0.045	14.38	57.86
B511	32.07	2.68	26.52	13.57	-8.20	-74.59	-0.050	14.29	57.86

a. T.E. - TOTAL ENERGY; UNIT: Kcal/mol

b. BOND - BOND STRETCHING

g. H-B - HYDROGEN BONDING

c. B.A. - BOND ANGLE BENDING

h. 1-4VDW - 1-4 VAN DER WAALS

d. DIH. - TORSIONAL

i. 1-4EEL - 1-4 ELECTROSTATIC

e. VDW - VAN DER WAALS

f. ELEC - ELECTROSTATIC

TABLE - 4F

SCALING FACTOR STUDY OF FUNCTIONALIZED NORBORNANE MIMIC^aCOMPARISON AT CONSTANT EEL^b

FILE	T.E.	BOND	B.A.	DIH.	VDW	ELEC	H-B	1-4 VDW	1-4 EEL	NB ^c	EEL
A	100.70	7.94	30.59	13.02	-9.19	-72.48	-0.0322	22.56	108.30	0.5	0.5
B	88.04	4.88	29.74	12.39	-9.07	-72.51	-0.0481	14.32	108.30	1.0	0.5
C	82.99	3.99	29.52	12.21	-9.06	-72.56	-0.0510	10.59	108.40	1.5	0.5
D	80.24	3.62	29.39	12.13	-9.07	-72.58	-0.0385	8.42	108.40	2.0	0.5
G	44.91	5.52	27.57	14.12	-8.56	-74.23	-0.0350	22.97	57.56	0.5	1.0
F	32.12	2.63	26.20	14.02	-8.46	-74.56	-0.0109	14.35	57.96	1.0	1.0
H	27.12	1.83	25.77	14.05	-8.42	-74.69	-0.0116	10.43	58.16	1.5	1.0
I	24.39	1.48	25.53	14.01	-8.46	-74.67	-0.0435	8.33	58.21	2.0	1.0
J	25.26	4.69	26.22	15.77	-8.49	-75.15	-0.0872	22.76	39.57	0.5	1.5
K	12.77	2.51	26.21	14.02	-8.43	-74.68	-0.0029	14.39	38.76	1.0	1.5
L	7.56	1.44	25.26	14.14	-8.15	-75.18	-0.0213	10.64	39.43	1.5	1.5
M	4.81	1.11	24.96	14.14	-8.09	-75.28	-0.0163	8.45	39.54	2.0	1.5
N	15.32	4.41	25.84	16.17	-8.39	-75.51	-0.1060	22.87	30.04	0.5	2.0
O	2.53	1.84	24.74	15.31	-8.17	-75.70	-0.1072	14.45	30.17	1.0	2.0
P	-2.53	1.16	24.38	14.97	-8.03	-75.78	-0.1021	10.68	30.19	1.5	2.0
Q	-5.27	0.88	24.23	14.80	-7.96	-75.80	-0.1066	8.482	30.21	2.0	2.0

a. The same starting structure (minimized B510) was used for each calculation.

b. NB: 1-4 nonbonded term scaling factor.

c. EEL: 1-4 electrostatic term scaling factor.

TABLE - 4G

SCALING FACTOR STUDY OF FUNCTIONALIZED NORBORNANE MIMIC^aCOMPARISON AT CONSTANT NB^b

FILE	T.E.	BOND	B.A.	DIH.	VDW	ELEC	H-B	1-4 VDW	1-4 EEL	NB	EEL ^c
A	100.70	7.94	30.59	13.02	-9.19	-72.48	-0.0322	22.56	108.30	0.5	0.5
G	44.91	5.52	27.57	14.12	-8.56	-74.23	-0.0350	22.97	57.56	0.5	1.0
J	25.26	4.69	26.22	15.77	-8.49	-75.15	-0.0872	22.76	39.57	0.5	1.5
N	15.32	4.41	25.84	16.17	-8.39	-75.51	-0.1060	22.87	30.04	0.5	2.0
B	88.04	4.88	29.74	12.39	-9.07	-72.51	-0.0481	14.32	108.30	1.0	0.5
F	32.12	2.63	26.20	14.02	-8.46	-74.56	-0.0109	14.35	57.96	1.0	1.0
K	12.77	2.51	26.21	14.02	-8.43	-74.68	-0.0029	14.39	38.76	1.0	1.5
O	2.53	1.84	24.74	15.31	-8.17	-75.70	-0.1072	14.45	30.17	1.0	2.0
C	82.99	3.99	29.52	12.21	-9.06	-72.56	-0.0510	10.59	108.40	1.5	0.5
H	27.12	1.83	25.77	14.05	-8.42	-74.69	-0.0116	10.43	58.16	1.5	1.0
L	7.56	1.44	25.26	14.14	-8.15	-75.18	-0.0213	10.64	39.43	1.5	1.5
P	-2.53	1.16	24.38	14.97	-8.03	-75.78	-0.1021	10.68	30.19	1.5	2.0
D	80.24	3.62	29.39	12.13	-9.07	-72.58	-0.0385	8.42	108.40	2.0	0.5
I	24.39	1.48	25.53	14.01	-8.46	-74.67	-0.0435	8.33	58.21	2.0	1.0
M	4.81	1.11	24.96	14.14	-8.09	-75.28	-0.0163	8.45	39.54	2.0	1.5
Q	-5.27	0.88	24.23	14.80	-7.96	-75.80	-0.1066	8.48	30.21	2.0	2.0

a. The same starting structure (minimized B510) was used for each calculation.

b. EEL: 1-4 electrostatic term scaling factor.

c. NB: 1-4 nonbonded term scaling factor.

TABLE - 5A

OPTIMIZATION OF ALPHA ANGLE : O10-C9-O11-C12

Distance^{a,b} Between Atoms in Functionalized Norbornane Mimic

FILE	Imidazolyl Nitrogen (N23) to Ester Oxygens		Imidazolyl Hydrogen (H22) to Carboxylate Oxygens	
	N23-O11	N23-O10	H22-O33	H22-O32
B11M	3.149	4.877	3.654	1.689
B12M	3.572	4.553	3.591	1.693
B13M	3.343	4.097	3.674	1.686
B14M	3.545	4.562	3.663	1.697
B15M	3.685	4.742	3.682	1.706
B16M	3.353	4.383	3.639	1.690
B17M	3.379	4.465	3.643	1.690
B18M	4.250	5.141	3.510	1.677
B19M	4.021	4.910	3.574	1.689
B110	3.589	4.666	3.614	1.684
B111	3.264	5.205	3.684	1.688

a. Distance given in Angstroms.

b. Refer to Figure 11A for atomic labelling scheme.

TABLE - 5B

OPTIMIZATION OF BETA ANGLE : C17-C18-C19-N23

Distance^{a,b} Between Atoms in Functionalized Norbornane Mimic

FILE	Imidazolyl Nitrogen (N23) to Ester Oxygens		Imidazolyl Hydrogen (H22) to Carboxylate Oxygens	
	N23-O11	N23-O10	H22-O33	H22-O32
B21M	3.149	4.877	3.655	1.689
B22M	3.324	5.124	3.646	1.692
B23M	3.817	5.234	3.655	1.690
B24M	4.336	5.754	3.652	1.686
B25M	4.892	6.353	3.764	1.705
B26M	5.143	6.745	3.772	1.702
B27M	5.131	6.909	3.651	1.685
B28M	4.988	6.897	3.650	1.684
B29M	4.651	6.640	3.651	1.684
B210	4.132	6.165	3.757	1.711
B211	3.633	5.623	3.768	1.714
B212	3.199	5.046	3.807	1.713

a. Distance given in Angstroms.

b. Refer to Figure 11A for atomic labelling scheme.

TABLE - 5C

OPTIMIZATION OF GAMMA ANGLE : C25-C30-C31-O32

Distance^{a,b} Between Atoms in Functionalized Norbornane Mimic

FILE	Imidazolyl Nitrogen (N23) to Ester Oxygens		Imidazolyl Hydrogen (H22) to Carboxylate Oxygens	
	N23-O11	N23-O10	H22-O33	H22-O32
B31M	3.149	4.877	3.655	1.689
B32M	3.152	4.863	3.697	1.690
B33M	3.112	4.839	3.716	1.698
B34M	3.065	4.764	1.701	3.724
B35M	3.155	4.865	1.687	3.563
B36M	3.157	4.813	1.705	3.745
B37M	3.084	4.797	1.708	3.721
B38M	3.151	4.870	1.697	3.709
B39M	3.132	4.834	1.693	3.664
B310	3.231	4.891	3.813	1.705
B311	3.165	4.845	3.643	1.691
B312	3.158	4.822	3.750	1.708

a. Distance given in Angstroms.

b. Refer to Figure 11A for atomic labelling scheme.

TABLE - 5D

OPTIMIZATION OF ALPHA ANGLE : O10-C9-O11-C12

Distance^{a,b} Between Atoms in Functionalized Norbornane Mimic

FILE	Imidazolyl Nitrogen (N23) to Ester Oxygens		Imidazolyl Hydrogen (H22) to Carboxylate Oxygens	
	N23-O11	N23-O10	H22-O33	H22-O32
B41M	3.165	4.844	3.642	1.692
B42M	3.094	4.769	3.709	1.699
B43M	3.176	4.849	3.771	1.711
B44M	3.254	4.947	3.757	1.702
B45M	3.324	5.010	3.744	1.696
B46M	3.450	5.136	3.723	1.699
B47M	3.348	4.895	3.733	1.692
B48M	3.239	3.218	3.698	1.694
B49M	3.059	4.771	3.741	1.697
B410	3.073	4.746	3.695	1.690
B411	3.118	4.756	3.747	1.691

a. Distance given in Angstroms.

b. Refer to Figure 11A for atomic labelling scheme.

TABLE - 5E

OPTIMIZATION OF DELTA ANGLE : N21-C24-C25-C30

Distance^{a,b} Between Atoms in Functionalized Norbornane Mimic

FILE	Imidazolyl Nitrogen (N23) to Ester Oxygens		Imidazolyl Hydrogen (H22) to Carboxylate Oxygens	
	N23-O11	N23-O10	H22-O33	H22-O32
B51M	3.058	4.752	3.729	1.698
B52M	3.281	5.146	3.782	1.687
B53M	3.120	4.970	3.755	1.709
B54M	3.017	4.972	3.775	1.713
B55M	3.153	5.029	3.782	1.712
B56M	3.187	4.863	3.816	1.730
B57M	3.055	4.692	4.620	2.755
B58M	4.157	6.042	3.692	1.697
B59M	4.252	6.119	3.731	1.704
B510	3.083	4.754	3.743	1.694
B511	3.078	4.755	3.745	1.694

a. Distance given in Angstroms.

b. Refer to Figure 11A for atomic labelling scheme.

TABLE - 6A RMS COMPARISONS FOR SELECTED MINIMIZED STRUCTURES^b

File	RMS ^b Deviation For 6 Atoms ^c	RMS Deviation For All Atoms	Mean	Standard deviation	Maximum deviation	For Atom
B16M ^d	0.0273	0.0116	0.0044	0.0108	12.7379	C3
B111	0.0157	0.0067	0.0139	0.0074	3.3702	C4
B24M	0.0114	0.0049	0.0101	0.0053	6.5912	C27
B38M	0.0094	0.0040	0.0015	0.0037	2.4143	O33
B31M	0.0122	0.0056	0.0020	0.0056	2.2164	C4
B311	0.0077	0.0033	0.0071	0.0039	1.2557	C3

TABLE - 6B RMS COMPARISONS FOR SELECTED MINIMIZED STRUCTURES WITH DIFFERENT VALUES OF NB AND EEL SCALING FACTOR^a

File	RMS Deviation For 6 Atoms	RMS Deviation For All Atoms	Mean	Standard deviation	Maximum deviation	For Atom
B5A ^e NB=0.5 EEL=0.5	0.0238	0.0101	0.0038	0.0094	0.4015	O32
B5N NB=0.5 EEL=2.0	0.0185	0.0079	0.0030	0.0073	0.3497	C2
B5Q NB=2.0 EEL=2.0	0.0168	0.0072	0.0027	0.0067	0.2151	O32

a. The statistical information is given for the fit of the structure to the global energy minimum, B510.

b. RMS: Root Mean Square, refer to Section II.F.

c. 6 Atoms: C12, C13, C14, C15, C16, and C17, see Figure 11A.

d. See Figure 12 - 17.

e. See Figure 18 - 20.

TABLE - 7

COMPARISON OF DISTANCES^a BETWEEN FUNCTIONAL GROUPS IN MIMIC
AND IN ENZYME

FILE	O32-N23 ^b	O32-N21	O33-N23	O33-N21	O11-N23	O11-N21	T.E. ^c
B16M	4.398	2.571	5.537	4.277	3.353	5.525	42.68
B111	4.390	2.567	5.652	4.359	3.264	5.483	36.82
B24M	4.400	2.566	5.563	4.298	4.336	4.889	38.76
B38M	5.568	4.354	4.371	2.568	3.151	5.379	34.43
B31M	4.400	2.567	5.564	4.298	3.149	5.375	34.07
B311	4.404	2.572	5.582	4.301	3.165	5.384	33.37
B410	4.378	2.564	5.760	4.343	3.073	5.280	32.12
B510	4.376	2.564	5.761	4.343	3.073	5.280	32.06
CHYM ^d	4.606	2.613	5.408	3.310	2.816	4.684	

a. Distances given in Angstroms.

b. See Figure 11A for relative atomic positions.

c. T.E. - TOTAL ENERGY.

d. Distances taken from alpha-chymotrypsin X-ray structure [10]. See Figure 21 for relative atomic positions. The O32-N23 distance in the mimic corresponds to OD2-NE2 in the enzyme. In addition, O32-N21 corresponds to OD2-ND1; O33-N23 to OD1-NE2; O33-N21 to OD1-ND1; O11-N23 to OG-NE2; and O11-N21 to OG-ND1.

TABLE - 8

STRUCTURAL SUPERPOSITION OF MIMIC^a ONTO THE ACTIVE SITE OF
ALPHA-CHYMOTRYPSIN

Atom of Norbornane Mimic	Atom of Alpha-chymotrypsin	Relative ^b Distance
N21	ND1 of His-57	0.811
N23	NE2 of His-57	0.472
O33	OD1 of Asp-102	1.325
O32	OD2 of Asp-102	0.994
O11	OG of Ser-195	0.503

a. Structure B510, minimized.

b. Relative distances are given in Angstroms.

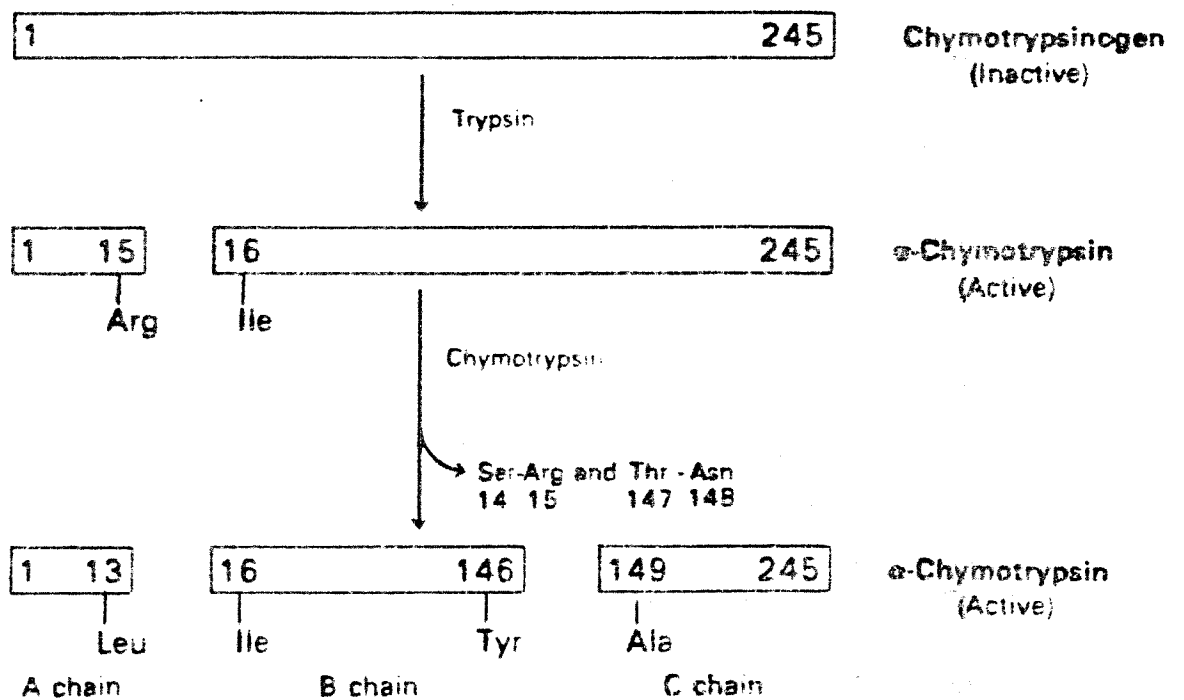


Figure 1

The activation process of chymotrypsinogen. Reproduced from: Stryer, L. Biochemistry, 2d. ed., W.H. Freeman and Co., 1981, p.158.

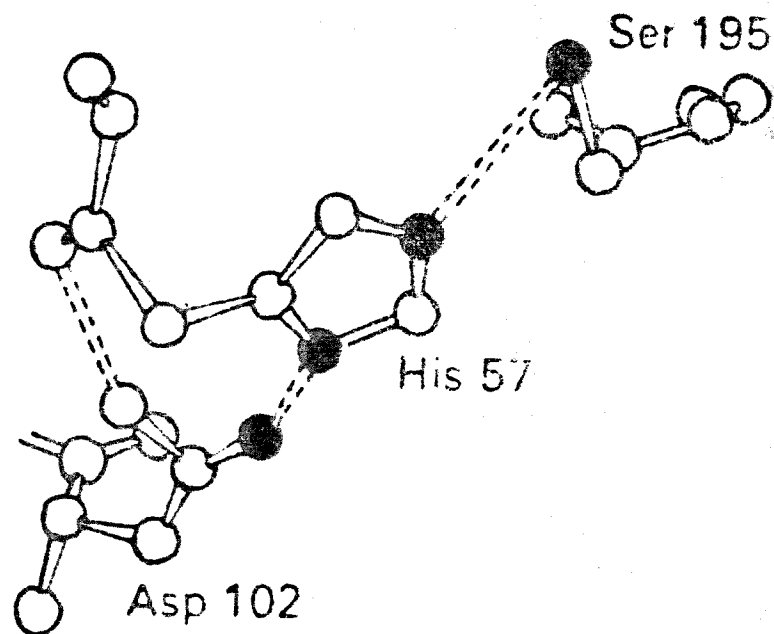


Figure 2

Conformation of the charge relay system in chymotrypsin.
Reproduced from: Stryer, L. Biochemistry, 2d. ed., W.H.
Freeman and Co., 1981, p.163.

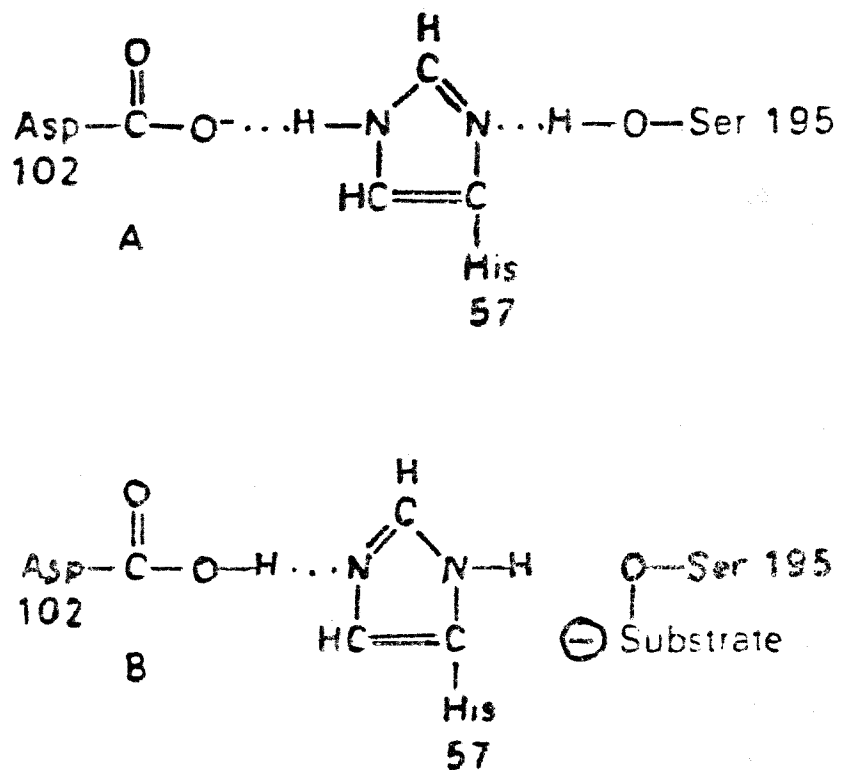


Figure 3

Charge relay network in chymotrypsin: (A) enzyme alone; (B) on addition of a substrate, Aspartate 102 and Histidine 57 transiently bind a proton. Reproduced from: Stryer, L. Biochemistry, 2d. ed., W.H. Freeman and Co., 1981, p.163.

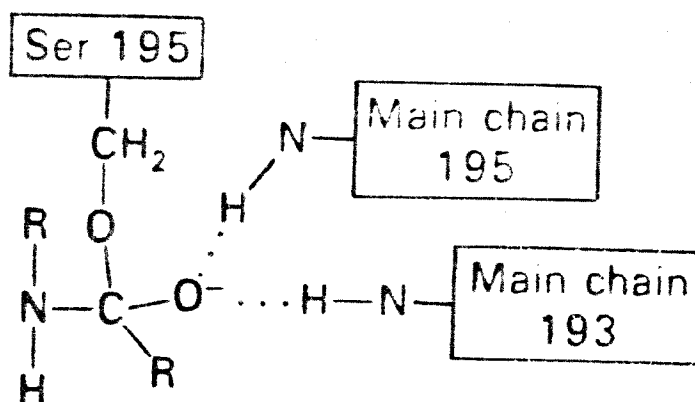


Figure 4

The tetrahedral transition-state intermediate in the acylation and deacylation reactions of chymotrypsin. The hydrogen bonds formed by two NH groups from the main chain of the enzyme are critical in stabilizing this intermediate. Reproduced from: Stryer, L. Biochemistry, 2d. ed., W.H. Freeman and Co., 1981, p.164.

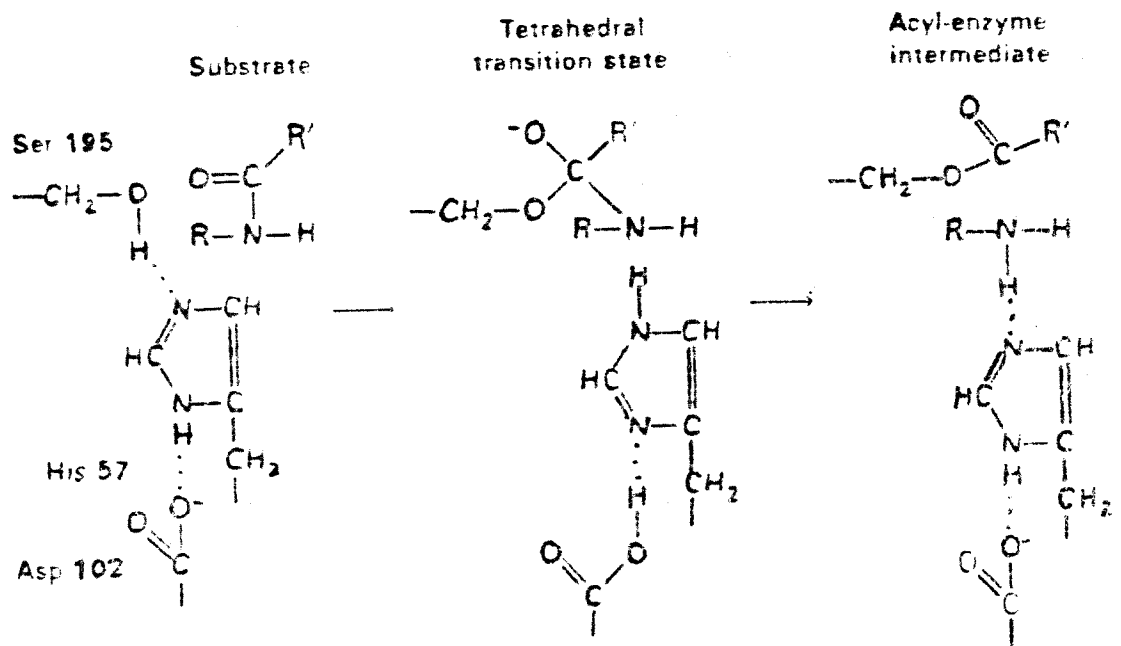


Figure 5

First stage in the hydrolysis of a peptide by chymotrypsin: acylation. A tetrahedral transition state is formed. The amine component then rapidly diffuses away, which leaves an acyl-enzyme intermediate. Reproduced from: Stryer, L. Biochemistry, 2d. ed., W.H. Freeman and Co., 1981, p.164.

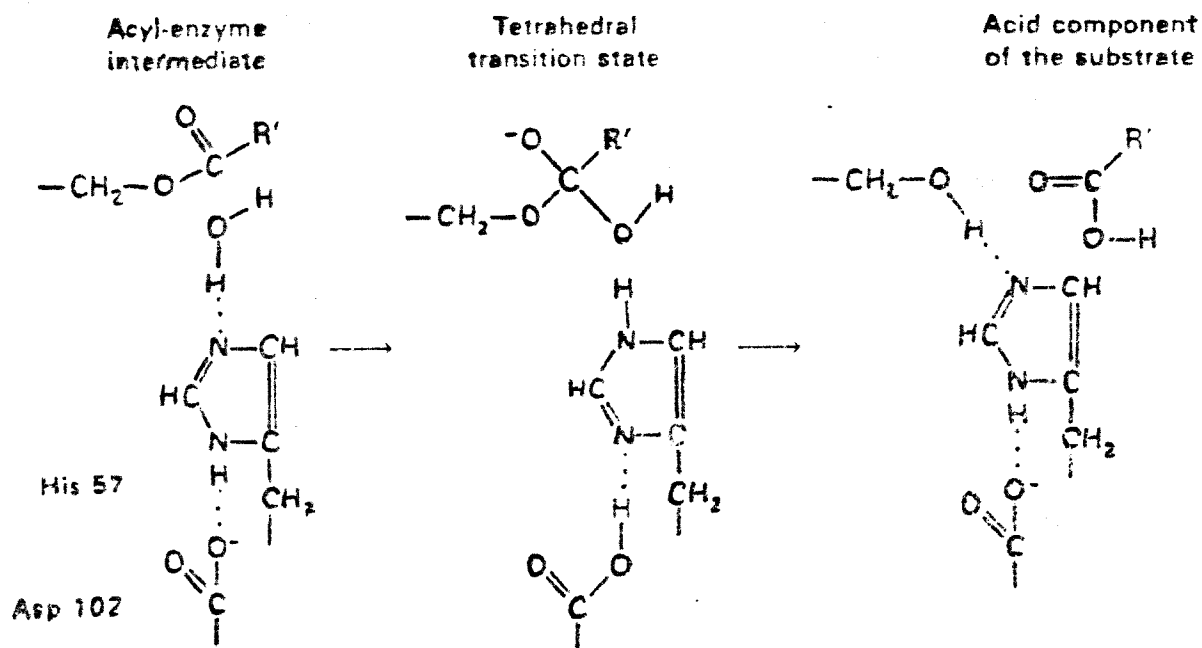
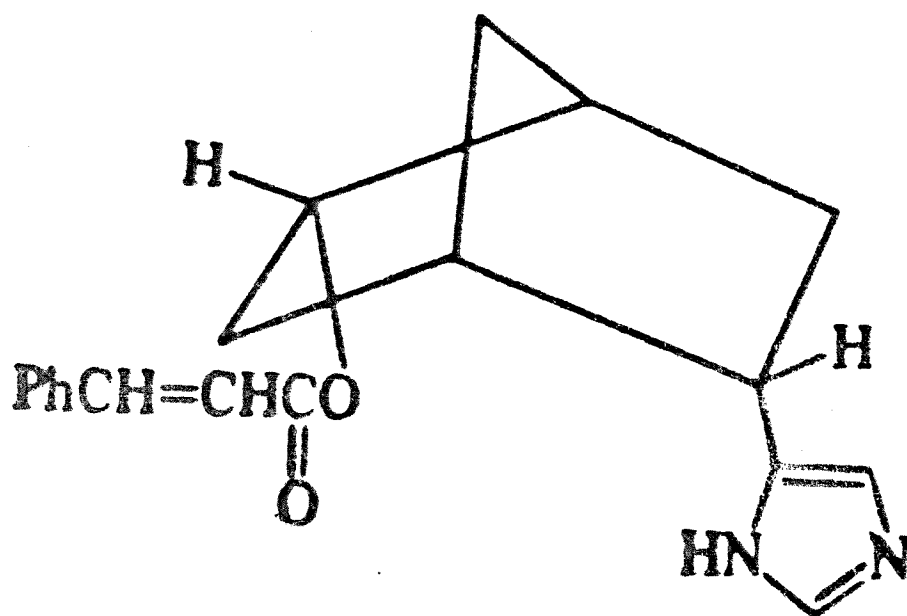


Figure 6

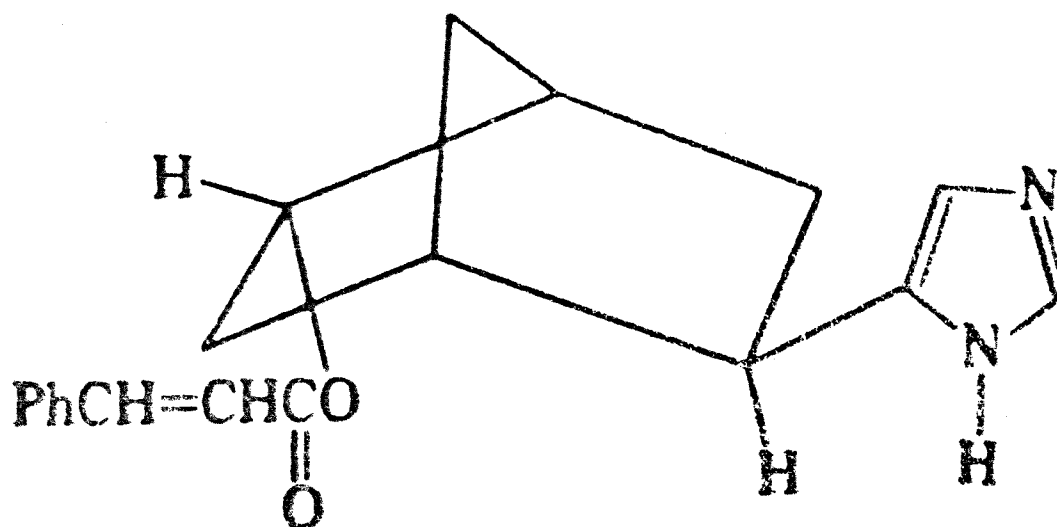
Second stage in the hydrolysis of a peptide of chymotrypsin: deacylation. The acyl-enzyme intermediate is hydrolyzed by water. Note that deacylation is essentially the reverse of acylation, with water replacing the amine component of the substrate. Reproduced from: Stryer, L. Biochemistry, 2d. ed., W.H. Freeman and Co., 1981, p.165.



1

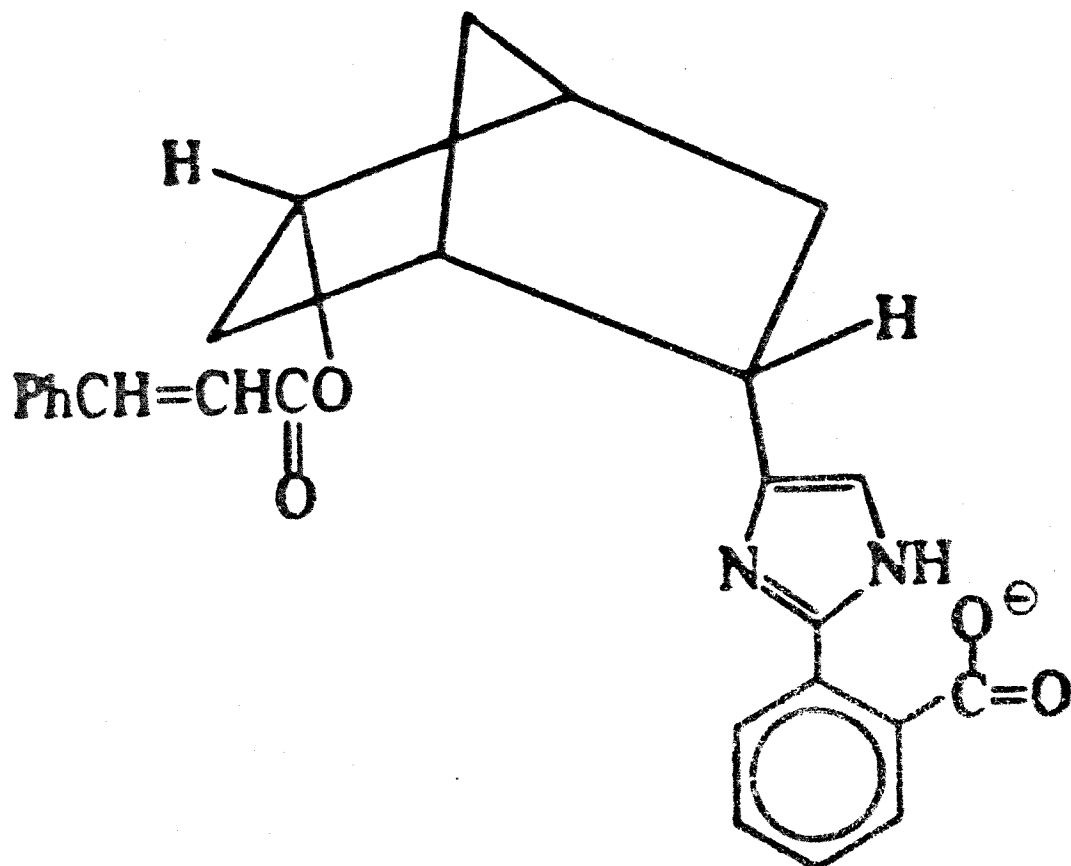
Figure 7

Structure of endo - 5 - [4'(5') - imidazolyl] bicyclo
[2.2.1] - hept - endo - 2 - yl trans-cinnamate.



2

Figure 8
Structure of exo - 5 - [4'(5') - imidazolyl] bicyclo [2.2.1]
-hept - endo - 3 - yl trans-cinnamate which is basically
the endo-exo isomer of structure 1, Figure 7.



3

Figure 9

Structure of endo, endo - 5 - [2-(2-carboxylphenyl)-4-(5)-imidazolyl] bicyclo [2.2.1]-hept-2-yl trans-cinnamate. This molecule has an additional benzoate group, compared to structure 1.

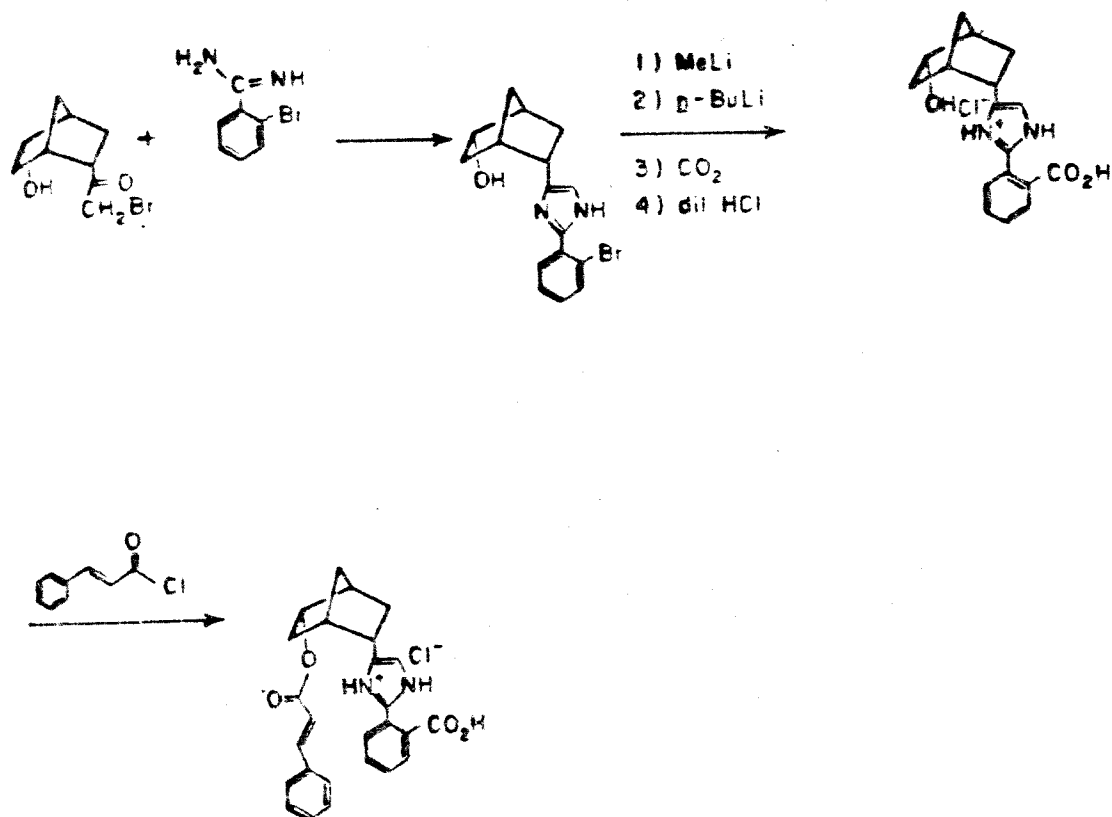


Figure 10

Synthesis of structure 3 (Figure 9) by: (1) Condensation of 2-bromobenzamide with endo, endo- 5 - (bromoacetyl)- 2 - hydroxybicyclo [2.2.1] heptane; (2) Followed by lithium exchange of bromine atom; (3) Carboxylation of the lithium derivative; and (4) Cinnamoylation of the hydroxyl group [5].

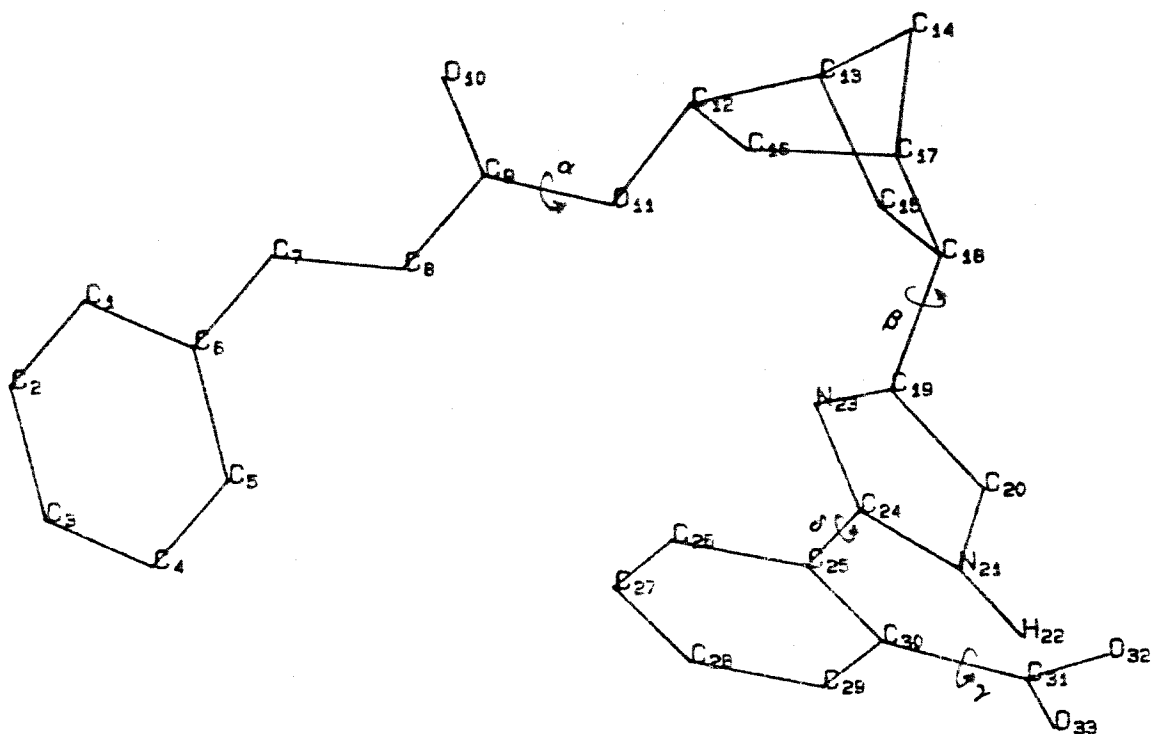


Figure 11A

The starting structure of the norbornane mimic. The molecule is shown in the united atom approximation in which hydrogen atoms attached to the aliphatic and aromatic carbons are not explicitly indicated. The dihedral angles used for the conformational analysis are indicated: alpha (O10-C9-O11-C12), beta (C17-C18-C19-N23), gamma (C25-C30-C31-O32), delta (N21-C24-C25-C30). The norbornane atoms used in the structural superposition procedure are C12, C13, C14, C15, C16, C17.

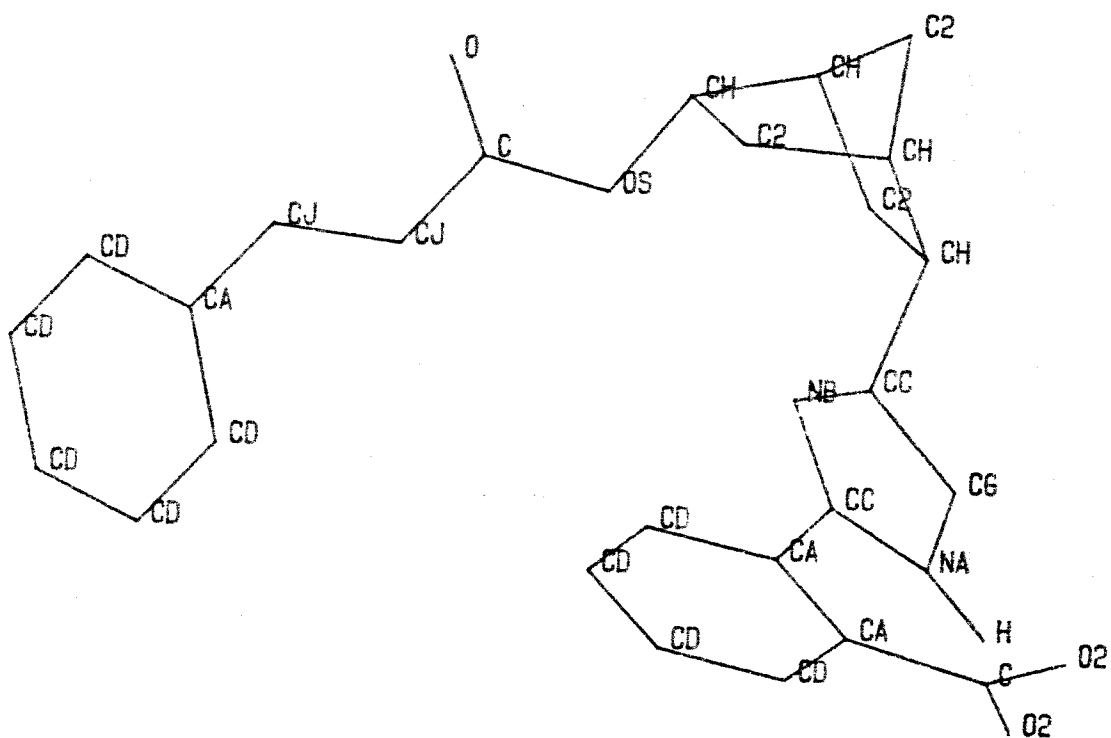


Figure 11B

The norbornane mimic with atoms label according to Amber atom type (See Table 1 and accompanying Chart 1).

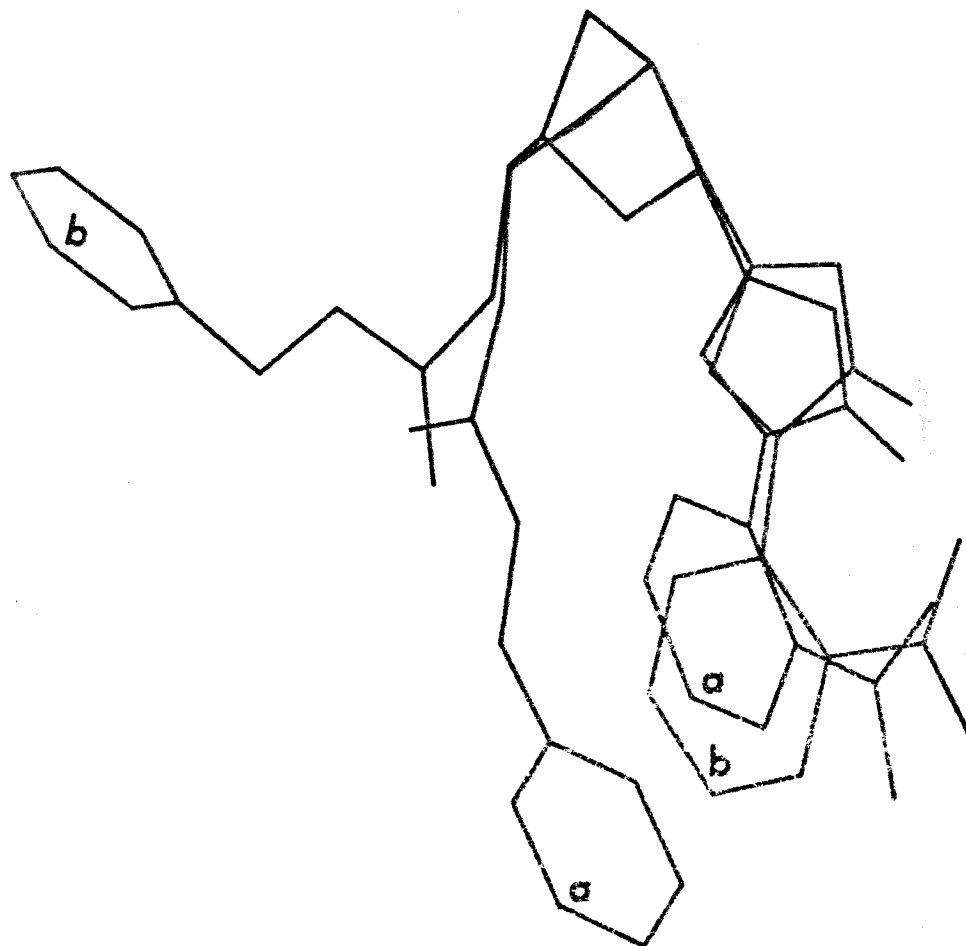


Figure 12

Superposition of two minimized structures of the norbornane mimic. Structure a is the optimized norbornane mimic obtained from run B510 (Table 4E) which corresponds to the global energy minimum of 32.06 Kcal/mol, whereas structure b corresponds to the energy maximum for the rotation around the alpha angle, run B16M of Table 4A, at 42.68 Kcal/mol.

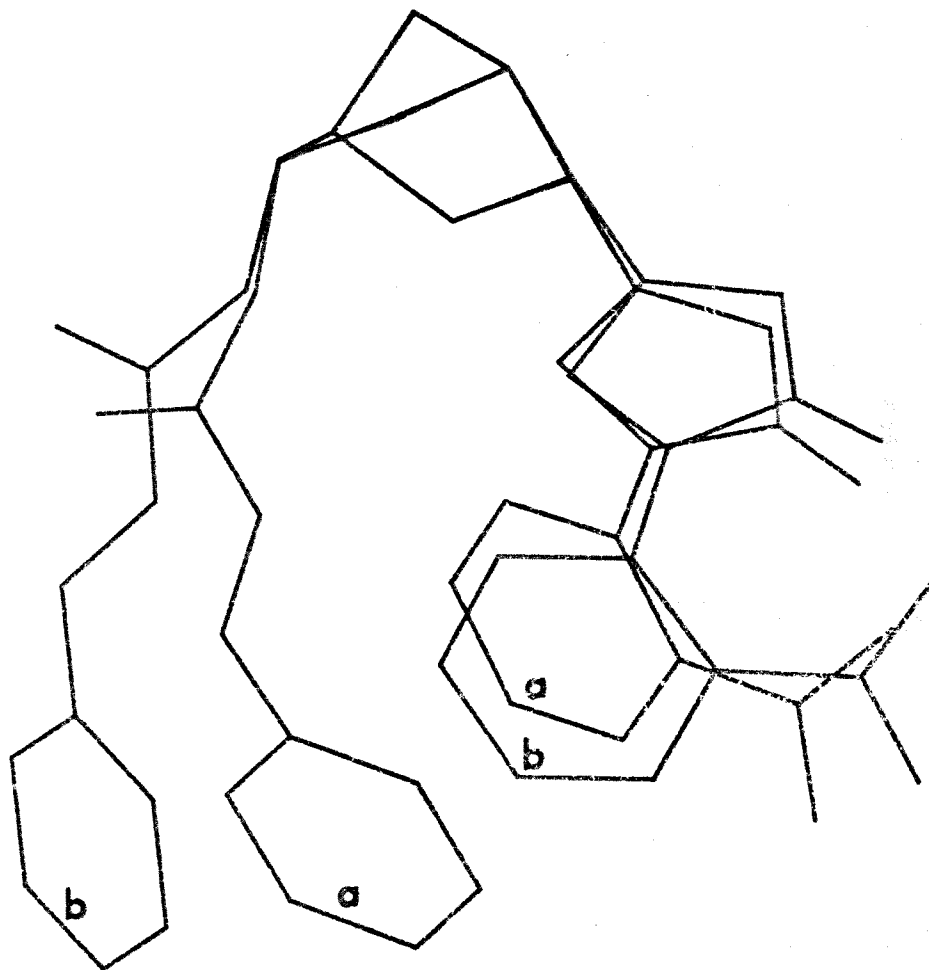


Figure 13

Superposition of two minimized structures of the norbornane mimic. Structure a is the optimized norbornane mimic obtained from run B510 (Table 4E) which corresponds to the global energy minimum of 32.06 Kcal/mol, whereas structure b corresponds to the mid-range energy for the rotation around the alpha angle, run B111 of Table 4A, at 36.82 Kcal/mol.

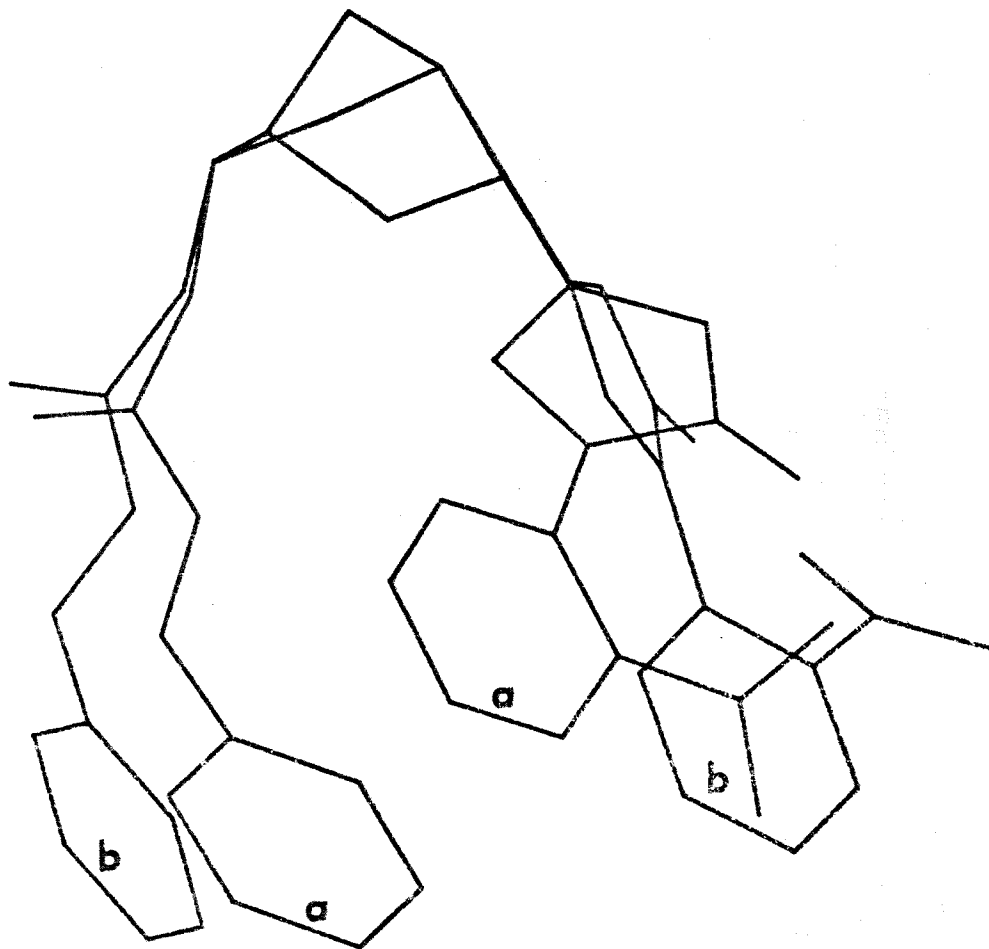


Figure 14

Superposition of two minimized structures of the norbornane mimic. Structure a is the optimized norbornane mimic obtained from run B510 (Table 4E) which corresponds to the global energy minimum of 32.06 Kcal/mol, whereas structure b corresponds to the energy maximum for the rotation around the beta angle, run B24M of Table 4B, at 38.76 Kcal/mol.

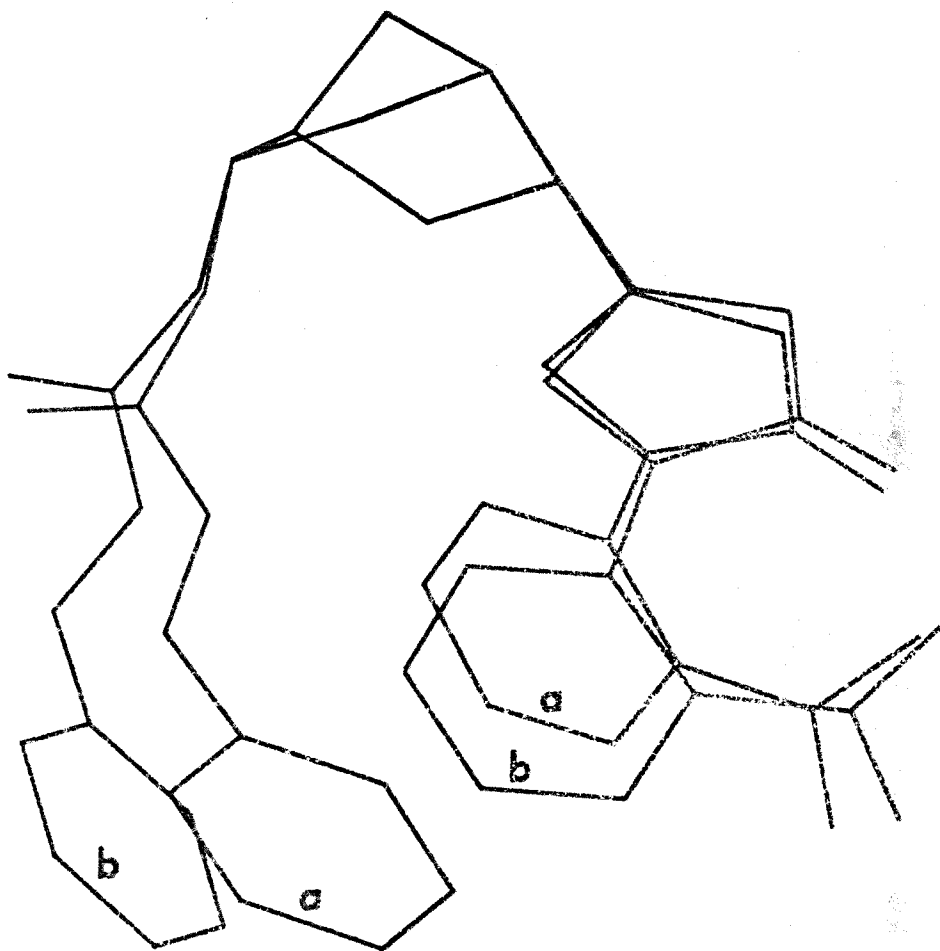


Figure 15

Superposition of two minimized structures of the norbornane mimic. Structure a is the optimized norbornane mimic obtained from run B510 (Table 4E) which corresponds to the global energy minimum of 32.06 Kcal/mol, whereas structure b corresponds to the energy maximum for the rotation around the gamma angle, run B38M of Table 4C, at 34.43 Kcal/mol.

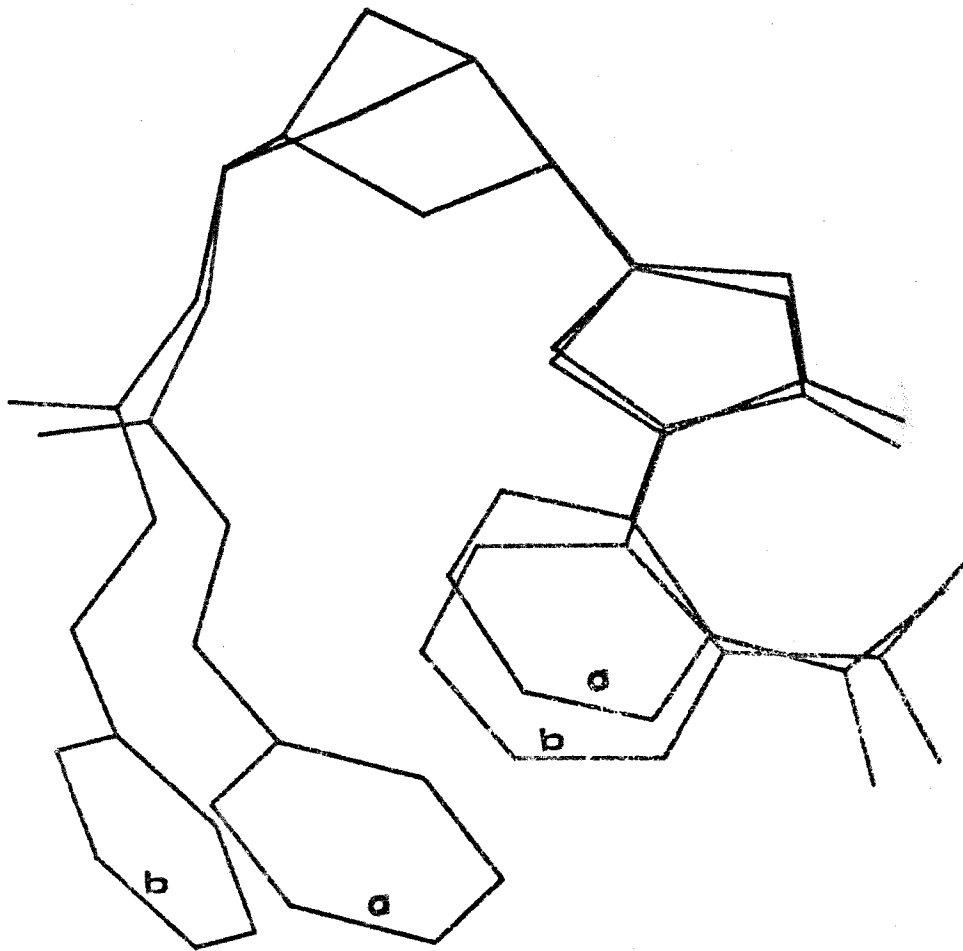


Figure 16

Superposition of two minimized structures of the norbornane mimic. Structure a is the optimized norbornane mimic obtained from run B510 (Table 4E) which corresponds to the global energy minimum of 32.06 Kcal/mol, whereas structure b corresponds to the mid-range energy for the rotation around the gamma angle, run B31M of Table 4C, at 34.07 Kcal/mol.

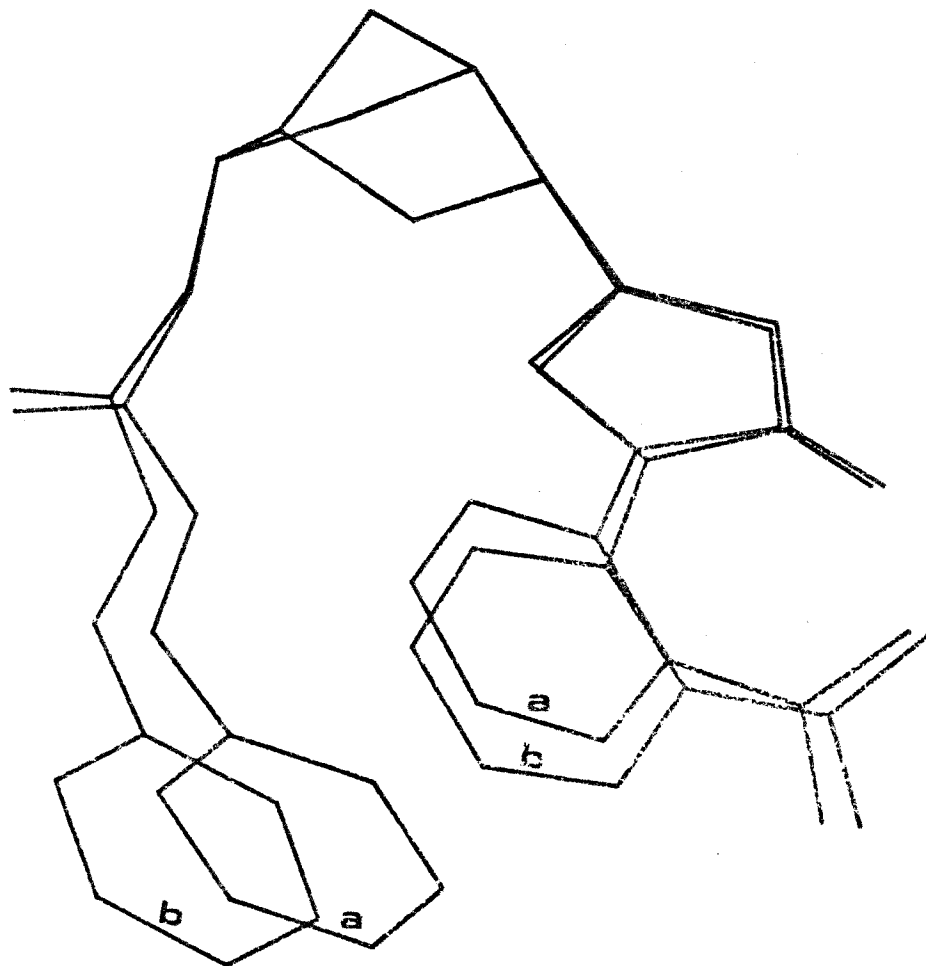


Figure 17

Superposition of two minimized structures of the norbornane mimic. Structure a is the optimized norbornane mimic obtained from run B510 (Table 4E) which corresponds to the global energy minimum of 32.06 Kcal/mol, whereas structure b corresponds to the energy minimum for the rotation around the gamma angle, run B311 of Table 4C, at 33.37 Kcal/mol.

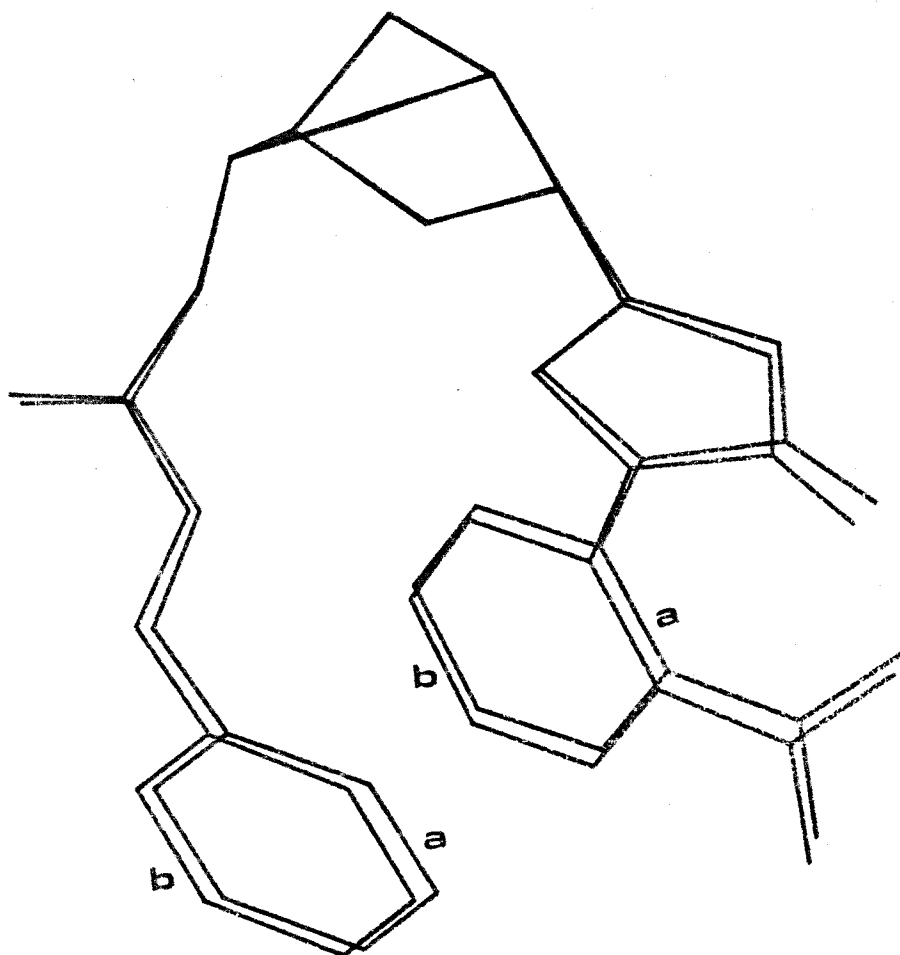


Figure 18

Superposition of two minimized structures of the norbornane mimic calculated with values of NB and EEL (i.e. 1-4 van der Waals, 1-4 Electrostatic scaling factors, see Tables 4F and 4G). Structure a is obtained from run F, NB=EEL=1.0 (energy=32.06 Kcal/mol), whereas structure b is obtained from run A, NB = 0.5, EEL = 0.5 (energy=100.70 Kcal/mol).

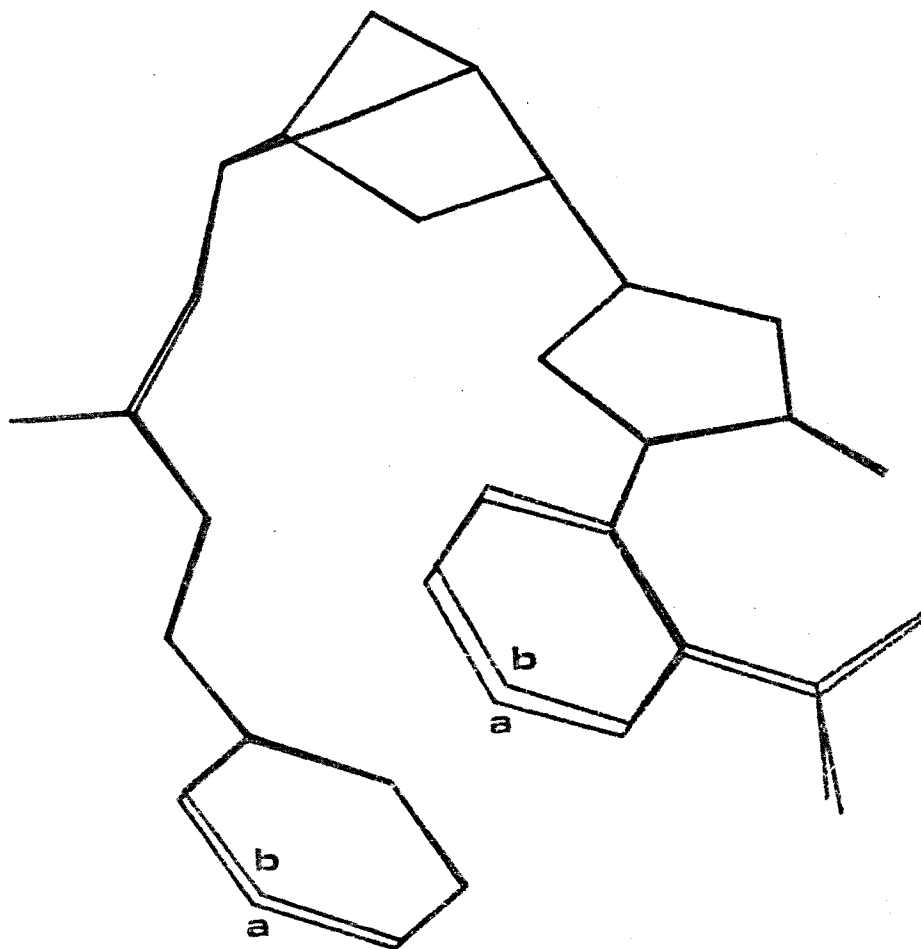


Figure 19

Superposition of two minimized structures of the norbornane mimic calculated with values of NB and EEL (i.e. 1-4 van der Waals, 1-4 Electrostatic scaling factors, see Tables 4F and 4G). Structure a is obtained from run F, NB=EEL=1.0 (energy=32.06 Kcal/mol), whereas structure b is obtained from run N, NB = 0.5, EEL = 2.0 (energy=15.32 Kcal/mol).

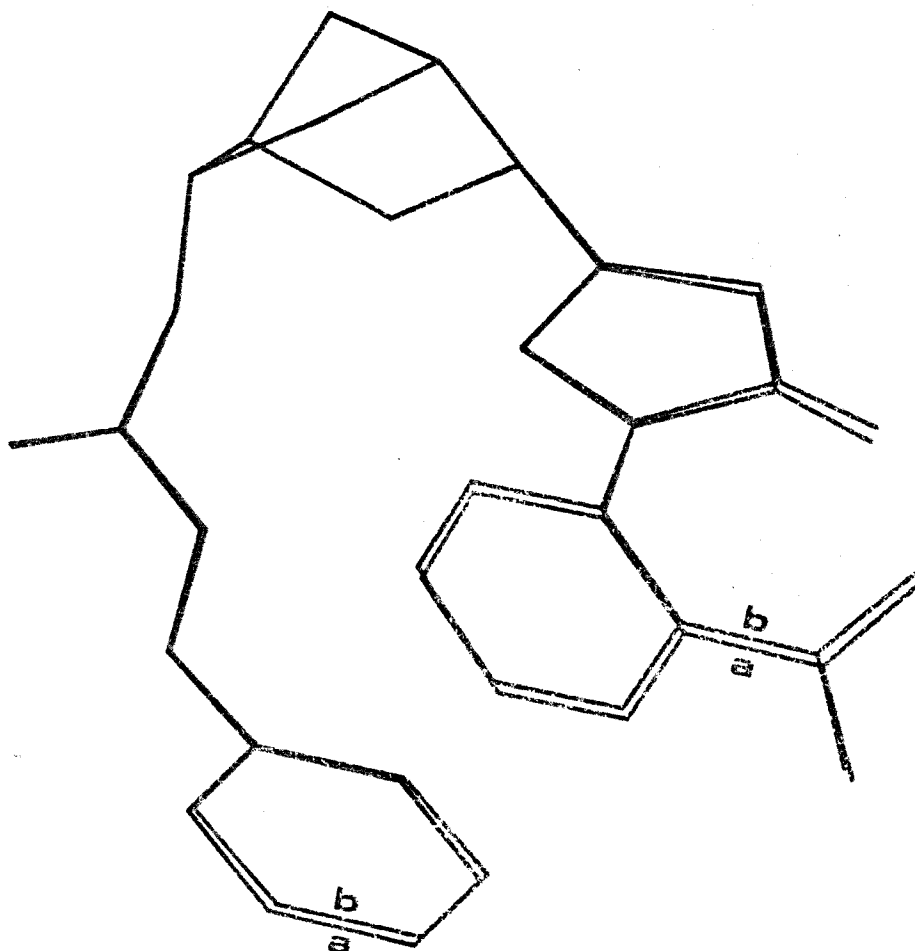


Figure 20

Superposition of two minimized structures of the norbornane mimic calculated with values of NB and EEL (i.e. 1-4 van der Waals, 1-4 Electrostatic scaling factors, see Tables 4F and 4G). Structure a is obtained from run F, NB=EEL=1.0 (energy=32.06 Kcal/mol), whereas structure b is obtained from run Q, NB = 2.0, EEL = 2.0 (energy=-5.27 Kcal/mol).

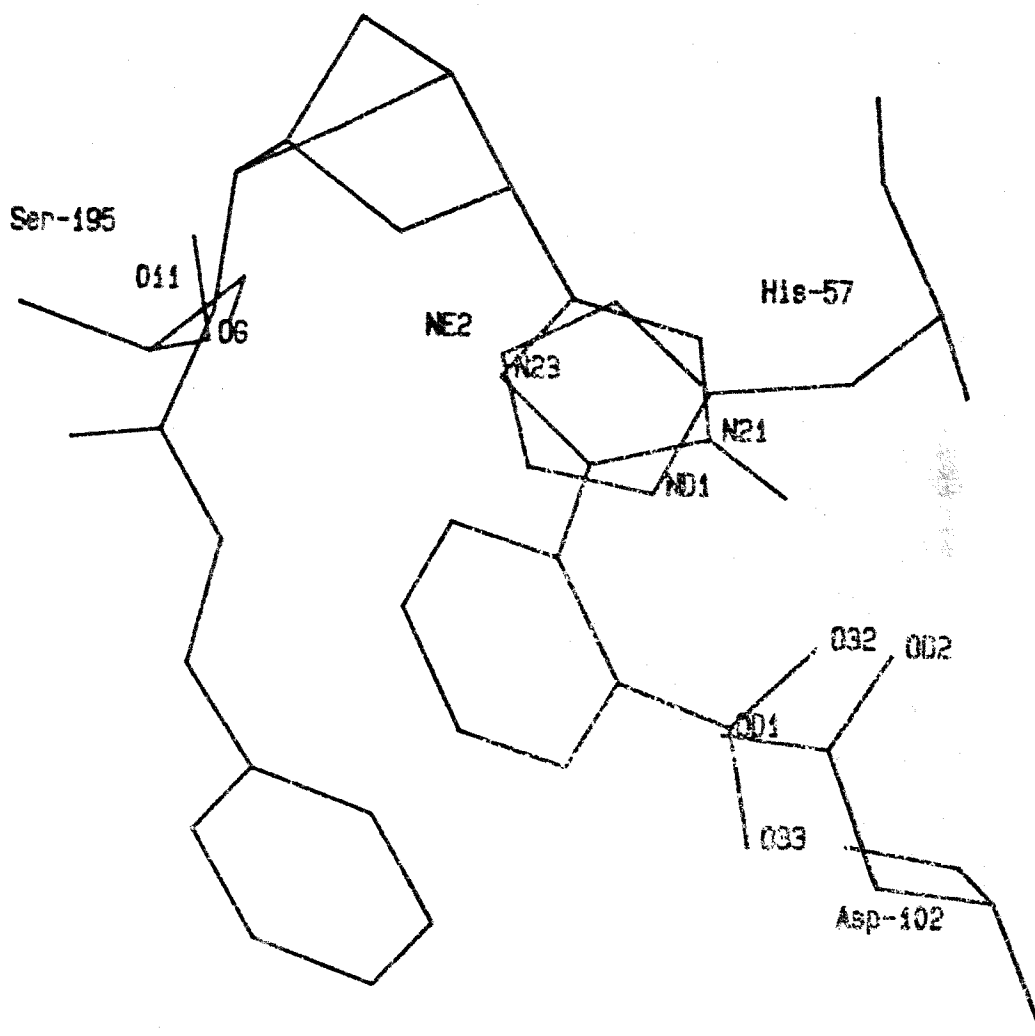


Figure 21
 Superposition of the optimized norbornane mimic structure onto the active site of alpha-chymotrypsin [11]. The structure of the mimic is that of the global conformational energy minimum obtained from run B510 (Table 5E) at 32.06 Kcal/mol. The potential proton transfer partners are: O32-N21 (mimic) and OD2-ND1 (enzyme); and O11-N23 (mimic) and O6-NE2 (enzyme).

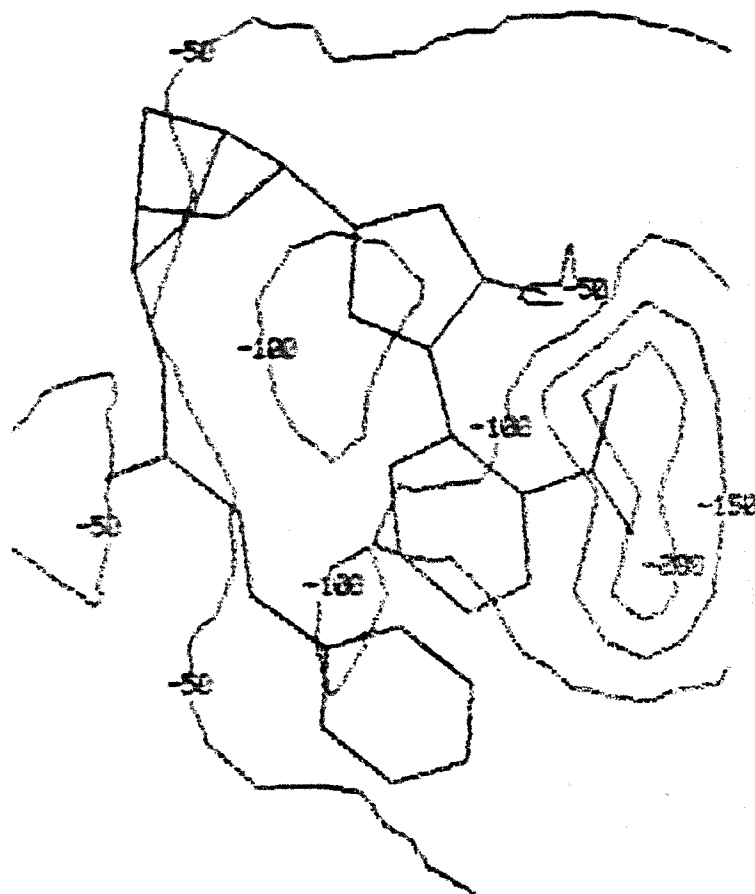


Figure 22

The molecular electrostatic potential contour map of the norbornane mimic (global energy minimum structure) calculated in the x-y plane at $z = 0.0$ Å. The molecule is oriented so that the x-y plane at $z = 0.0$ Å passes through atoms O10, O12, N21, and O32 (see Figure 11A). The values of the equi-energy contours are indicated on the figure in Kcal/mol.

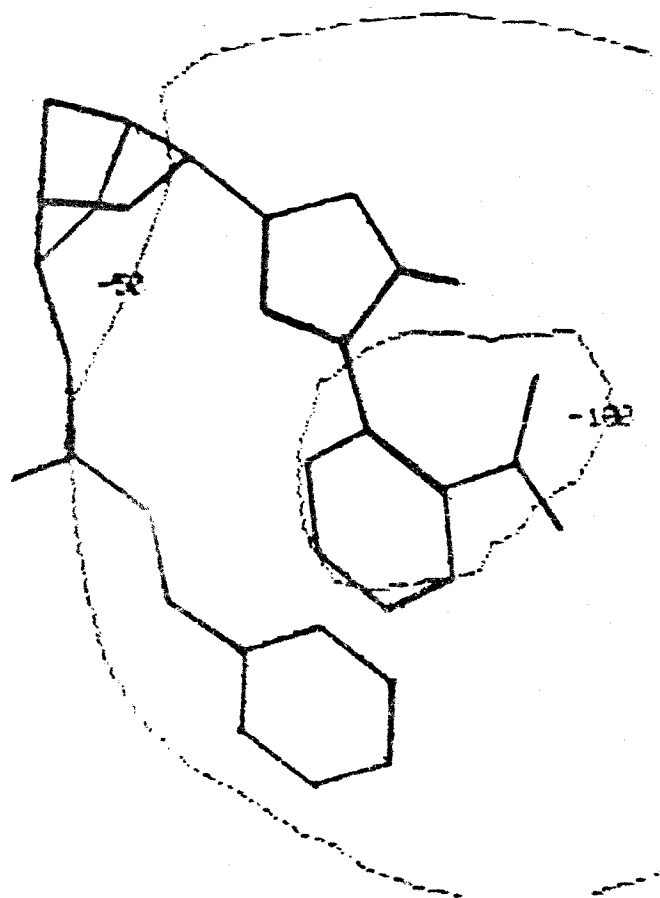


Figure 23

The molecular electrostatic potential contour map of the norbornane mimic (global energy minimum structure) calculated in the x-y plane at $z = 2.0$ Å. The molecule is oriented so that the x-y plane at $z = 0.0$ Å passes through atoms O10, O12, N21, and O32 (see Figure 11A). The values of the equi-energy contours are indicated on the figure in Kcal/mol.

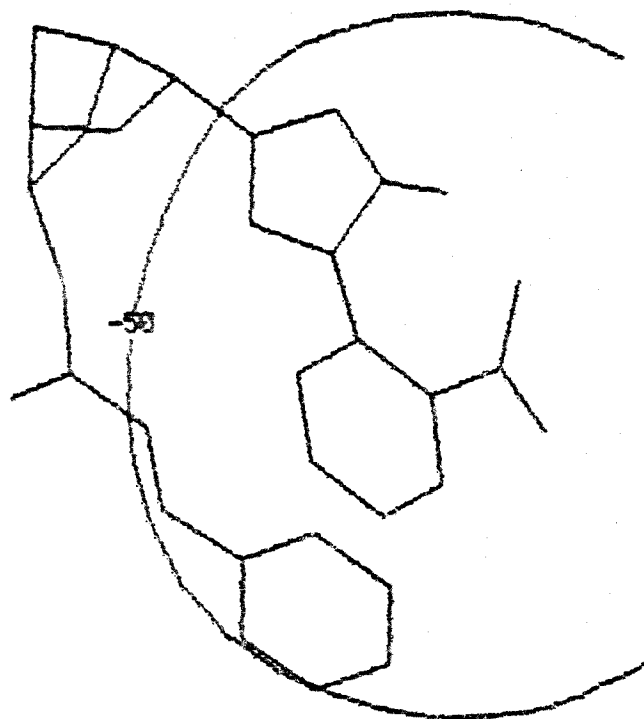


Figure 24

The molecular electrostatic potential contour map of the norbornane mimic (global energy minimum structure) calculated in the x-y plane at $z = 4.0$ Å. The molecule is oriented so that the x-y plane at $z = 0.0$ Å passes through atoms O10, O12, N21, and O32 (see Figure 11A). The values of the equi-energy contours are indicated on the figure in Kcal/mol.

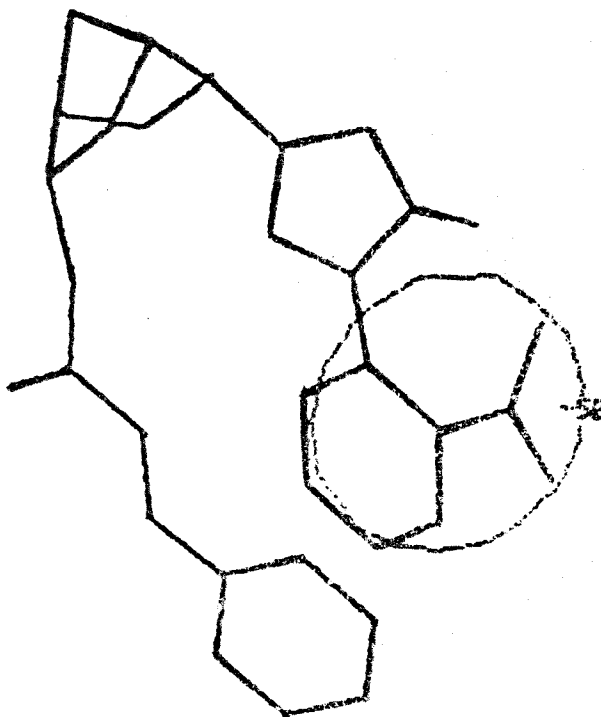


Figure 25

The molecular electrostatic potential contour map of the norbornane mimic (global energy minimum structure) calculated in the x-y plane at $z = 6.0$ Å. The molecule is oriented so that the x-y plane at $z = 0.0$ Å passes through atoms O10, O12, N21, and O32 (see Figure 11A). The values of the equi-energy contours are indicated on the figure in Kcal/mol.

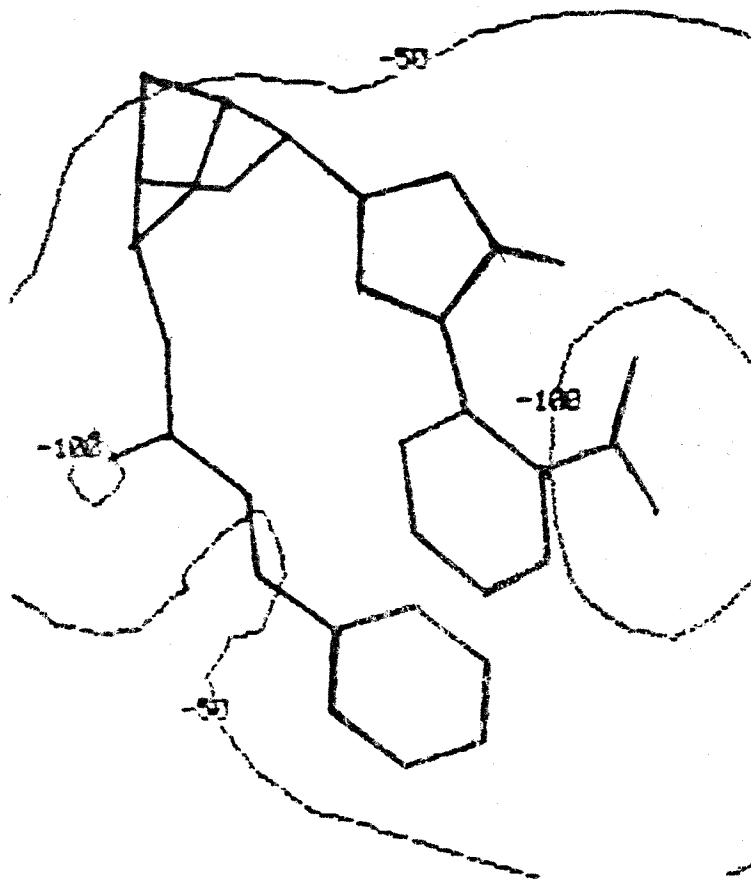


Figure 26

The molecular electrostatic potential contour map of the norbornane mimic (global energy minimum structure) calculated in the x-y plane at $z = -2.0$ Å. The molecule is oriented so that the x-y plane at $z = 0.0$ Å passes through atoms O10, O12, N21, and O32 (see Figure 11A). The values of the equi-energy contours are indicated on the figure in Kcal/mol.

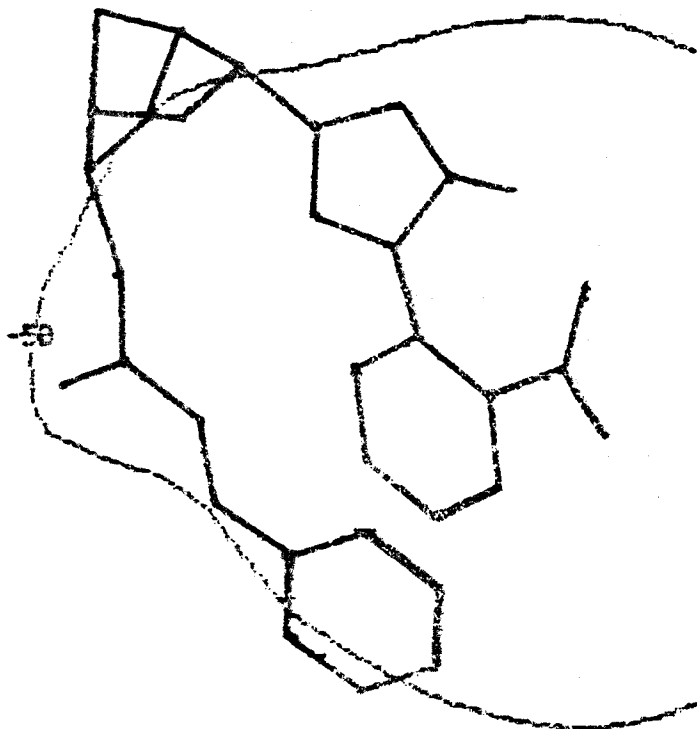


Figure 27

The molecular electrostatic potential contour map of the norbornane mimic (global energy minimum structure) calculated in the x-y plane at $z = -4.0$ Å. The molecule is oriented so that the x-y plane at $z = 0.0$ Å passes through atoms O10, O12, N21, and O32 (see Figure 11A). The values of the equi-energy contours are indicated on the figure in Kcal/mol.

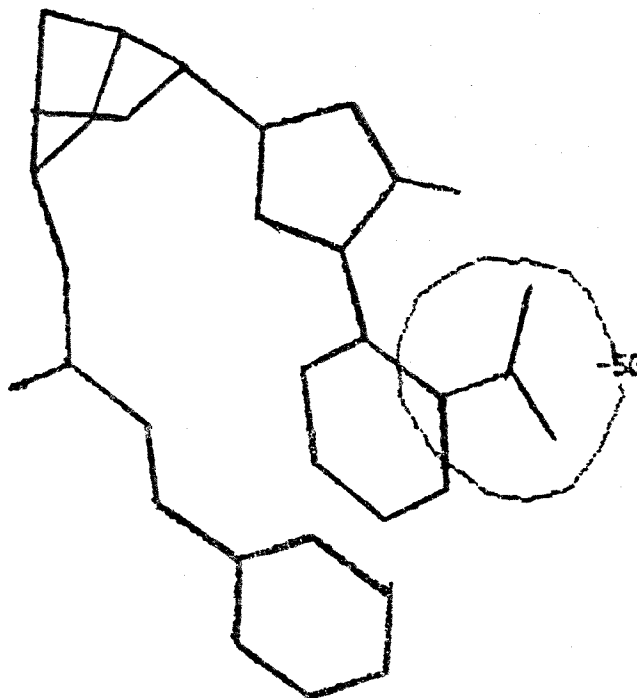


Figure 28

The molecular electrostatic potential contour map of the norbornane mimic (global energy minimum structure) calculated in the x-y plane at $z = -6.0$ Å. The molecule is oriented so that the x-y plane at $z = 0.0$ Å passes through atoms O10, O12, N21, and O32 (see Figure 11A). The values of the equi-energy contours are indicated on the figure in Kcal/mol.

APPENDIX 1

ALTERNATION OF TORSIONAL ANGLE USING CHEMGRAF/CHEM-X

Read pdb bender1a.pdb

Calculate Bond

Nominate aed767

Set Torsion
O10 C9 O11 C12
120.00

Write pdb ben*.pdb

EXIT

APPENDIX 2

CALCULATION OF ANGLES AND DISTANCES USING CHEMGRAF/CHEM-X

Read pdb benderla.pdb

Calculate Bond

Nominate aed767

CALCULATE GEOMETRY

O10 C9 O11 C12

C17 C18 C19 N23

C29 C30 C31 O32

O11 N23

O10 N23

H22 O33

H22 O32

N21 C24 C25 C30

/FINISH

EXIT

APPENDIX 3

ORIENTATION OF MOLECULE WITH PLANE PASSING THROUGH SELECTED
ATOMS USING CHEMGRAF/CHEM-X

Read css ben510m.css

Calculate Bond

Nominate aed767

Set View
/plane O11 N21 N23 O32

Write css ben510mmv.css

EXIT

APPENDIX 4

CALCULATION OF ELECTROSTATIC POTENTIAL USING CHEMGRAF/CHEM-X

Read css ben510mmv.css

Calculate Bond

Nominate aed767

SET TITLE

/ROOT_NAME BEN510MMV.CSS (NB=1.0 EEL=1.0) Z = 0.0

/ROOT_NAME/POS 110 250

/ROOT_NAME/COL RED

/ROOTNAME/DIS

SET DUMMY

/C CEN1 O11 N21 N23 O32

MODIFY

/GEO CEN1

-4.0744, -4.7725, 0.000

SET MAP

/VDW 0.5

/2 CEN1

/ADD (*)

/P 20

/CON -250 DRED -200 RED -150 ORANGE -100 GREEN -50 LBLUE 0

BLUE

/Finish

DISPLAY

EXIT

APPENDIX 5

CALCULATION OF 3-DIMENSIONAL ELECTROSTATIC POTENTIAL USING
CHEMGRAF/CHEM-X

Read css ben510mmv.css

Calculate Bond

Nominate aed767

SET TITLE

/ROOT_NAME BEN510MMV.CSS (NB=1.0 EEL=1.0) Z = 0.0

/ROOT_NAME/POS 110 250

/ROOT_NAME/COL RED

/ROOTNAME/DIS

SET MAP

/VDW 0.5

/3 CEN1

/ADD (*)

/P 20

/CON -250 DRED -200 RED -150 ORANGE -100 GREEN -50 LBLUE 0

BLUE

/Finish

DISPLAY

EXIT

VIII. References

- 1 Dugas, H.; Penney, C. Bioorganic Chemistry, A Chemical Approach to Enzyme Action, Springer Verlag, 1981, Chapter 4.
- 2 Stryer, L. Biochemistry, 2d. ed., W.H. Freeman and Co., 1981, Chapters 5 and 6.
- 3 Walsh, C. Enzymatic Reaction Mechanisms, W.H. Freeman and Co., 1979, pp.56-96.
- 4 Bender, M. L.; Bergeron, R. J.; Komiyama, M. The Bioorganic Chemistry of Enzymatic Catalysis; John Wiley, 1984, Chapters 2,5, and 10.
- 5 Mallick, I. M.; D'Souza, V. T.; Yamaguchi, M.; Lee, J.; Chalabi, P.; Gadwood, R. C.; Bender, M. L. J. Am. Chem. Soc. 1984, 106, 7252-7254.
- 6 Cram, D.J.; Katz, H. E. J. Am. Chem. Soc. 1983, 105, 135-137.
- 7 Cram, D. J.; Dicker, I. B.; Knobler, C. B.; Trueblood, K. N. J. Am. Chem. Soc. 1982, 104, 6828-6830.
- 8 Breslow, R.; Czarniecki M.F.; Emert, J.; Hamaguchi, H. J. Am. Chem. Soc. 1980, 102, 762-769.
- 9 Komiyama, T.; Roesel, T. R.; Bender, M.L. Proc. Natl. Acad. Sci. 1977, 74, 23-25.
- 10 (a) Vandlen, R.L.; Tulinsky, A. Acta Crystallogr., Sect. B 1971, B27, 437.; and (b) Ibid. 1973, B29, 1309.
- 11 Birktoft, J.J.; Blow, D.M. J. Mol. Biol. 1972, 68, 187.
- 12 (a) Venanzi, C. A.; Bunce, J. D. Int. J. Quant. Chem. 1986, QBS12, 69-87. (b) Venanzi, C. A.; Bunce, J. D. Ann. N.Y. Acad. Sci. 1986, 471, 318-320.
- 13 Venanzi, C. A.; Bunce, J. D. Enzyme 1986, 36, 79-92.
- 14 Venanzi, C. A.; Molecular Structure and Energetics, 9, (Principles of Enzyme Activity), Liebman, J.F.; Greenburg, A. Eds.; VCH Publishers: Deerfield Beach, Florida, in press.
- 15 Weinstein, H.; Maayani, S.; Pazhenchevsky, B.; Venanzi, C.; Osman, R. Int. J. Quant. Chem. 1983, QBS12, 309-320.
- 16 Weiner, P. K.; Kollman, P. A. J. Comput. Chem. 1981, 2, 287-303.

- 17 Weiner, S. J.; Kollman, P. A.; Case, D. A.; Singh, U. C.; Ghio, C.; Alagona, G.; Profeta, S., Jr.; Weiner, P. J. Am. Chem. Soc. 1984, 106, 765-784.
- 18 Gelin, B.; Karplus, M. Proc. Nat. Acad. Sci. 1975, 72, 2002.
- 19 Allinger, N. J. Amer. Chem. Soc. 1977, 99, 8127.
- 20 Davies, E. K.: Chem-X; Chemical Crystallographic Laboratory, Oxford University (Chemical Design Ltd., Oxford, UK).
- 21 (a) Dewar, M. S.; Thiel, W. J. Amer. Chem. Soc. 1977, 99, 4899; (b) Stewart, J. J. P.: MOPAC: a general molecular orbital package. Quantum Chemistry Program Exchange Bull. 1983, 3, 43.
- 22 (a) Allen, F.H.; Kennard, O. Perspectives in Computing 1983, 3, 28-43. (b) Bryan, R.F.; Freyberg, D.P. J. Chem. Soc., Perkin 2, 1975, 188, 1835.
- 23 Wipff, G; Weiner, P.; Kollman, P. J. Am. Chem. Soc. 1982, 104, 3249.
- 24 Kollman, P.; Wipff, G.; Singh, U. C. J. Amer. Chem. Soc. 1985, 107, 2212.
- 25 Hollis, J.M.; Ridley, T. Chem. Phys. Let 1980, 75, 94-98.
- 26 (a) Singh, U.C.; Kollman, P. "GAUSSIAN 80 UCSF", Quantum Chemistry Program Exchange Bull. 1982, 2, 17; (b) Singh, U.C.; Kollman, P.A. J. Comp. Chem. 1984, 5, 129-145.
- 27 Weiner, P. RMS Module of Amber, Modified 1986.
- 28 Bernstein, F.C.; Koetzle, T.F.; Williams, G.J.B.; Meyer, E.F., Jr.; Brice, M.D.; Rodgers, J.R.; Kennard, O.; Shimamouchi, T.; Tasumi, M. J. Mol. Biol. 1977, 112, 535-542.
- 29 Pollitzer, P.; Truhlar, D.G. Chemical Applications of Atomic and Molecular Electrostatic Potential, Plenum Press, New York, 1981, pp.3.